

**THE REPUBLIC OF TURKEY
MUGLA SITKI KOCMAN UNIVERSITY
GRADUATE SCHOOL OF NATURAL AND APPLIED
SCIENCES**

DEPARTMENT OF GEOLOGICAL ENGINEERING

**IDENTIFICATION OF HOT AND COLD SPRINGS
USING THERMAL INFRARED REMOTE SENSING
AND IN-SITU MEASUREMENTS IN
MEDITERRANEAN REGION**

MASTER THESIS

TUĞBA GÜRCAN

JULY 2017

MUĞLA

MUGLA SITKI KOCMAN UNIVERSITY
Graduate School of Natural and Applied Sciences

THESIS CONFIRMATION

The thesis, prepared by TUĞBA GÜRCAN, titled as “**“IDENTIFICATION OF HOT AND COLD SPRINGS USING THERMAL INFRARED REMOTE SENSING AND IN-SITU MEASUREMENTS IN MEDITERRANEAN REGION”** has been accepted unanimously/majority by the jury listed below that fulfils the necessary conditions for master degree of Department of Geological Engineering at 21/09/2016.

THEESIS DEFENCE JURY

Prof. Dr. Mountaz RAZACK (**Head of Jury**)
Department of Geosciences,
University of Poitiers, Poitiers, France

Signature:

Asst. Prof. Dr. Bedri KURTULUŞ (**Supervisor**)
Department of Geological Engineering,
Mugla Sitki Kocman University, Muğla

Signature:

Asst. Prof. Dr. Mathieu LE COZ (**Member**)
Department of Geosciences,
University of Poitiers, Poitiers, France

Signature:

Asst. Prof. Dr. Özgür AVŞAR (**Member**)
Department of Geological Engineering,
Mugla Sitki Kocman University, Muğla

Signature:

Asst. Prof. Dr. Gilles POREL (**Member**)
Department of Geosciences,
University of Poitiers, Poitiers, France

Signature:

Asst. Prof. Dr. Jacques BODIN (**Member**)
Department of Geosciences,
University of Poitiers, Poitiers, France

Signature:

Asst. Prof. Dr. Aude NAVEAU (**Member**)
Department of Geosciences,
University of Poitiers, Poitiers, France

Signature:

Date of Defence: 21/09/2016

MUGLA SITKI KOCMAN UNIVERSITY
Graduate School of Natural and Applied Sciences

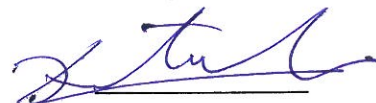
THESIS CONFIRMATION

The thesis, prepared by **TUĞBA GÜRCAN**, titled as "**IDENTIFICATION OF HOT AND COLD SPRINGS USING THERMAL INFRARED REMOTE SENSING AND IN-SITU MEASUREMENTS IN MEDITERRANEAN REGION**" has been accepted unanimously/majority by the jury listed below that fulfils the necessary conditions for master degree of Department of Geological Engineering at 21/09/2016.

DEPARTMENT CONFIRMATION

Asst. Prof. Dr. Bedri KURTULUŞ

Signature:



Head of Department of Geological Engineering,
Mugla Sitki Kocman University, Muğla

Asst. Prof. Dr. Bedri KURTULUŞ

Signature:



Supervisor, Department of Geological Engineering,
Mugla Sitki Kocman University, Muğla

Date of Defence: 21/09/2016

I declare all results and information in this document have been obtained and presented in accordance with scientific and academic ethic rules. I also declare that all original information and results belong to someone else that were not achieved within the study of this thesis were referenced by ethic rules of academy and science.



Tuğba GÜRCAN

21/09/2016

ÖZET

AKDENİZ BÖLGESİNDEN SOĞUK VE SICAK SU KAYNAKLARININ TERMAL KIZİLÖTESİ UZAKTAN ALGILAMA VE YERİNDE ÖLÇÜMLER İLE BELİRLENMESİ

Tuğba GÜRCAN

Yüksek Lisans Tezi

Fen Bilimleri Enstitüsü

Jeoloji Mühendisliği Anabilim Dalı

Danışman: Yrd. Doç. Dr. Bedri KURTULUŞ

Haziran 2017, 90 sayfa

Bu tezde, yerinde ölçümler ve termal kızılılolesi görüntüleri kullanılarak sıcak ve soğuk su kaynaklarının Türkiye'de Akdeniz Bölgesinde haritalaması yapılmıştır. Yerinde yüzey, derinlik su sıcaklığı, iklim verileri ve derinlik ölçümleri veri kaydediciler kullanılarak toplanmıştır. Landsat 8 TIRS bant (Termal Kızılılolesi Sensörleri) görüntüleri yerinde ölçümler ile karşılaştırılmıştır. Elektriksel iletkenlik, pH ve tuzluluk ölçümleri de toplanarak gölün dibindeki giriş yerlerinin daha iyi tanımlanması yapılmıştır. Yerinde ölçümler Ampirik Bayes Kriging (EBK) kullanılarak tahmin haritaları oluşturulmuştur. Yerinde ölçümler ve Landsat 8 görüntüleri hücre hücre karşılaştırılarak korelasyon katsayısı en iyi (R^2) olana göre hesaplanmıştır ve en uygun regresyon denklemi oluşturulmuştur. Sonuçlar yerinde su sıcaklığın ölçümleri ile Landsat 8 TIR görüntülerinin iyi bir korelasyon katsayısına ($R^2 \geq 0.86$) ulaşabilirliğini göstermektedir. Yerinde ölçümlerinin haritalama sonuçları da Köyceğiz Gölü'nün kuzey doğu kısmında göl dibinde soğuk su girişlerinin olduğunu ortaya koymaktadır. Sıcak su kanıtları ise Sultanije bölgesinin yakınında Köyceğiz Gölü'nün güney batı kesiminde bulunmaktadır. Köyceğiz gölünün derinliğe göre şekilleri de çizilerek gölün termal istifi de çıkarılmıştır. Göcek-Fethiye Körfezi'nde kıyı kesiminde soğuk su girişleri tespit edilmiştir. Bu bağlamda, bu tezin çıkışmasında finansal olarak katkıları olan TÜBİTAK (112Y137) projesine, Sıtkı Koçman Vakfı'na ve Fransa Konsolosluğuna teşekkür ederim.

Anahtar Kelimeler: Sıcaklık, Uzaktan Algılama, Kaynak, Köyceğiz Gölü, Fethiye Göcek Körefezi

ABSTRACT

IDENTIFICATION OF HOT AND COLD SPRINGS USING THERMAL INFRARED REMOTE SENSING AND IN-SITU MEASUREMENTS IN MEDITERRANEAN REGION

Tuğba GÜRCAN

Master of Science (M.Sc.)

Graduate School of Natural and Applied Sciences

Department of Geological Engineering

Supervisor: Asst. Prof. Dr. Bedri KURTULUŞ

Haziran 2017, 90 pages

In this thesis, in-situ measurement and thermal infrared imagery was used to map hot and cold springs of Mediterranean Region in Turkey. In-situ surface, depth water temperature, climatic data and bathymetry measurement were collected using data loggers. Landsat 8 TIRS Bands (Thermal Infrared Sensors) images were compared with in-situ measurements. Electrical conductivity, pH and salinity measurement were also collected at the bottom of the lake to better understand the groundwater discharge evidence in the lake. In-situ measurement was interpolated using Empirical Bayesian Kriging (EBK). In-Situ measurement and Landsat 8 Images were compared pixel by pixel and appropriate regression equation were calculated according to the best coefficient of correlation (R^2). The results show that in-situ measurement of the temperature of the water surface can reach a good correlation ($R^2 \geq 0.86$) with Landsat 8 TIR images. The mapping results of in-situ measurements also reveal that at the north east part of the Köyceğiz Lake there exist several evidence of cold spring at the bottom of the Lake. Hot spring evidence was located in the South-West part of the Köyceğiz Lake near the Sultaniye region. Thermal stratification of Köyceğiz Lake is also demonstrated using the depth vs. temperature graphs. There exist also some evidence of cold spring at Göcek-Fethiye Bay, which are located on the coastal line. In this regard, we would like also to thank TUBITAK project (112Y137), French Embassy in Turkey and Sıtkı Kocman Foundation for their financial support.

Keywords: Temperature, Remote sensing, Spring, Köyceğiz Lake, Göcek Bay

RESUME

IDENTIFICATION DE SOURCE CHAUD ET FROID EN UTILISANT TÉLÉDÉTECTION INFRAROUGE THERMIQUE ET MESURES IN SITU EN REGION DE LA MEDITERRANEE

Tugba GURCAN

Thèse du Master

Faculté des Sciences Fondamentales et Appliquées

Superviseur: Asst. Prof. Dr. Bedri KURTULUŞ

Juin 2017, 90 pages

Dans cette thèse, Les mesure in-situ et l'imagerie infrarouge thermique a été utilisée pour cartographier les sources chaudes et froides de la région méditerranéenne en Turquie. In-situ surface, température de l'eau de profondeur, les données climatiques et la mesure de bathymétrie ont été recueillies à l'aide des enregistreurs de données. Landsat 8 TIRS Bands images (capteurs infrarouges thermiques) ont été comparés avec des mesures in-situ. La conductivité électrique, le pH et la mesure de la salinité ont également été recueillies au fond du lac afin de mieux comprendre les éléments de preuve à décharge des eaux souterraines dans le lac. Mesure in situ ont été interpolées à l'aide Empirique Bayésien Krigeage (EBK). In-Situ mesure et Landsat 8 images ont été comparés pixel par pixel et l'équation de régression appropriée ont été calculés selon le meilleur coefficient de corrélation (R^2). Les résultats montrent que in situ mesure de la température à la surface de l'eau peut atteindre une bonne corrélation ($R^2 \geq 0,86$) avec des images Landsat 8 TIR. Les résultats de la cartographie des mesures in-situ révèlent également que dans la partie nord-est du lac Köyceğiz il existe plusieurs preuves de la source froide au fond du lac. Les preuves de source chaude ont été situées dans la partie sud-ouest du lac Köyceğiz près de la région Sultanije. Il existe également des preuves de la source froide à Göcek-Fethiye Baie qui sont situés sur la ligne côtière. Stratification thermique du Köyceğiz lac est également démontrée en utilisant la profondeur par rapport à des graphiques de température. À cet égard, nous aimerais également remercier projet TUBITAK (112Y137), Ambassade de la France en Turquie et Fondation Sıtkı Kocman pour leur soutien financier.

Mots Clés : Température, Télédétection, Source, Köyceğiz Lac, Fethiye-Göcek Baie



Dedicated to my family.

ACKNOWLEDGEMENT

I would like to thank to my supervisor Asst. Prof. Dr. Bedri KURTULUŞ for their help, ongoing support and supervising me to write this thesis.

I would like to thank very much to Asst. Prof. Dr. Özgür Avşar who gave very valuable data of TUBİTAK project and support to write this thesis and also participate to my thesis defense in Poitiers/France.

I am grateful to Prof. Dr. Mountaz Razack for his valuable advices and to accept me to do my Master degree in Poitiers University.

I would like to special thanks to Dr. Jacques Bodin, Dr. Giles Porel, Dr. Mathieu Le Coz, Dr. Aude Nevau to participate and be a jury member of my master thesis.

I give my special thanks to my my B.Sc. lecturer Assoc. Prof. Dr. K. Kadir Eriş and my M.Sc. lecturer Asst. Prof. Dr. Sena Akçer Ön for his unforgettable help, turning my back to Academia.

I would like to thank to Dean Prof. Dr. İlkay KUŞCU, Haşim KOÇ, and Erkan DÜZTAŞ for their motivational and financial supports...

I also owe a special thanks to Assoc. Prof. Dr. D. Funda KURTULUŞ and her father Yaşar KURTULUŞ and his wife Aynur KURTULUŞ for their motivation supports.

I am really indebted to the organization which gave me a scholarship, Muğla Sıtkı Koçman Vakfı (SKV) and French Government (CAMPUS FRANCE). This thesis was started and completed on time by using this financial help they provided. Thank you for your generous financial support.

My friends Günseli Erdem (PhD), Çağdaş Sağır (PhD), Engin Günay (M.Sc.), Ersin Ateş (M.Sc) and anyone who helped and I could not remember their name here, I thank to all for their supports.

I owe more than a thank you to my dearest family. I also dedicate this thesis to my father and my mother for their motivation and financial support all the time, additionally, likewise to my brother.

TABLE OF CONTENTS

ACKNOWLEDGEMENT	ix
TABLE OF CONTENTS.....	x
LIST OF TABLES	xii
LIST OF FIGURES	xiii
SYMBOLS AND ABBREVIATIONS.....	xviii
1. INTRODUCTION.....	1
1.1. Research Goal and Questions	1
1.2. Scope of the Study	2
1.3. Thesis Outline	2
1.4. Literature Review.....	3
2. STUDY AREA.....	8
2.1. Localization of the Study Area	8
2.2. Geology/Hydrogeology of the Study Area	11
3. RESEARCH METHODOLOGY AND MATERIAL.....	14
3.1. In-Situ Measurement.....	14
3.2 Interpolation Methodology: Empirical Bayesian Kriging	16
3.2.1. EBK Process	16
3.3. Thermal Infrared (TIR) Remote Sensing	18
3.3.1. Mathematical Background For TIR Remote Sensing of Surface Water.....	21
3.4. Advantages, Disadvantages and Limitations of TIR Remote Sensing Methods.....	23
3.5. Sensitivity Analysis	24
4. RESULTS	25
4.1. EBK Interpolation Results for in-situ Measurement	25
4.2. Comparison of Landsat 8 OLI with in-situ temperature measurement.....	31
4.3. Evidence of cold and hot spring results for Köycegiz Lake and Fethiye-Göcek Bay	34
4.4. Thermal Stratification (thermocline) of Köycegiz Lake.....	39
5. CONCLUSION.....	45

6. DISCUSSION AND RECOMMENDATION.....	47
REFERENCES	48
APPENDICES	54
Appendix A. EBK Interpolation For Salinity and Specific Conductance For Köyceğiz Lake	54
Appendix B. EBK Interpolations Maps for Specific Conductance, pH and salinity for Fethiye-Göcek Bay	56
Appendix C. EBK Eror Maps and Variograms for Köyceğiz Lake	59
Appendix D. EBK error maps and variograms for Fethiye-Göcek Bay	69
Appendix E. Temperature vs. Depth Graphs for Fethiye-Göcek Bay	85
CURRICULUM VITAE	88



LIST OF TABLES

Table 1.1.	Literature survey related to surface temperature estimation	3
Table 1.2.	Chemical analysis results of Köycegiz Bay waters according to Avsar et al. (2016)	6
Table 2.1.	Mean annual meteorological values between 1950 and 2015 in Mugla Station.	8
Table 3.1.	In-Situ measurement information (Avsar et al., 2015).....	15
Table 3.2.	TIR imaging for different type of satellites	18
Table 3.3.	Details describing selected LANDSAT 8 scenes	20
Table 3.4.	Metadata for Landsat 8 TIR for Band 10	20
Table 3.5.	Temperature values at the capture time (hourly temperature average of 10:00-11:00) of the LANDSAT 8 images.	20
Table 3.6.	Advantages and disadvantages of TIR remote sensing	23
Table 3.7.	An overview of the uncertainty analysis for internal and external factor to calculate temperature prediction	24
Table 4.1.	The Numbering the interpolation maps.....	25
Table 4.2.	The numbering the interpolation maps (cont...)	26

LIST OF FIGURES

Figure 2.1.	Localization of the Study Area.....	9
Figure 2.2.	Digital Elevation Model and Batymetry Map of the Study Area.....	10
Figure 2.3.	A general view of Köyceğiz Lake from Google Earth.....	10
Figure 2.4.	A general view of Fethiye-Göcek Bay from Google Earth.....	11
Figure 2.5.	The detailed geological map of Study Area	13
Figure 3.1.	Muğla Sıtkı Kocman University floating platform (Avsar et al., 2015).....	14
Figure 3.2.	Specified in-situ measurement grid	14
Figure 3.3.	An example of EBK interporpolation for a. semi variogram cloud b. cross validation results and best fit.....	17
Figure 3.4.	Landsat 8 Spectral response function	19
Figure 3.5.	An example view of Landsat 8 download web page (http://earthexplorer.usgs.gov/)	19
Figure 3.6.	Suggested flowchart for Landsat 8 image processing (Handcock et al., 2012).....	22
Figure 4.1.	EBK interpolation for temperature at surface of Köyceğiz Lake.....	27
Figure 4.2.	EBK interpolation for temperature at depth of Köyceğiz Lake	28
Figure 4.3.	EBK interpolation for temperature at surface of Fethiye-Göcek Bay.....	29
Figure 4.4.	EBK interpolation for temperature at depth of Fethiye-Göcek Bay... ...	30
Figure 4.5.	Corrected Landsat 8 TIR image according to regression equaiton for Koycegiz Lake (23/07/2013)	32
Figure 4.6.	Corrected Landsat 8 TIR image according to regression equaiton for Koycegiz Lake (30/07/2013)	32
Figure 4.7.	Corrected Landsat 8 TIR image according to regression equaiton for Göcek-Fethiye Bay (27/08/2014)	33
Figure 4.8.	Corrected Landsat 8 TIR image according to regression equaiton for Göcek-Fethiye Bay (08/06/2014)	33
Figure 4.9.	Corrected Landsat 8 TIR image according to regression equaiton for Göcek-Fethiye Bay (24/08/2013)	34
Figure 4.10.	Surface Water Temperature interpolations for Köyceğiz Lake (July and August 2013).	35
Figure 4.11.	Surface Water Temperature interpolations for Fethiye-Göcek Bay (August 2013 and June 2014).....	36

Figure 4.12.	Normalize Depth Water Temperature Interpolation maps for Köyceğiz Lake (July and August 2013)	37
Figure 4.13.	Normalize Depth water temperature Interpolations maps for Fethiye-Göcek Bay (August 2013 and June 2014).....	38
Figure 4.14.	Temperature and Specific Conductivity vs Depth plots for Köyceğiz Lake.....	39
Figure 4.15.	Temperature and Specific Conductivity vs Depth plots for Köyceğiz Lake (cont...)	40
Figure 4.16.	Temperature and Specific Conductivity vs Depth plots for Köyceğiz Lake (cont...)	41
Figure 4.17.	Temperature and Specific Conductivity vs Depth plots for Köyceğiz Lake (cont...)	42
Figure 4.18.	Temperature and Specific Conductivity vs Depth plots for Köyceğiz Lake (cont...)	43
Figure 4.19.	Temperature and Specific Conductivity vs Depth plots for Köyceğiz Lake (cont...)	44
Figure A.1.	EBK interpolation for salinity at depth of Köyceğiz Lake	54
Figure A.2.	EBK interpolation for Specific Conductivty at depth of Köyceğiz Lake	55
Figure B.1.	EBK interpolation for Specific Conductivity at depth of Fethiye-Göcek Bay	56
Figure B.2.	EBK interpolation for pH at depth of Fethiye-Göcek Bay	57
Figure B.3.	EBK interpolation for salinity at depth of Fethiye- Göcek Bay	58
Figure C.1.	The surface temperature eror map of Köyceğiz Lake	59
Figure C.2.	The surface temperature variogram of Köyceğiz Lake in 19.07.2013	60
Figure C.3.	The surface temperature variogram of Köyceğiz Lake in 20.07.2013	60
Figure C.4.	The surface temperature variogram of Köyceğiz Lake in 22.07.2013	60
Figure C.5.	The surface temperature variogram of Köyceğiz Lake in 23.07.2013	61
Figure C.6.	The surface temperature variogram of Köyceğiz Lake in 24.07.2013	61
Figure C.7.	The surface temperature variogram of Köyceğiz Lake in 25.07.2013	61
Figure C.8.	The surface temperature variogram of Köyceğiz Lake in 26.07.2013	62
Figure C.9.	The surface temperature variogram of Köyceğiz Lake in 18.08.2013	62

Figure C.10.	The surface temperature variogram of Köyceğiz Lake in 19.08.2013	62
Figure C.11.	The surface temperature variogram of Köyceğiz Lake in 20.08.2013	63
Figure C.12.	The surface temperature variogram of Köyceğiz Lake in 21.08.2013	63
Figure C.13.	The depth temperature eror map of Köyceğiz Lake	64
Figure C.14.	The depht temperature variogram of Köyceğiz Lake in 19.07.2013..	65
Figure C.15.	The depht temperature variogram of Köyceğiz Lake in 20.07.2013..	65
Figure C.16.	The depht temperature variogram of Köyceğiz Lake in 22.07.2013..	65
Figure C.17.	The depht temperature variogram of Köyceğiz Lake in 23.07.2013..	66
Figure C.18.	The depht temperature variogram of Köyceğiz Lake in 24.07.2013..	66
Figure C.19.	The depht temperature variogram of Köyceğiz Lake in 25.07.2013..	66
Figure C.20.	The depht temperature variogram of Köyceğiz Lake in 26.07.2013..	67
Figure C.21.	The depht temperature variogram of Köyceğiz Lake in 18.08.2013..	67
Figure C.22.	The depht temperature variogram of Köyceğiz Lake in 19.08.2013..	67
Figure C.23.	The depht temperature variogram of Köyceğiz Lake in 20.08.2013..	68
Figure C.24.	The depht temperature variogram of Köyceğiz Lake in 21.08.2013..	68
Figure D.1.	The surface temperature eror map of Fethiye-Göcek Bay	69
Figure D.2.	The surface temperature variogram of Fethiye-Göcek Lake in 23.08.2013	70
Figure D.3.	The surface temperature variogram of Fethiye-Göcek Lake in	70
Figure D.4.	The surface temperature variogram of Fethiye-Göcek Lake in 25.08.2013	70
Figure D.5.	The surface temperature variogram of Fethiye-Göcek Lake in 26.08.2013	71
Figure D.6.	The surface temperature variogram of Fethiye-Göcek Lake in 27.08.2013	71
Figure D.7.	The surface temperature variogram of Fethiye-Göcek Lake in 30.08.2013	71
Figure D.8.	The surface temperature variogram of Fethiye-Göcek Lake in 31.08.2013	72
Figure D.9.	The surface temperature variogram of Fethiye-Göcek Lake in 03.06.2014	72
Figure D.10.	The surface temperature variogram of Fethiye-Göcek Lake in 04.06.2014	72

Figure D.11.	The surface temperature variogram of Fethiye-Göcek Lake in 05.06.2014	73
Figure D.12.	The surface temperature variogram of Fethiye-Göcek Lake in 06.06.2014	73
Figure D.13.	The surface temperature variogram of Fethiye-Göcek Lake in 07.06.2014	73
Figure D.14.	The surface temperature variogram of Fethiye-Göcek Lake in 26.08.2014	74
Figure D.15.	The surface temperature variogram of Fethiye-Göcek Lake in 27.08.2014	74
Figure D.16.	The surface temperature variogram of Fethiye-Göcek Lake in 28.08.2014	74
Figure D.17.	The surface temperature variogram of Fethiye-Göcek Lake in 29.08.2014	75
Figure D.18.	The surface temperature variogram of Fethiye-Göcek Lake in 30.08.2014	75
Figure D.19.	The surface temperature variogram of Fethiye-Göcek Lake in 30.08.2014	75
Figure D.20.	The surface temperature variogram of Fethiye-Göcek Lake in 30.08.2014	76
Figure D.21.	The surface temperature variogram of Fethiye-Göcek Lake in 31.08.2014	76
Figure D.22.	The depth temperature error map of Fethiye-Göcek Bay	77
Figure D.23.	The depth temperature variogram of Fethiye-Göcek Lake in 23.08.2013	78
Figure D.24.	The depth temperature variogram of Fethiye-Göcek Lake in 24.08.2013	78
Figure D.25.	The depth temperature variogram of Fethiye-Göcek Lake in 25.08.2013	78
Figure D.26.	The depth temperature variogram of Fethiye-Göcek Lake in 26.08.2013	79
Figure D.27.	The depth temperature variogram of Fethiye-Göcek Lake in 27.08.2013	79
Figure D.28.	The depth temperature variogram of Fethiye-Göcek Lake in 30.08.2013	79
Figure D.29.	The depth temperature variogram of Fethiye-Göcek Lake in 31.08.2013	80
Figure D.30.	The depth temperature variogram of Fethiye-Göcek Lake in 02.06.2014	80

Figure D.31.	The depth temperature variogram of Fethiye-Göcek Lake in 03.06.2014	80
Figure D.32.	The depth temperature variogram of Fethiye-Göcek Lake in 05.06.2014	81
Figure D.33.	The depth temperature variogram of Fethiye-Göcek Lake in 06.06.2014	81
Figure D.34.	The depth temperature variogram of Fethiye-Göcek Lake in 07.06.2014	81
Figure D.35.	The depth temperature variogram of Fethiye-Göcek Lake in 27.08.2014	82
Figure D.36.	The depth temperature variogram of Fethiye-Göcek Lake in 28.08.2014	82
Figure D.37.	The depth temperature variogram of Fethiye-Göcek Lake in 29.08.2014	82
Figure D.38.	The depth temperature variogram of Fethiye-Göcek Lake in 30.08.2014	83
Figure D.39.	The depth temperature variogram of Fethiye-Göcek Lake in 30.08.2014	83
Figure D.40.	The depth temperature variogram of Fethiye-Göcek Lake in 30.08.2014	83
Figure D.41.	The depth temperature variogram of Fethiye-Göcek Lake in 31.08.2014	84
Figure E.1.	Temperature and Specific Conductivity vs Depth plots for Fethiye-Göcek Bay	85
Figure E.2.	Temperature and Specific Conductivity vs Depth plots for Fethiye-Göcek Bay (cont...)	86
Figure E.3.	Temperature and Specific Conductivity vs Depth plots for Fethiye-Göcek Bay (cont...)	87

SYMBOLS AND ABBREVIATIONS

$^{\circ}\text{C/C}$	Celsius Degree
%	Percent sign
σ	Sigma (Stefan-Boltzmann constant)
c	Speed of light
h	Planck's constant
K	Kelvin
R^2	Coefficient of determination
Kg / m^2	Kilogram Per Square Meter
Km	Kilometer
μm	Micrometer
m	Meter
mm	Milimeter
km^2	Square Kilometer
m^2	Square Meters
m^3/s	Cubic Meters Per Second
m/s	Metre Per second
EC	Electrical Conductivity
W	Watt
λ	Lambda
ρ	Rho
ε	Reversed Ze (Epsilon)
min	Minimum
max	Maximum
$\mu\text{S/cm}$	Micro Siemens Centimeter
pH	Negative Logarithm Of $[\text{H}^+]$
Ppm	Parts per million
EBK	Empirical Bayesian Kriging
RS	Remote Sensing
GIS	Geographic Information System
Vs	Versus
ETM	Enhanced Thematic Mapper

TIR	Thermal Infrared
TIRS	Thermal Infrared Sensors
OLI	Operational Land Imager
AVHRR	Advanced Very High Resolution Radiometer
NOAA	National Oceanic and Atmospheric Administration
MODIS	Moderate resolution Imaging Spectroradiometer
ASTER	Advanced Spaceborne Thermal Emission and Reflection Radiometer
SLSTR	Sea and Land Surface Temperature Radiometer
NASA	National Aeronautics and Space Administration
VIS	Visible-Infrared
NIR	Near-Infrared
SWIR	Short-wavelength Infrared
LWIR	Long-wavelength Infrared
SGD	Submarine Groundwater Discharge
CDT	Conductivity Depth temperature
T	Temperature
LST	Land Surface Temperature
TOA	Top Atmospheric Radiance
TDS	Total Dissolved Solids
MGM	Turkish State Meteorological Service
MTA	General Directorate of Mineral Research and Exploration
USGS	United States Geological Survey
U.S	United States
NY	New York
YSI 6600	Multi-Parameter Water Quality Sonde
HOBO	Data Logger
DN	Digital Number
UTM	Universal Transverse Mercator
WGS	World Geodetic System
GMT	Greenwich Mean Time
M	Radiance Multiplier
B	Radiance Add
K ₁	Thermal conversion constant for the band (W/m ² x ster x μm)
K ₂	Thermal conversion constant for the band (Kelvin)

Na	Sodium
Ca	Calcium
K	Potassium
Ca	Calcium
Mg	Magnezyum
HCO_3	Bicarbonete
Cl	Chloride
SO_4	Sulfate
SiO_2	Silica
NO_3	Nitrate
B	Boron
Al	Aluminum
Fe	Iron
Br	Bromine

1. INTRODUCTION

1.1. Research Goal and Questions

Evaluating physicochemical parameter of surface and ground/water is a key tool in water management. A number of in-situ water samples can be collected in the field, which can be time consuming and costly. In addition, if there exist few samples, spatial variability of the study area cannot be mapped accurately. Water temperature is one the most important physicochemical parameter to understand the intrusion of hot and/or cold spring in the water environment. Water temperature can also be estimated from satellite images (Landsat thermal infrared data). The accuracy of temperature estimated from these satellite image data is comparable to in-situ monitoring. Other important physicochemical parameters such as specific electrical conductivity, salinity and pH are also useful to validate the spatial distribution of the water parameters. The research goal is to find an appropriate methodology to estimate the water temperature and other physicochemical parameter using in-situ measurement and compare with remote sensing data in the Mediterranean region.

The research questions, according to the defined goal above will basically try to answer the following questions:

- Estimation of surface temperature from Landsat satellite thermal infrared image can be used to identify hot and cold spring?
- What kind of information can give us a high resolution surface and depth in-situ measurement? Can we find new discover of hot and cold spring in a large Lake and Bay in Mediterranean region?
- Can we determine the type of stratification of Lake Köyceğiz and Fethiye-Göcek Bay? Surfer 9. Data type transformations were implemented by Global Mapper v12. All other mapping and visualisation were done by ArcGIS 10.

1.2. Scope of the Study

This study is motivated by the physicochemical water parameter mapping and as well as to identify existing and new discover of hot and cold springs in the Mediterranean region (Köycegiz Lake and Fethiye-Göcek Bay) using in situ-measurement and remote sensing data. The study has three overall scopes:

1. To map surface and depth water physicochemical in-situ measurement using Empirical Bayesian Interpolation (EBK) method and identify hot and cold spring area;
2. To establish atmospheric/Geometric corrections of Landsat 8 Thermal images and transform the Digital Number to surface water temperature using RS and GIS software (ARCGIS 10.3.1);
3. To compare surface temperature with satellite images over different areas in the Mediterranean Region for an appropriate linear regression analysis.
4. Using the in-situ measurement the temperature stratification of Lake Köyceğiz and Fethiye-Göcek Bay was determined.

1.3. Thesis Outline

The general outline of the thesis is separated in the two main parts. The first part of the thesis covers three chapters which started with a general content describing the introduction, literature review the description of the study area. The second part of the thesis focus on the methodology applied and obtained results and conclusion.

Chapter 2 deals with the localization, general description of the geology and hydrogeology of the study area. Chapter 3, the first part deals with in-situ measurement and data mining. The second part mainly focused on the mathematical background of the interpolation technique and satellite thermal image analysis. The quality of the data is also discussed in this chapter.

Chapter 4 is dedicated to the result comparison based on the result derived from interpolation and LANDSAT 8 derived surface temperature. The depth vs temperature was plotted and evidence of thermal stratification for Lake Köyceğiz

was determined. Eventually, Chapter 5 ends up with conclusion, discussion, and recommendation and also suggests further areas of the study.

1.4. Literature Review

Water temperature in lakes, streams and coastal areas is an important indicator for several purposes (water quality, aquatic organism, land use, etc..) that is affected primarily by ground/surface water inputs (Brown and Krygier, 1970; Beschta et al., 1987; Poole and Berman, 2001; Hannah et al. 2008; Handcock 2012; Dörnhöfer and Oppelt, 2016). Water temperature change can be due to the anthropogenic effects and/or irrigation, energy production, transportation, fishery and also natural conditions. Table 1 show literature related to use for surface temperature products for monitoring purposes. Table 1 present also the literature for different types of temperature satellite sensors with coarse/fine resolutions on a daily basis. All authors agree that if there exist in-situ measurement, high accuracies can be achieved to predict the water temperature with different kind of instrumentations.

Table 1 1.Literature survey related to surface temperature estimation

Authors	Sensor	Range	Study Area	Time	Process
Torgersen et al. (2001)	Airborne thermal infrared	5 to 27 °C	Western and Eastern Oregon, USA	1999	Evaluating the physical factors that influence the accuracy of thermal remote sensing
Handcock et al. (2006)	MODIS, ASTER, LANDSAT T 7ETM+	Average temperature 17.2 ± 5.2 °C	Washington State, USA	2001-2002	Stream temperature estimation for different scales
Alcantara et al., (2010)	MODIS	12 to 35 °C	Brazil	2003-2008	Analyses of heat fluxes and calculation surface energy budget
Tonolla et al., (2010)	Thermal infrared Camera	7.4 to 30 °C	Alpine River floodplains Tagliamento, Italy	2004	TIR images to quantify surface temperature patterns at 12-15 minute interval over 24h cycles
Bresciani et al., (2011)	MODIS	0 to 30 °C	Lake Trasimeno Lake Garda, Italy	2005-2008 2004-2009	Temperature-Chla relationship

Politi et al., (2012)	AVHRR	0 to 30 °C	Lake Geneva, Switzerland Balaton, Hungary	1993-1996 2001-2005	Spatial distribution of temperature for European Lakes
Simon et al., (2014)	Landsat ETM+	4 to 25 °C	Lake Barriousses, Lake Bimont, France	2009-2013	Historical prediction of temperature for different lakes
Tamborshi et al. (2015)	Airborne thermal infrared (TIR)	17 to 23 °C	Long Island, NY, USA	2013-2014	Investigate submarine groundwater discharge (SGD)
Liu et al, (2016)	Airborne thermal infrared (TIR)	9 to 20 °C	Heihe River, China	2012	Investigate surface groundwater interaction

Temperature and specific conductance are the two environmentally friendly used physicochemical parameters. Surface water temperature is a key physical parameter to monitor fundamentals of water. Specific conductance of water is also an essential chemical parameter that measure the ability of a water to conduct electricity at a specific temperature. Especially, these two parameters can be used to detect hot/cold water inputs in sea, lakes and rivers.

Williams (1976) stated that underwater thermal springs can be found far away from the coastal line and depth water. However, he told also that there could exist also some springs near the coastal areas.

The study of groundwater discharge (hot/cold springs) into sea/lake via coastal or submarine outflows began to come out in the literature at the beginning of 1990s (Moore, 1996; Younger, 1996). The identification of the submarine groundwater discharge is also stated as very complicated and need specific techniques such as aerial thermal remote sensing or oceanographic surveying (Kazami, 2008).

Manga (1998), in his study record water temperature at springs in Oregon Cascades area. In this study, the surface water heat flux was compared with the regional groundwater heat flux. Anderson (2005) stated in his study that water temperature is an essential tracer to evaluate the groundwater system.

Torgersen et al. (2001) studies that the field of research about the remote sensing technology to predict the temperature is a very young and unexplored.

Baena (2008) has taken periodic in-situ measurement of water temperature and electrical conductivity values of a karstic springs located in Spain in order to evaluate the dynamics of the karstic system. He stated that the temperature and electrical conductivity had to be evaluated together.

Other studies about the groundwater temperature is done by Long (2009). He studies about groundwater modeling and calibrate the model with water temperature. Luhman (2011) show results that aquifer geometry can be predicted by using precipitation- temperature classification. He shows also that the temperature can be used as a tracer.

Mejias et al. (2012) stated that “The discharge of groundwater into the marine environment occurs when coastal aquifers possess a hydraulic connection with the sea and a great hydraulic head. Most discharges occur either on the coastline or the continental shelf and tend to concentrate few hundred meters from the coast.”

There are over a hundred lakes in Turkey. Most of them locates in the area known as the Lake District in southwestern Turkey. The area includes saline and freshwater lakes. These lake systems can be formed during the Pleistocene period or can be the remnants of a central Anatolian lake (Kazancı et al. 2004). In Turkey, the most important studies about the study area is done by Bayarı (1995). In this study, they discover that Koycegiz Lake is a meromictic lake and has a two thermocline level. They also emphasize in their study the importance of water recharge at the bottom of the lake. Kazancı and Girgin (2001) work on thermal spring’s hydrogeochemistry at Dalaman and Koycegiz. Another very important literature is done by Gökgöz and Tarcan (2006). They discover that the water temperature varies between 24 to 41 °C and enrich with Na, Ca. They also emphasize that lake water is influenced by thermal water inputs.

The latest work is done by Avsar et al. (2015) and Avsar et al. (2016). They collected 55 water samples from inland and coastal of Muğla. They found that 16 are geothermal and 10 are mineral water sources. The temperature of the water ranges between 18.3 and 39.2 °C. At the south west part of Koycegiz Lake (Sultaniye, Delibey, Kelgirme) the temperature of water is found hot. Near the Fethiye town, they also found a thermal spring called as Girmeler. The water properties in the region, according to laboratory analysis is given in Table 2.

Table 1 2.Chemical analysis results of Köycegiz Bay waters according to Avsar et al. (2016)

Location	Sultaniye-1	Sultaniye-2	Sultaniye-3	Kelgirme	Delibey-1	Delibey-2
X	642788	642853	642805	645593	644920	644921
Y	4082305	4082265	4082293	4078489	4080156	4080156
T (°C)	19.7	39.2	37	36.9	29.9	30.5
pH	7.29	6.45	6.54	6.39	6.81	6.3
TDS (ppm)	3419	25698	22965	29437	9885	27300
Na (ppm)	818	6904	6043	7808	2503	7344
K (ppm)	42	387	335	442	140	561
Ca (ppm)	255	1543	1436	1802	734	1465
Mg (ppm)	111	877	732	1031	363	907
HCO ₃ (ppm)	276	347	299	318	353	292
Cl (ppm)	1672	13584	12203	15697	4997	14549
SO ₄ (ppm)	228	1936	1811	2205	742	2088
SiO ₂ (ppm)	7	18	17	15	11	18
NO ₃ (ppm)	1	9	0	31	12	21
B (ppm)	0	4.6	3.6	0	1.4	4.4
Al (ppb)	124	886	0	487	234	5213
Fe (ppb)	230	1397	0	1269	460	7933
Br (ppb)	5	39	28	43	14	37
Water type	Na-Cl	Na-Cl	Na-Cl	Na-Cl	Na-Cl	Na-Cl

There exist several studies about water quality monitoring using remote sensing. Remote sensing data are used to extract some information about water quality such as suspended soils, chlorophyll a (Chawira et al., 2013; Dube et al., 2014; Kibena et al., 2013; Verstraete et al., 1999).

Remote sensing give also special importance to the water management for different kind of application for water monitoring. Spatio-temporal information can be used using different electromagnetic band spectrum Landsat 8 satellite is recently launched in February 2013. It provides remote sensing data at high spatial resolution using the Operational Land Imager (OLI) and the thermal infrared sensors (TIRS). TIRS bands measure radiance at 100 m spatial resolution using two bands (10 and 12 μm). They are resampled to 30 meters to match OLI multispectral bands (Lamaro et al. 2013). Landsat 7 ETM+ satellite providers also a remote sensing TIR image in the range 8 to 15 μm. However Landsat 7 ETM+ has one band of TIR image. The TIR band has a spatial resolution of 60 m. The image was processed after 25 February 2010 and resampled to 30 meter/pixel. Landsat 7 ETM+ and Landsat 8 OLI TIR

bands has been newly applied in the last 10 year to predict Land Surface Temperature (LST) (Vlassova et al. 2014).

In this thesis, a new method of Kriging is used also to interpolate in-situ measurement (temperature, electrical conductivity, etc...) which named as Empirical Bayesian Kriging which was developed by Krivoruchko (2011). Empirical Bayesian Kriging method used a Bayesian rule to predict several variogram instead of single semi-variogram.

The present study focuses on determining possible hot/cold spring of Lake Koyceğiz and Fethiye-Göcek Bay by in-situ measurements and comparisons with Landsat 8 images (thermal bands). All the spatial interpolations maps were done using Empirical Bayesian Kriging (EBK) method and its results were correlated by in-situ measurements. By using spatial interpolation maps, remote sensing images result the evidence of the possible cold and hot areas were presented by EBK interpolation maps.

There exist several studies about water quality monitoring using remote sensing. Remote sensing data are used to extract some information about water quality such as suspended soils, chlorophyll a (Chawira et al., 2013; Dube et al., 2014; Kibena et al., 2013; Verstraete et al., 1999).

2. STUDY AREA

2.1 Localization of the Study Area

The Study area is located at the south and southwest part of Turkey in Muğla region. It is just the corner of the Aegean and Mediterranean Sea (Figure 2.1). The altitudes vary up to 2265 meters for Köyceğiz watershed and 1951 meters for Göcek watershed. According to 30 year temperature measurement of meteorological station in the region of Muğla, annual mean temperature observed as 15 °C. The long term summer mean temperature observed at 25 °C degrees and the winter mean temperature is observed at 6 °C degrees. The annual mean precipitation is as 1159.2 mm. Muğla region is also one of the areas that has the highest annual precipitation rate in Turkey. Mean annual meteorological values between 1950 and 2015 is given in Table 2.1 (Anonymous, MGM, 2015).

Table 2 1.Mean annual meteorological values between 1950 and 2015 in Mugla Station.

MUGLA	Jan.	Feb.	Mar	Apr	May	June	July	Aug.	Sep.	Oct.	Nov.	Dec
Mean annual between (1950 - 2015)												
Mean Temperature (°C)	5.5	6.1	8.5	12.5	17.6	22.9	26.3	26.1	21.7	15.9	10.5	7
Mean Maximum Temperature (°C)	10	11	14.3	18.7	24.3	29.8	33.5	33.6	29.4	23	16.5	11.5
Mean Minimum Temperature (°C)	1.6	1.9	3.6	6.9	11.2	16.1	19.7	19.7	15.2	10.1	5.7	3.2
Average sun day (hour)	3.4	4.4	5.5	7.2	8.4	10.3	11.2	11	9.3	7	4.5	3.2
Average total day rainfall	14.9	13	11.1	9.5	8	3.7	1.7	1.3	2.7	6.6	9.9	14.6
Mean total rainfall (kg/m ²)	233.8	176.2	119.9	65.4	50.1	23.4	7.8	8	18.6	68.3	138.9	259
The minimum and maximum temperature between 1950 - 2015												
Maximum Temperature (°C)	20.9	21.2	28.8	31.2	35.7	40.8	42.1	41.2	38.8	35	27.6	20.8
Minimum Temperature (°C)	-11	-9.9	-8.5	-3.6	1	6.7	10.5	10.9	5.6	0.2	-6.1	-8.4

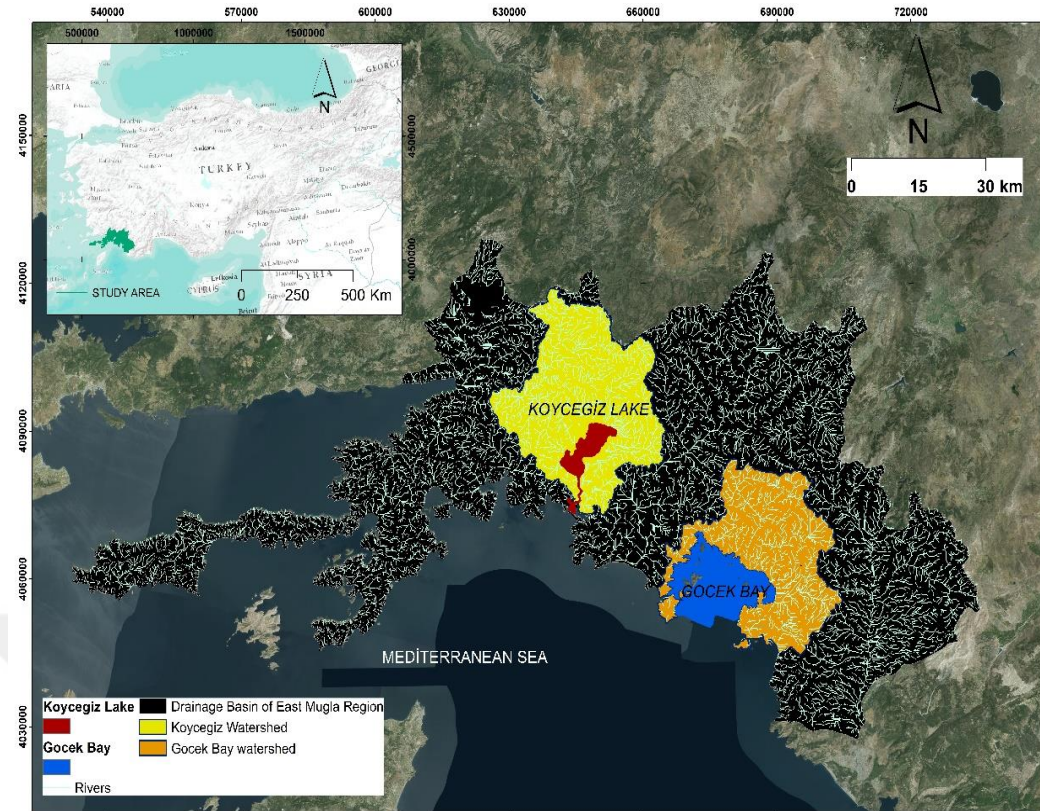


Figure 2 1.Localization of the Study Area.

The first study area is located near the Köycegiz region. The name of the lake is taken as the village name. The total square area of Köycegiz Lake and of the lagoon is approximately 830 km² and 130 km². Köycegiz Lake is directly connected through surface water in the lagoon and further into the Mediterranean Sea by the lagoon and its various branches. There are total 3 main rivers across the lake who's recharging the lake. The highest flow rate river is named as Namnam River, located at the south west part of the river (Figure 2.1). The discharge of the Koycegiz Lake is 33 m³/s according to Bayari et al. (2001). Alagöl and Sülüngür lakes are also inside of the lagoon and it's a branch of Dalyan Channel. Köycegiz Lake and Dalyan Lagoon, declared as a special protected area in 1988 with a diverse type of species. The Caretta Caretta turtles and the ruins of the Accient City of Caunos and Lycian rock tombs are found near the river (Gurel et al., 2005).

Göcek-Feyhiye Bay is located near the Göcek and Fethiye village. A Göcek-Fethiye watershed is about 450 km². The main geological formations are: various kinds of limestones, green rocks, such as serpentine, and alluviums. The main tectonic and

morphological characteristics are the numerous faults, karsts and flood cones. The altitude varies up to 1951 m.

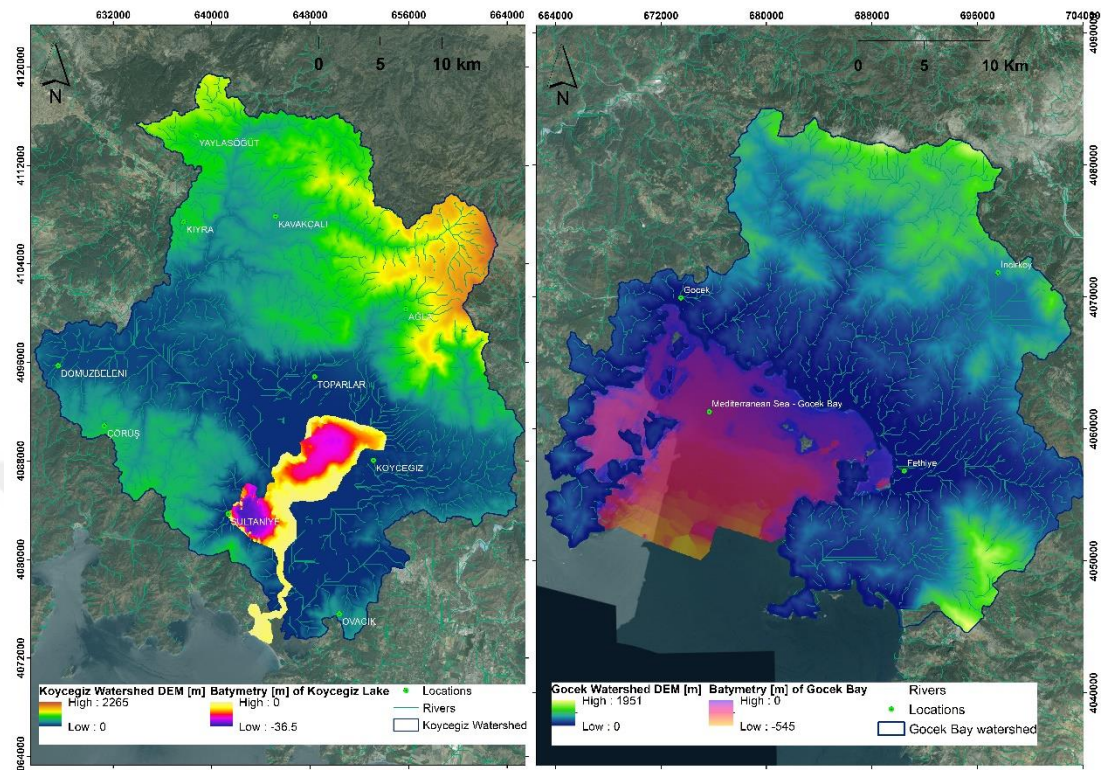


Figure 2 2.Digital Elevation Model and Bathymetry Map of the Study Area.

A general view of Köyceğiz Lake and Fethiye- Göcek Bay is given in Figure 2.3 and Figure 2.4.

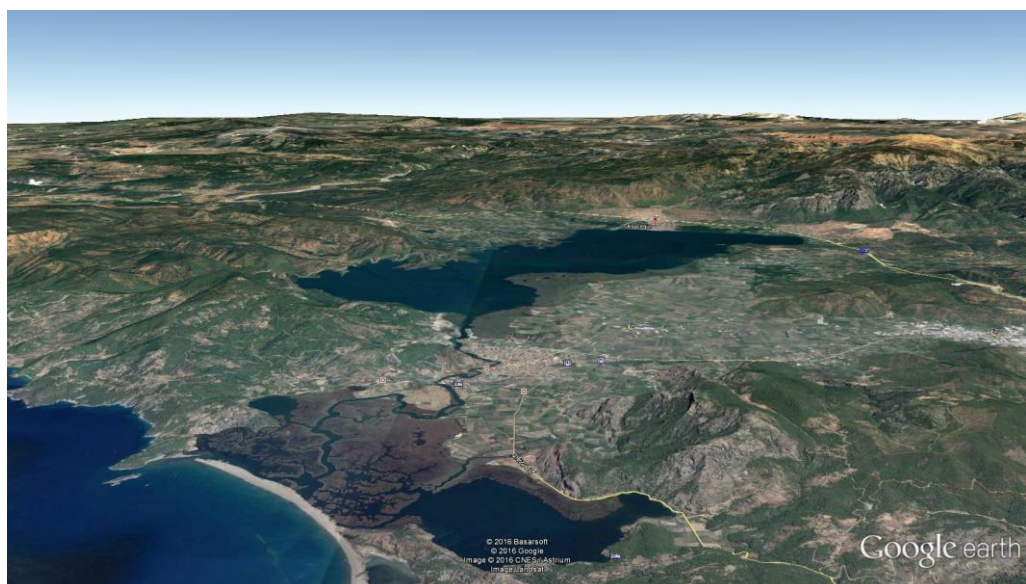


Figure 2 3.A general view of Köyceğiz Lake from Google Earth

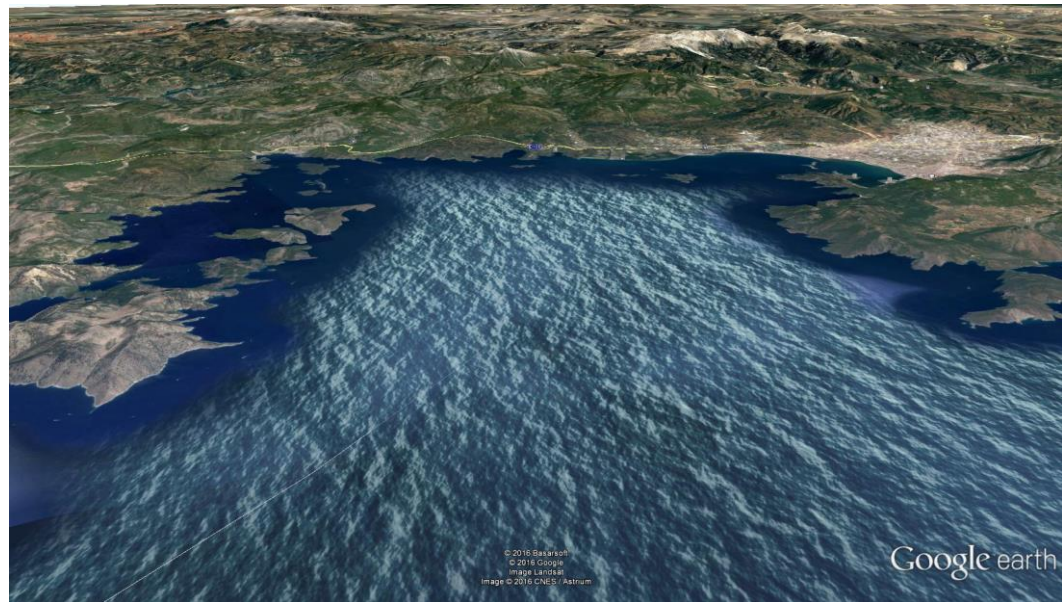


Figure 2 4.A general view of Fethiye-Göcek Bay from Google Earth

2.2 Geology/Hydrogeology of the Study Area

Turkey has a complex geological evolution due to its geographical and geological position between Eurasian, Pan African and Arabian plates. There exist several literature and discussion about the geology/hydrogeology of the study area (Collins and Robertson 1997; 1998; 1999; 2003; Gessner et al., 2001a; 2001b; 2001c; Candan et al., 2001; Whitney and Bozkurt, 2002; Sözbilir et al, 2011; Tansug and Oztunali, 1976; Gunay and Bayari, 1989; Kazancı et al., 1992).

The geology in this region is mainly composed of allochthonous and autochthonous Flysch and karstic facies overlain by plio-quaternary sediments (Graciansky, 1968). Due to tectonic activities, several faults were formed in this area. Details about the geology and more maps can be found in Bayari et al. (1995). The Dalaman, Sarisu, Tersakan, Namnamcay and Yuvarlakcay rivers are the major surface waters in the study area. The Namnamcay River flows within the ophiolitic melange of the Marmaris nappe and its flow is negligible during summer. Most of the discharges of the Dalaman and Namnamcay rivers are supplied by karstic discharges from the allochthonous limestones of the Lycian nappes (Bayari et al., 1995). The Namnamcay and Yuvarlakcay rivers, rain and alluvial groundwater (Bayari et al., 1995) and discharged to the Mediterranean Sea by the Dalyan Channel.

Köycegiz Lake is composed of two water layers, with the boundary between the two layers being around 12 m from the surface. The bottom water chemistry is similar to thermal water in Sultaniye due to thermal groundwater discharges located at the lake bottom, whereas the upper layer water chemistry is similar to fresh water (Bayarı et al., 1995, 2000). According to the lake water balance equation Bayarı et al. (1995) stated that the amount of water must be supplied by the lake bottom springs.

The mountains of the Fethiye-Göcek watershed are mainly covered by karstic areas and groundwater is coming from the carbonate aquifers. The main rivers are Değirmendere, Karacasu, Cerci and Kargı and Eldirek rivers. Groundwater is used also for irrigation and drinking water purposes in the area. Major aquifers for cold groundwater in the study area are found in the brackish and locally karstic limestones of the Lycian nappes and Quaternary alluvium. The cold springs discharge from the contact between limestone and alluvium or ultramafic and alluvium (Yesertener, 1986). In this study, MTA (2002) maps are used and shown in figure 2.5.

We can divide the geological formations according to the hydrogeological point of view as fallow:

The permeable formations are mainly composed with limestones. The study area covered by Triassic, Cretaceous and Eocene limestone. The alluvium also is considered as permeable formation in the area. Semi- permeable formation are schistous sandstones, sandstone. The area is covered by Eocene Flysch. The impermeable formations are considered as peridotite and basalt.

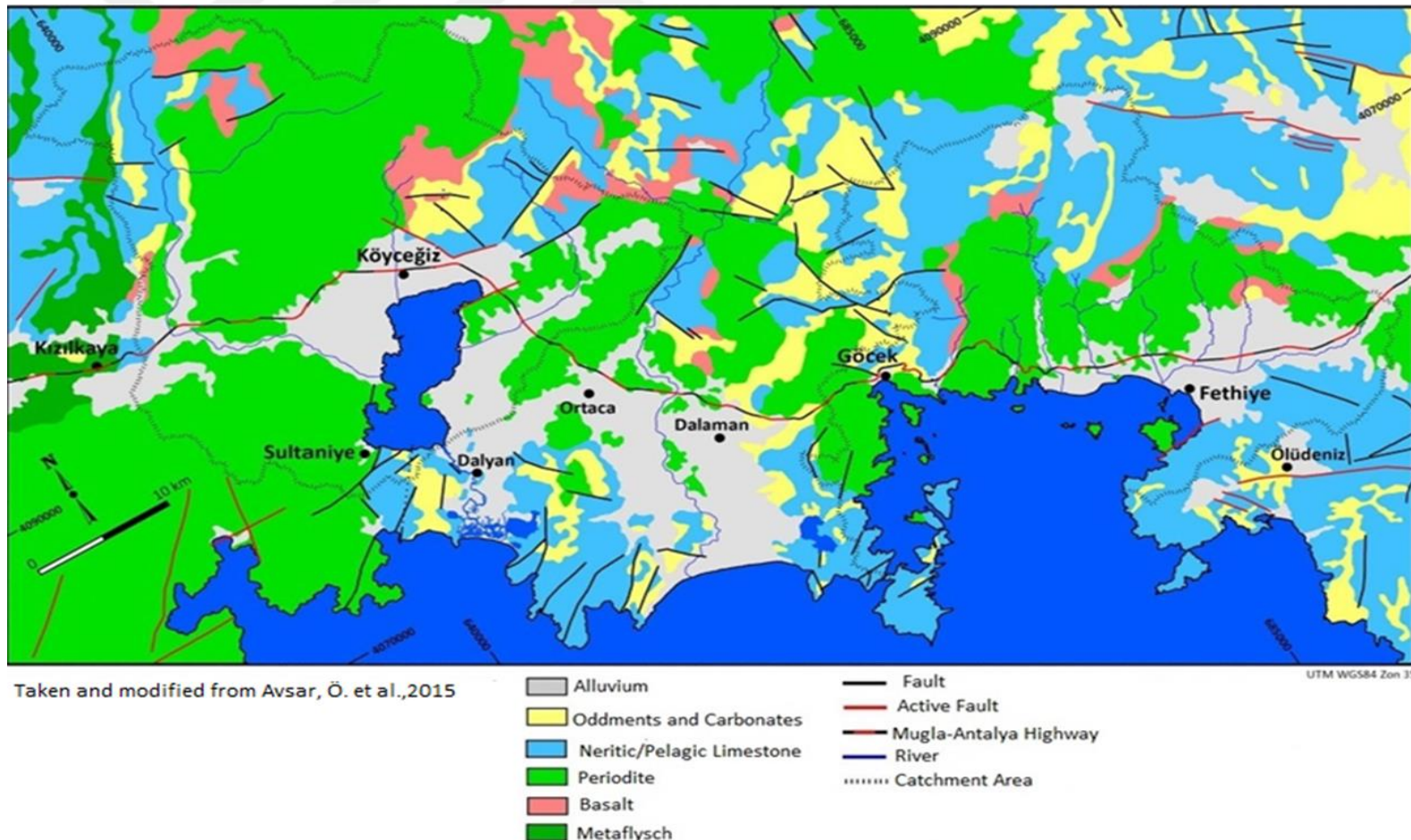


Figure 2.5. The detailed geological map of Study Area

3. RESEARCH METHODOLOGY AND MATERIAL

3.1. In-Situ Measurement

Using Mugla Sıtkı Kocman University geological engineering floating platform (Fig3.1), specific conductance, temperature, pH and depth values were measured with the YSI 6600 and Horiba U2 devices in surface and depth of Lake Köyceğiz and Fethiye-Göcek Bay at specific grid (Fig 3.2). When the depth of the water and the coordinates were measured by GPS. The in-situ measurement details are given in Table 3.1.



Figure 3 1.Muğla Sıtkı Kocman University floating platform (Avsar et al., 2015)

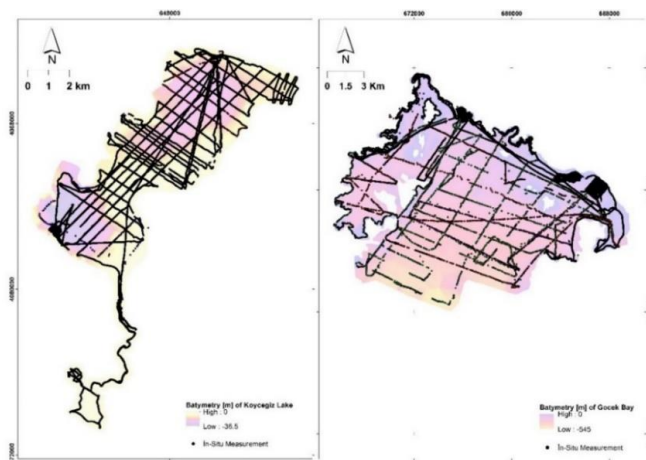


Figure 3 2.Specified in-situ measurement grid

Table 3 1.In-Situ measurement information (Avsar et al., 2015)

Date	Parameters		Satellite Availability (Landsat 8)	In-Situ Measurement time interval	
	Surface Temperature	Depth CDT		Start	End
19.07.2013	+	+	-	08:45	13:28
20.07.2013	+	+	-	07:34	15:34
22.07.2013	+	+	-	10:29	18:23
23.07.2013	+	+	+	08:32	17:43
24.07.2013	+	+	-	09:39	12:23
25.07.2013	+	+	-	11:55	14:19
26.07.2013	+	+	+	09:27	10:27
18.08.2013	+	+	-	11:16	18:22
19.08.2013	+	+	-	11:33	14:28
20.08.2013	+	+	-	11:05	14:26
23.08.2013	+	+	-	12:42	16:09
24.08.2013	+	+	+	13:51	18:02
25.08.2013	+	+	-	12:37	18:07
26.08.2013	+	+	-	11:33	18:07
27.08.2013	+	+	-	10:30	19:14
28.08.2013	+	+	-	11:03	17:04
29.08.2013	+	+	-	13:18	17:26
30.08.2013	+	+	-	09:31	16:32
31.08.2013	+	+	-	09:43	15:17
2.06.2014	+	+	-	12:27	19:31
3.06.2014	+	+	-	09:19	19:12
5.06.2014	+	+	-	08:50	19:18
6.06.2014	+	+	-	09:10	19:45
7.06.2014	+	+	+	08:46	19:17
27.08.2014	+	+	+	09:59	19:53
28.08.2014	+	+	-	10:53	17:59
29.08.2014	+	+	-	10:00	16:55
30.08.2014	+	+	-	09:26	19:07
31.08.2014	+	+	-	10:20	15:22

CDT : Conductivity, Depth, Temperature

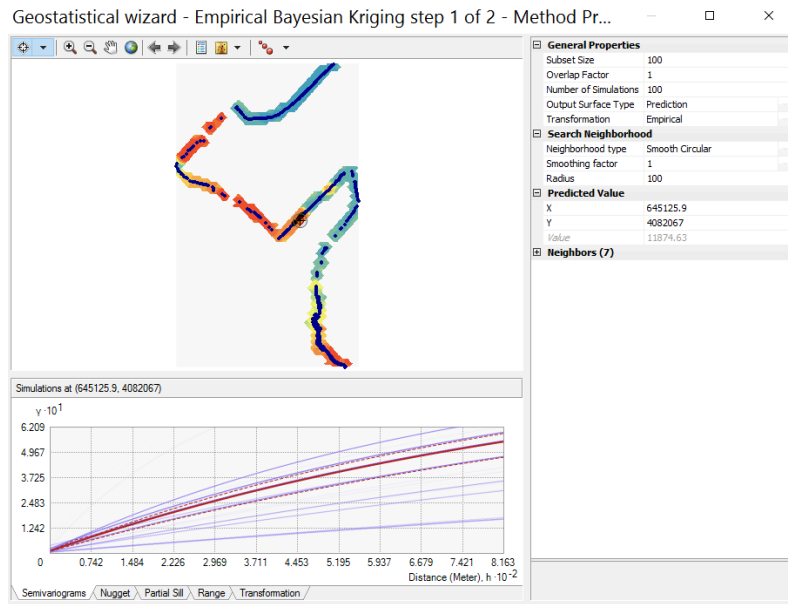
3.2 Interpolation Methodology: Empirical Bayesian Kriging

Empirical Bayesian Kriging is a geostatistical interpolation method that automates the difficult aspects of building a valid kriging model. Other kriging methods require to manually adjust parameters, but EBK automatically calculates these parameters through a process of subsetting and simulations (Chiles and Delfiner, 1999). EBK method can handle moderately nonstationary input data estimates and then uses many semivariogram models rather than a single semivariogram. EBK accounts for the error introduced by estimating the underlying semivariogram through repeated simulations (Finzgar et al., 2014).

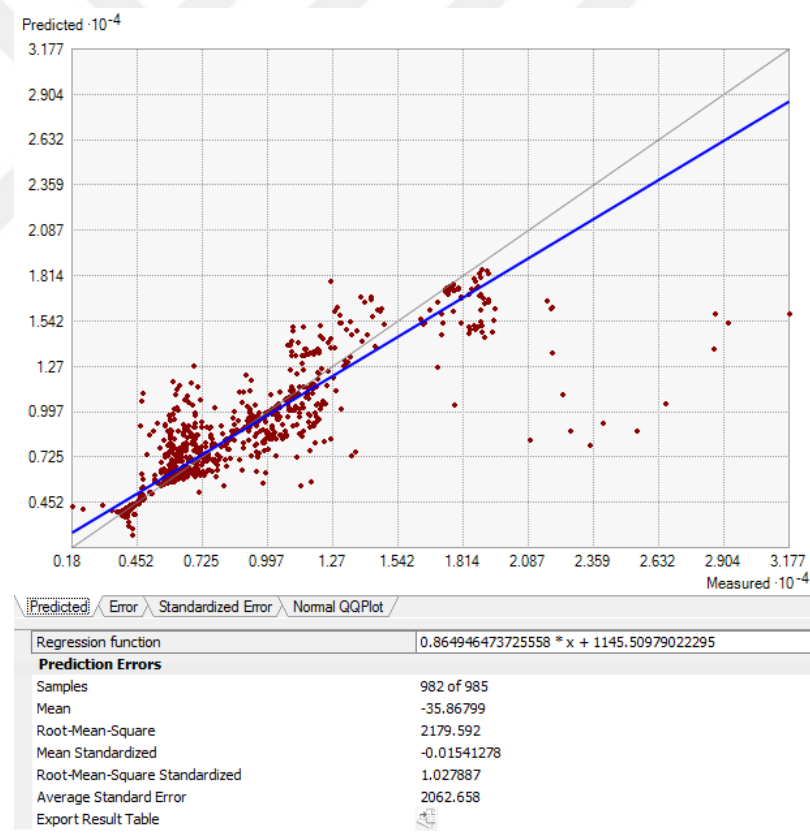
EBK method is based on 3 main steps: Firstly, a semivariogram model is estimated from the observed data set. Secondly, a new value is simulated at each of the observed data locations by using the semivariogram estimated on the previous step. Thirdly, a new semivariogram model is estimated from the newly simulated data at the second step. By using Bayes' rule, a weight for this semivariogram model is calculated which shows how likely the observed data can be generated from the semivariogram. Second and third steps are repeated. This process creates a spectrum of semivariograms (Pilz and Spöck, 2007). New parameters are needed also for EBK such as subset size which defines the number of points in each subset, overlap factor which specifies the degree of overlap between subsets and number of simulation which specifies the number of semivariogram that will be simulated for each subset.

3.2.1. EBK Process

For the creation of semi-variogram cloud in EBK; subset size, overlap factor, the number of simulations, maximum neighbors, minimum neighbors and radius (m) are determined by order: 100, 1, 100, 50, 25 and 100. The solid line semi-variogram cloud shows the best performance for the obtained results. Cross validation results also derived for each interpolation and used to select for best fit (Fig 3.3).



a. Semi variogram cloud according to bayesing kriking (solid line show the best fit semi-variogram)



b. cross validation and best fit results

Figure 3 3.An example of EBK interpolation for a. semi variogram cloud b. cross validation results and best fit

3.3. Thermal Infrared (TIR) Remote Sensing

Understanding the temperature of ocean, sea, lakes, and rivers are crucial for understanding the hydrosystem (Flipo et al. 2014, Vilmin et al. 2016). The temperature data coming from ships buoys and other type instruments can be very expensive and were very insufficient to characterize the area. The spatial resolution (pixel size) of remote sensing technology has recently developed and have the possibility to fill the gap to collect the spatial data. Table 3.1 shows the currently available TIR imaging satellites with their pixel size.

Table 3 2.TIR imaging for different type of satellites

TIR Satellites	Pixel size [m]	Source
Landsat 7 and 8	100, 60 (30)	NASA (2013a)
ASTER	90	Satellite Imaging Corporation (2013a,b)
MODIS	250,500,1000	NASA (2013b)
AVHRR-NOAA	1100	NOAA (1997)
Sentinel-3A SLSTR	1000	COPERNICUS (2016)

Landsat-8 was successfully launched on 11 February 2013 and deployed into orbit with two instruments on-board: (1) the Operational Land Imager (OLI) with nine spectral bands in the visual (VIS), near infrared (NIR), and the shortwave infrared (SWIR) spectral regions; and (2) the Thermal Infrared Sensor (TIRS) with two spectral bands in the LWIR. The relative spectral response of the TIRS bands is presented in Figure 3.4 The spatial resolution of TIRS data is 100 m with a revisit time of 16 days, and as a result, applications are different than those of other sensors with coarser spatial resolutions and shorter revisiting times. Landsat-8 images are already freely distributed through the U.S. Geological Survey (USGS) (Figure 3.5).

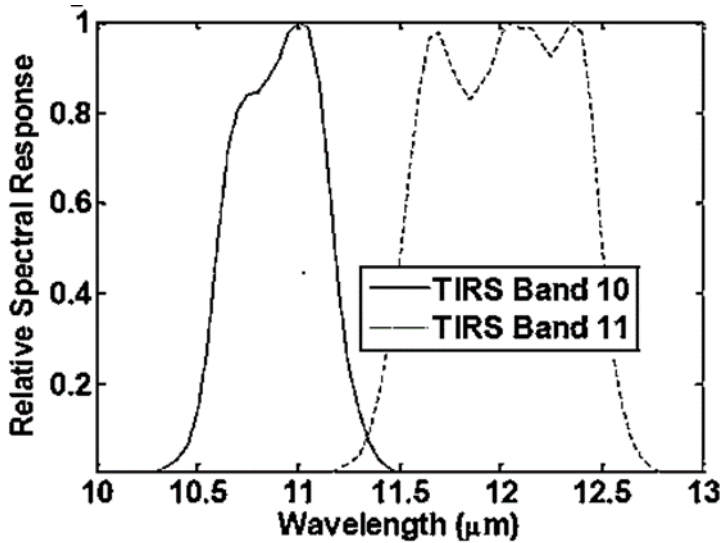


Figure 3.4.Landsat 8 Spectral response function

The satellite instrument measures the emitted thermal and/or reflected solar energy of/by the earth and expresses the intensity measured in each part of the spectrum (the ‘bands’ of the instrument) as a Digital Number (DN). This DN of each image pixel is the characteristic output of the satellite instrument. High DN values represent high intensities, while low DN values represent low intensities (USGS, 2016).

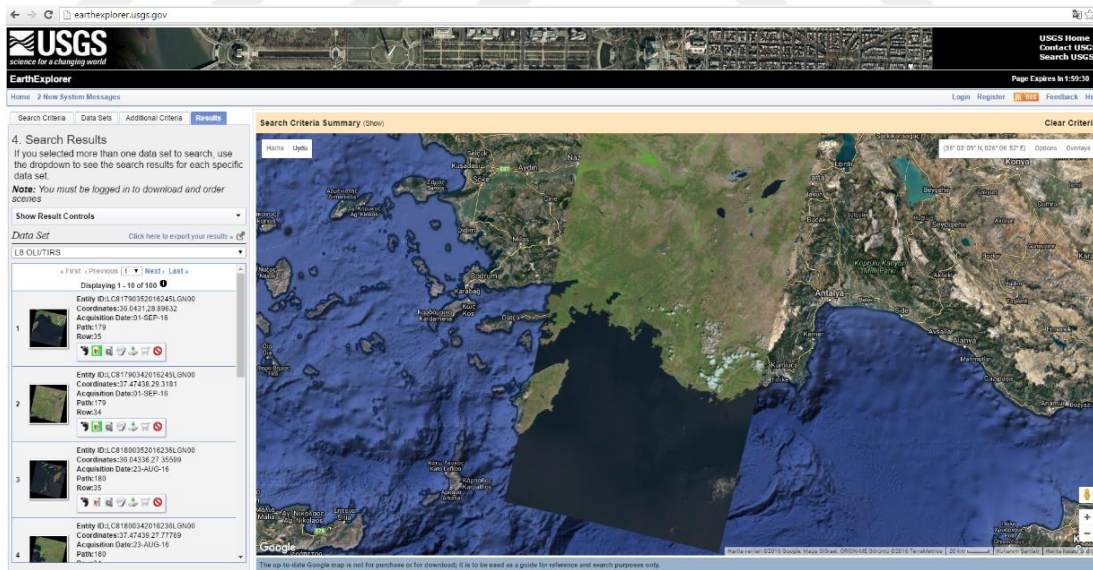


Figure 3.5.An example view of Landsat 8 download web page (<http://earthexplorer.usgs.gov/>)

The dataset used in this study included images is presented in Table 3.2. The metadata used for Landsat 8 TIR for Band10 is given in Table 3.3. For Landsat 8, bands 10 are used to estimate the temperature data value of each pixel in the image.

All Landsat images were further rectified to a common Universal Transverse Mercator (UTM) WGS 84 coordinate system. Table 3.4 give the temperature values at the time of accruing the images.

Table 3 3.Details describing selected LANDSAT 8 scenes

Landsat 8 Name	Acquisition date	Cloud Cover (%)	Sun Elevation	Sun Azimuth
LC81790352013204LGN00	23.07.2013 10:42:46 GMT+2, K	1.10	65.00	123.46
LC81800342013211LGN00	30.07.2013 10:48:35 GMT+2, K	0.06	63.23	128.85
LC81790342013236LGN00	24.08.2013 10:42:27 GMT+2, G	1.16	57.80	139.42
LC81790352014159LGN00	08.06.2014 10:40:28 GMT +2, G	14.20	67.80	120.22
LC81790352014239LGN00	27.08.2014 10:40:53 GMT+2, G	0.08	57.75	137.96

G: Göcek-Fethiye; K: Köyceğiz Study area

Table 3 4.Metadata for Landsat 8 TIR for Band 10

	Band 10
Radiance Multiplier (M)	0.0003342
Radiance Add (B)	0.1
K1 (watts/meter ² x ster x μm)	774.89
K2 (Kelvin)	1321.08

Table 3 5.Temperature values at the capture time (hourly temperature average of 10:00-11:00) of the LANDSAT 8 images.

Landsat 8 Name	Acquisition date	Mugla Meteorological Station (°C)	Köyceğiz Meteorological Station (°C)	Fethiye Meteorological Station (°C)
LC81790352013204LGN00	23.07.2013 10:42:46 GMT+2, K	32.00	35.40	35.35
LC81800342013211LGN00	30.07.2013 10:48:35 GMT+2, K	34.70	36.90	37.00
LC81790342013236LGN00	24.08.2013 10:42:27 GMT+2, G	30.95	34.45	34.25
LC81790352014159LGN00	08.06.2014 10:40:28 GMT+2, G	28.00	28.40	28.50
LC81790352014239LGN00	27.08.2014 10:40:53 GMT+2, G	34.90	36.00	32.50

G: Göcek-Fethiye; K: Köyceğiz Study area, all meteorological station are located in the city center.

3.3.1. Mathematical Background For TIR Remote Sensing of Surface Water

In Figure 3.6 a flowchart with a recommended processing procedure for TIR images is presented (Handcock, et al., 2012).

The methodology to convert Digital Number (DN) of the TIRS to temperature value can be done first by converting DN to Top Atmospheric Radiance (TOA) and then using TOA values, brightness temperature can be calculated as shown in Eq. (1) and Eq. (2). Table 2 shows the parameters that are needed for brightness temperature calculations.

$$\text{TOA} = M \times \text{DN} + B \quad (1)$$

Where; M: is the Radiance Multiplier

B: is the Radiance Add

TOA is the spectral radiance in W/ (m² x ster x um)

$$\text{TB (Kelvin)} = K_2 / (\ln(K_1 / \text{TOA} + 1)) \quad (2)$$

Where K₁ and K₂ are parameters of band specific thermal conversion constant. TB is brightness temperature in Kelvin.

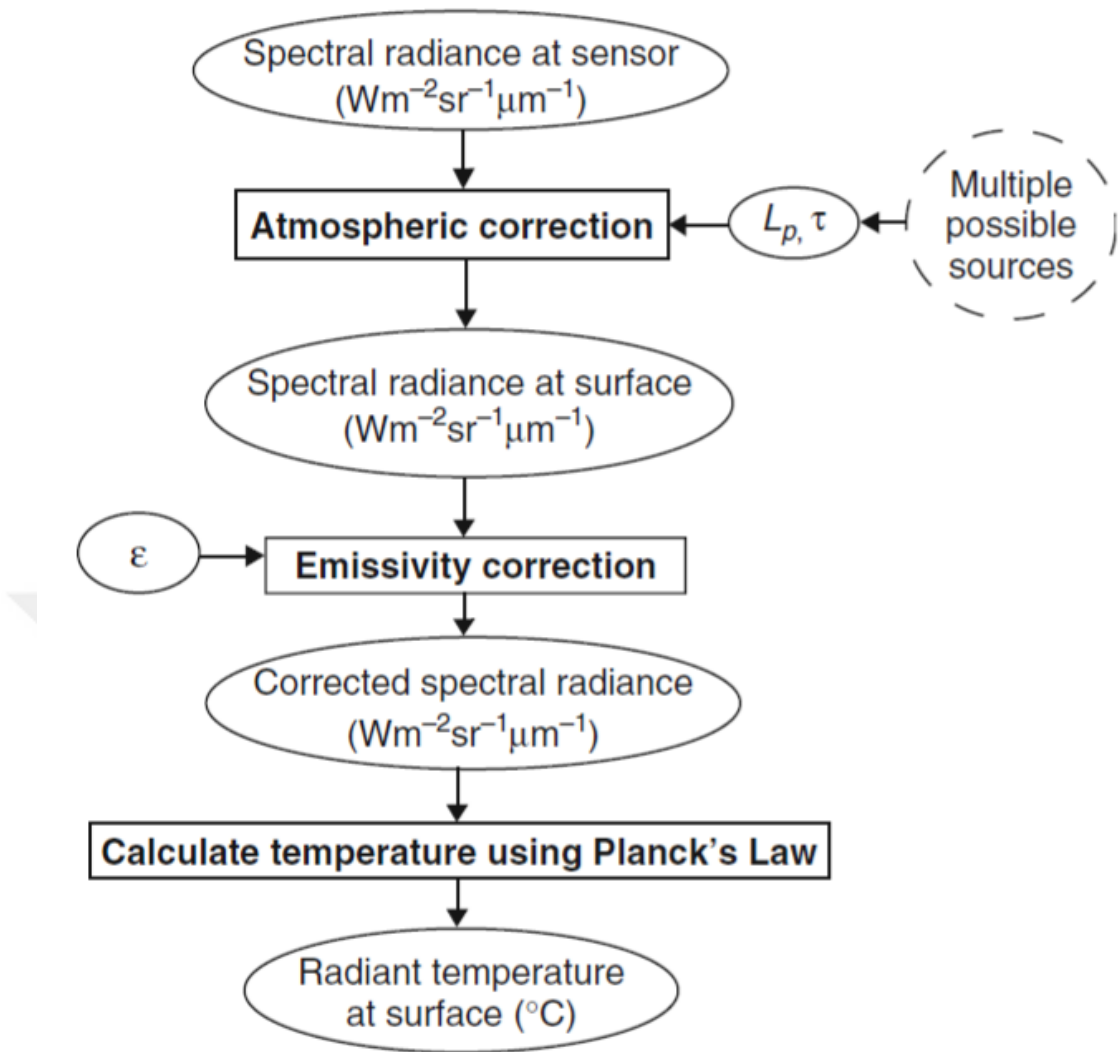


Figure 3.6.Suggested flowchart for Landsat 8 image processing (Handcock et al., 2012)

The temperature values obtained by TB are for black body. Therefore, the emissivity (ϵ) become necessary according to the nature of land cover. Land Surface Temperature can be calculated using Eq. (3) by using an average emissivity values for water ($\epsilon_{\text{water}} = 0.98$) as stated in Du et al. (2015).

$$T = \frac{TB}{(1 + (\lambda + TB/\rho) \times \ln \epsilon)} \quad (3)$$

λ =wavelength of emitted radiance ($\lambda = 11.5 \text{ um}$ for Landsat 7, $\lambda = 10.8 \text{ for Landsat 8 Band 10}$, $\lambda = 12 \text{ for Landsat 8 Band 11}$) (Markham and Barker, 1985)

$\rho = h * c / \sigma$ ($1.438 \times 10^{-2} \text{ m K}$), $\sigma = \text{Boltzmann constant}$ ($1.38 \times 10^{-23} \text{ J/K}$), $h = \text{Planck's constant}$ ($6.626 \times 10^{-34} \text{ J s}$), and $c = \text{velocity of light}$ ($2.998 \times 10^8 \text{ m/s}$).

The brightness temperature is calculated in degree Kelvin. Then, the temperature values can be convert in degree Celsius by subtracting 273.15° from degrees Kelvin. All these calculation are done using ArcGIS platform (ESRI, 2013).

Except minimum and maximum values, Geo-ANFIS provided more accurate results than Kriging for ⁶⁵Cu and ⁷⁵As.

3.4 Advantages, Disadvantages and Limitations of TIR Remote Sensing Methods

The potential of remote sensing for water management is generally well known. However, there are also some studies indicate a number of disadvantages. In order to better understand the potential of remote sensing, the advantages and disadvantages are summarized in Table 3.5.

Table 3.6. Advantages and disadvantages of TIR remote sensing

	Advantages	Disadvantages
Data Collection	Data can be collected from local to regional scale	The temporal image is limited
	The image are generally continuous and repeatedly, The image can be free of use and low cost	The image can be cloudy.
Image processing	If there exist no measurement of temperature in the field, the temperature pattern can be obtained from the data	Expert knowledge is required to interpret the data, Corrections of temperature can be time consuming and expensive due to commercial programs
Applications	The study area can be measured repeatedly	The surface temperature may not be representative. The Land body can influence the water body.
	The images are consistent and it can be used for calibration of models	The spatial resolution of image can be not sufficient to interpret for different scales. TIR measurement can only measure at the top layer of the surface.

The limitation of the airborne technology also is a discussion subject in the literature. The spatial resolution of the image determine the delineation of water body to the coastal site. Temporal resolution of satellite is limited and revisit time of a satellite depend on the orbit. Another limitation is the pixel size. The pixel size have an influence of the data and cause a heterogeneity of land and water. There is also effect

of other surface, object which can be found at the study area. Atmospheric absorption and scattering limits the accuracy of measure of the temperature.

3.5 Sensitivity Analysis

A sensitivity analysis also is needed to understand the uncertainty contribution of external and internal factors to approximate the water temperature distribution. The sensitivity analysis show that external and internal factor which influence on uncertainty could be reasonable and the results is not change extremely for this study. Unfortunately, all factors could not be analyzed due to time limitation of the thesis however the factor which can be influences the uncertainty by the literature is given in Table 3.6.

Table 3.7. An overview of the uncertainty analysis for internal and external factor to calculate temperature prediction

Influence factor	Type of factor	Estimated Bias for temperature (°C)
Atmospheric Correction	External	± 0.5 (1.5°C at coastal part)
Emissivity	External	± 0.5 °C
Surface effects	External	± 2-3 °C
Measurement error of Satellite	Internal	± 0.6 °C
Measurement error of data logger	Internal	± 0.22 °C
Undetected Cloud Cover	Internal	- 10 °C

4. RESULTS

4.1 EBK Interpolation Results for in-situ Measurement

Fig. 4.1, Fig. 4.2, Fig. 4.3 and Fig. 4.4 show the EBK prediction of temperature at surface and depth for Köyceğiz and Fethiye-Göcek Bay. Salinity, specific conductance at depth EBK maps of Köyceiz Lake are given in Appendix I. Specific conductance, pH, salinity at depth maps of the Fethiye-Göcek Bay are given in Appendix II. All Errors maps, statistics and semi-variograms for surface and depth temperature interpolations are given in Appendix III and Appendix IV

In order to better compare and analyze the interpolation results for each maps a number is given as shown in Table 4.1

Table 4.1.The Numbering the interpolation maps

Date	Numbering	Date	Numbering	Date	Numbering
19/07/2013	STK 1	20/07/2013	STK 2	22/07/2013	STK 3
23/07/2013	STK 4	24/07/2013	STK 5	25/07/2013	STK 6
26/07/2013	STK 7	18/08/2013	STK 8	19/08/2013	STK 9
20/06/2013	STK 10	21/08/2013	STK 11	STK: Surface Temperature Measurement of Köycegiz Lake	
Date	Numbering	Date	Numbering	Date	Numbering
19/07/2013	DTK 1	20/07/2013	DTK 2	22/07/2013	DTK 3
23/07/2013	DTK 4	24/07/2013	DTK 5	25/07/2013	DTK 6
26/07/2013	DTK 7	18/08/2013	DTK 8	19/08/2013	DTK 9
20/06/2013	DTK 10	21/08/2013	DTK 11	DTK: Depth Temperature Measurement of Köycegiz Lake	
Date	Numbering	Date	Numbering	Date	Numbering
19/07/2013	DSK 1	20/07/2013	DSK 2	22/07/2013	DSK 3
23/07/2013	DSK 4	24/07/2013	DSK 5	25/07/2013	DSK 6
26/07/2013	DSK 7	18/08/2013	DSK 8	19/08/2013	DSK 9
20/06/2013	DSK 10	21/08/2013	DSK 11	DSK: Depth Salinity Measurement of Köycegiz Lake	
Date	Numbering	Date	Numbering	Date	Numbering
19/07/2013	DScK 1	20/07/2013	DScK 2	22/07/2013	DScK 3
23/07/2013	DScK 4	24/07/2013	DScK 5	25/07/2013	DScK 6
26/07/2013	DScK 7	18/08/2013	DScK 8	19/08/2013	DScK

20/06/2013	DScK 10	21/08/2013	DScK 11	DScK: Depth Specific Conductivity Measurement of Köycegiz Lake
------------	---------	------------	---------	--

Table 4 2.The numbering the interpolation maps (cont...)

Date	Numbering	Date	Numbering	Date	Numbering
23-24-25/08/2013	STG 1	26/27/30/31/08/2013	STG 2	02/03/05/06/07/06/2014	STG 3
27/08/2014	STG 4	28/08/2014	STG 5	29/08/2014	STG 6
30/08/2014	STG 7a, 7b, 7c	31/08/2014	STG 8	STG: Surface Temperature Measurement of Göcek-Fethiye Bay	
Date	Numbering	Date	Numbering	Date	Numbering
23-24-25/08/2013	DTG 1	26/27/30/31/08/2013	DTG 2	02/03/05/06/07/06/2014	DTG 3
27/08/2014	DTG 4	28/08/2014	DTG 5	29/08/2014	DTG 6
30/08/2014	DTG 7a, 7b, 7c	31/08/2014	DTG 8	26/08/2014	DTG 9

STG: Depth Temperature Measurement of Göcek-Fethiye Bay

Date	Numbering	Date	Numbering	Date	Numbering
23-24-25/08/2013	DScG 1	26/27/30/31/08/2013	DScG 2	02/03/05/06/07/06/2014	DScG 3
27/08/2014	DScG 4	28/08/2014	DScG 5	29/08/2014	DScG 6
30/08/2014	DScG 7a, 7b, 7c	31/08/2014	DScG 8	26/08/2014	DScG 9

STG: Depth Specific Conductivity Measurement of Göcek-Fethiye Bay

Date	Numbering	Date	Numbering	Date	Numbering
23-24-25/08/2013	DpHG 1	26/27/30/31/08/2013	DpHG 2	02/03/05/06/07/06/2014	DpHG 3
27/08/2014	DpHG 4	28/08/2014	DpHG 5	29/08/2014	DpHG 6
30/08/2014	DpHG 7a, 7b, 7c	31/08/2014	DpHG 8	26/08/2014	DpHG 9

STG: Depth pH Measurement of Göcek-Fethiye Bay

Date	Numbering	Date	Numbering	Date	Numbering
23-24-25/08/2013	DSG 1	26/27/30/31/08/2013	DSG 2	02/03/05/06/07/06/2014	DSG 3
27/08/2014	DSG 4	28/08/2014	DSG 5	29/08/2014	DSG 6
30/08/2014	DSG 7a, 7b, 7c	31/08/2014	DSG 8	26/08/2014	DSG 9

STG: Depth Salinity Measurement of Göcek-Fethiye Bay

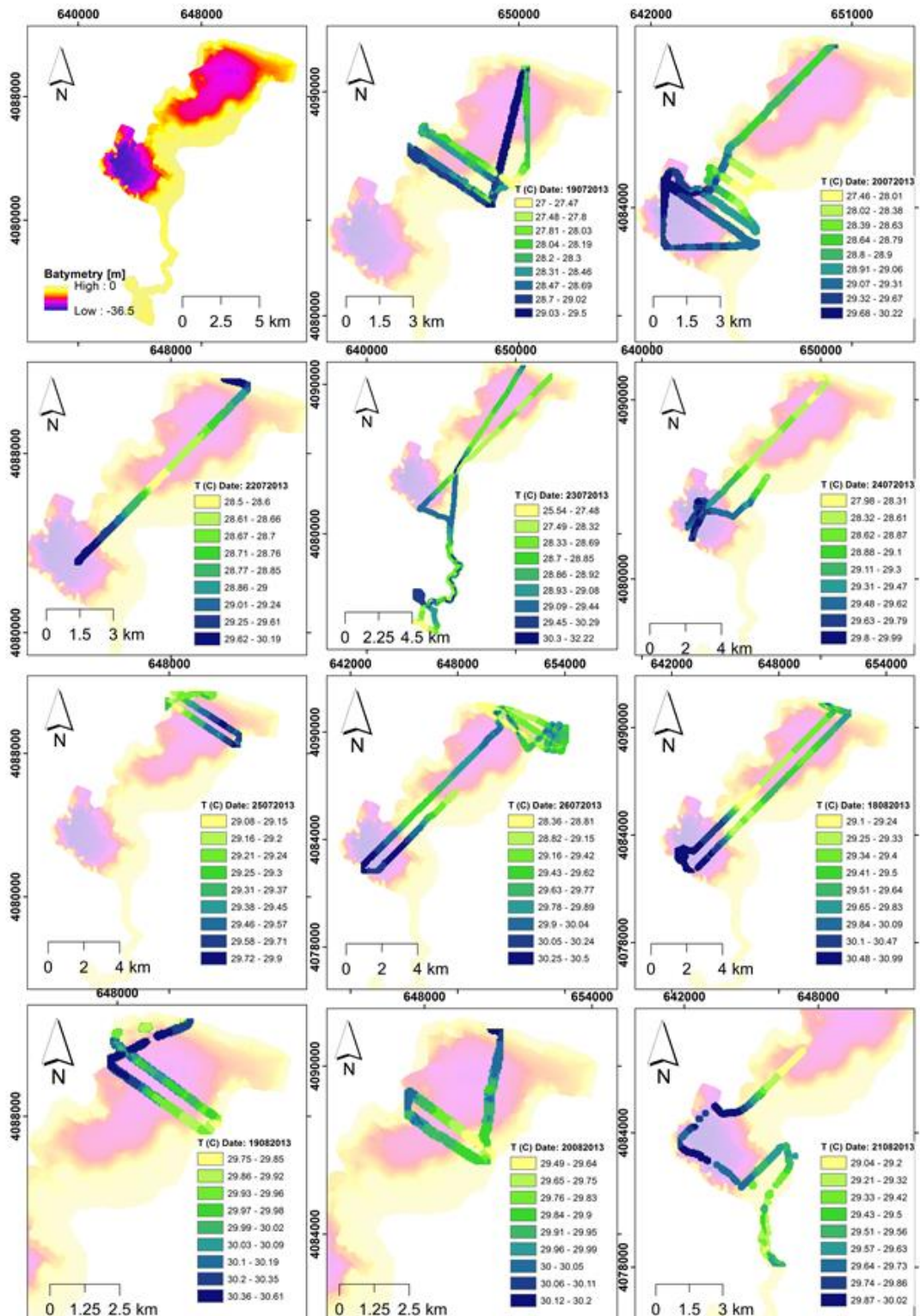


Figure 4 1.EBK interpolation for temperature at surface of Koycegiz Lake

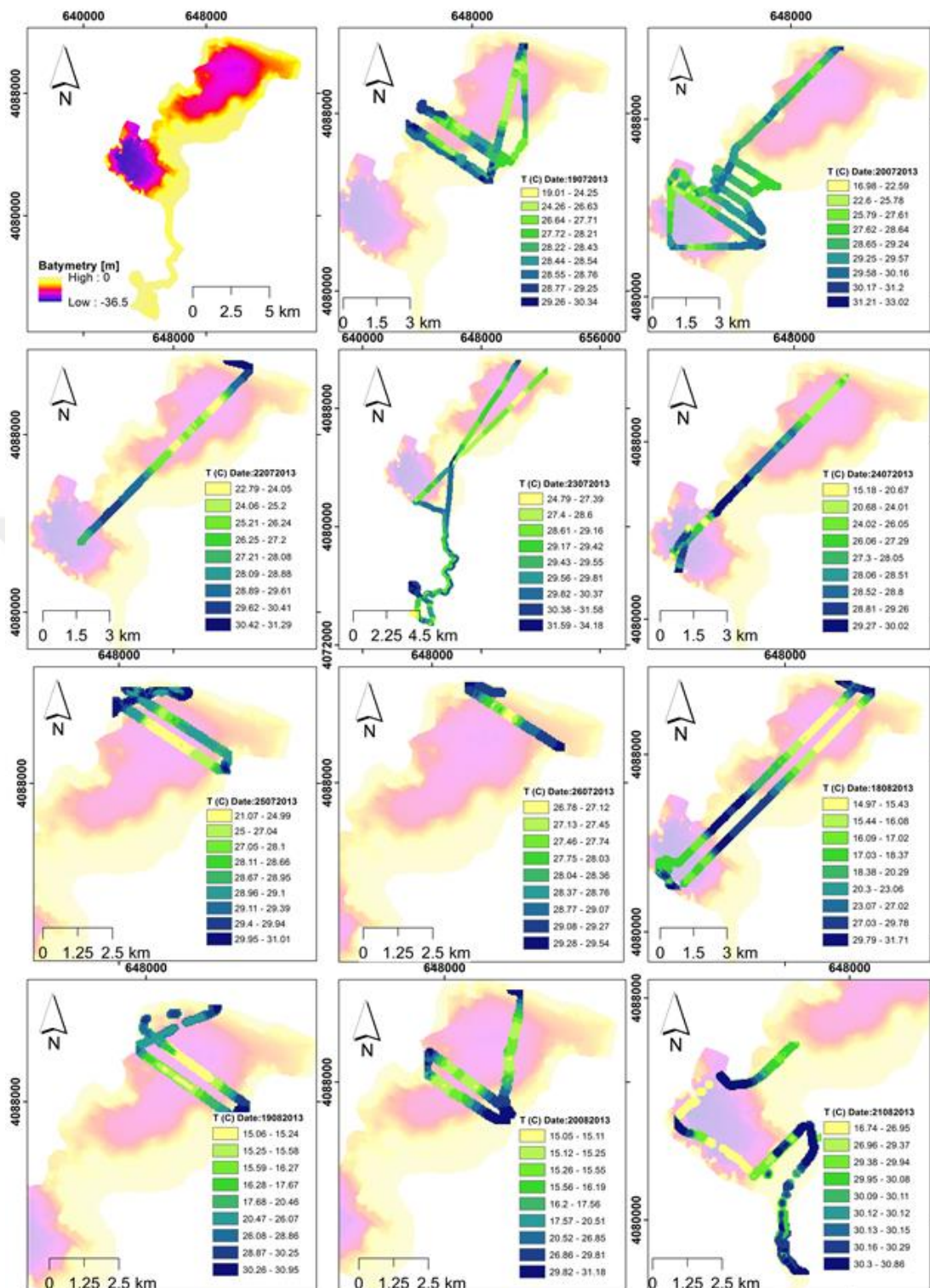


Figure 4 2.EBK interpolation for temperature at depth of Köyceğiz Lake

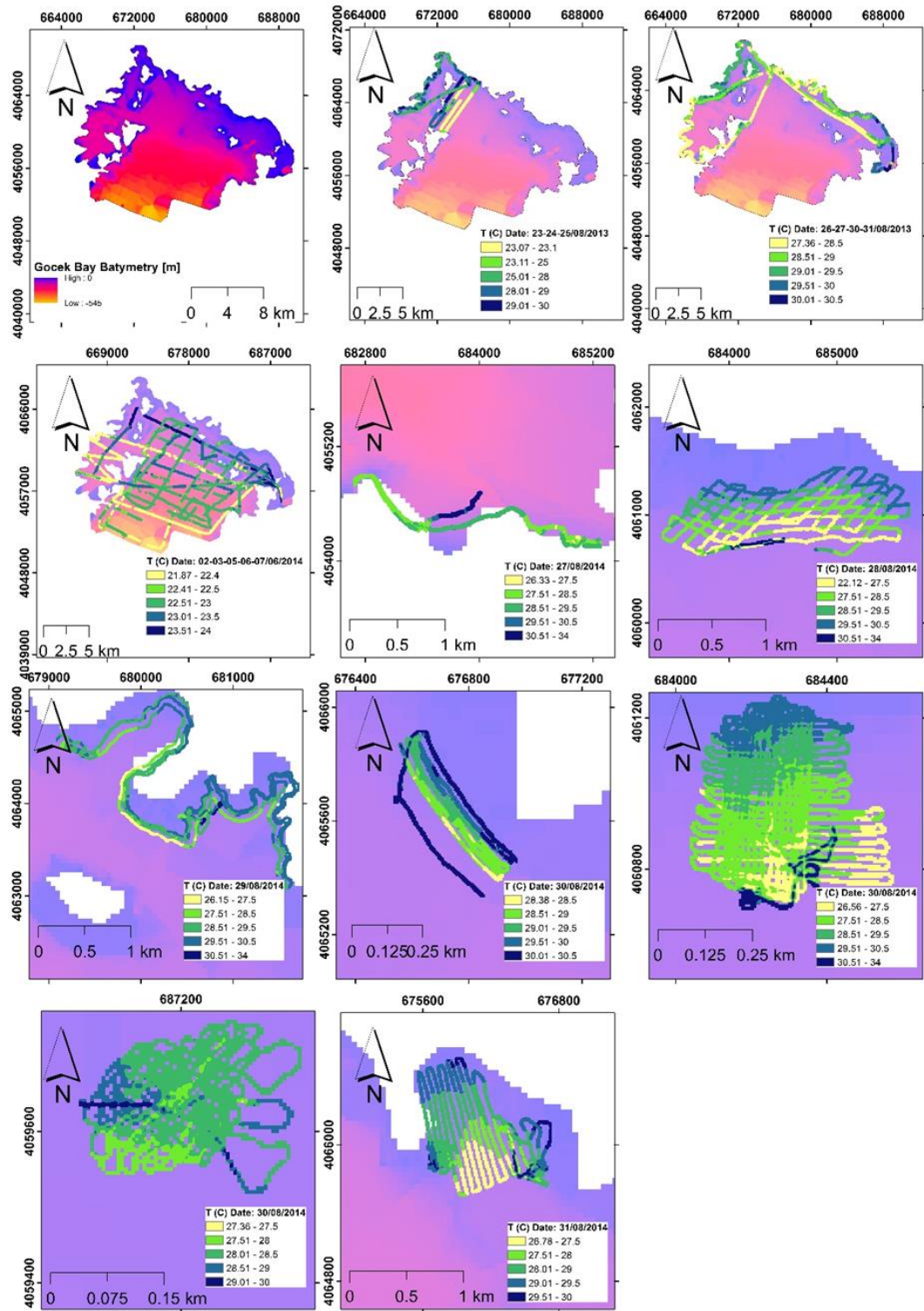
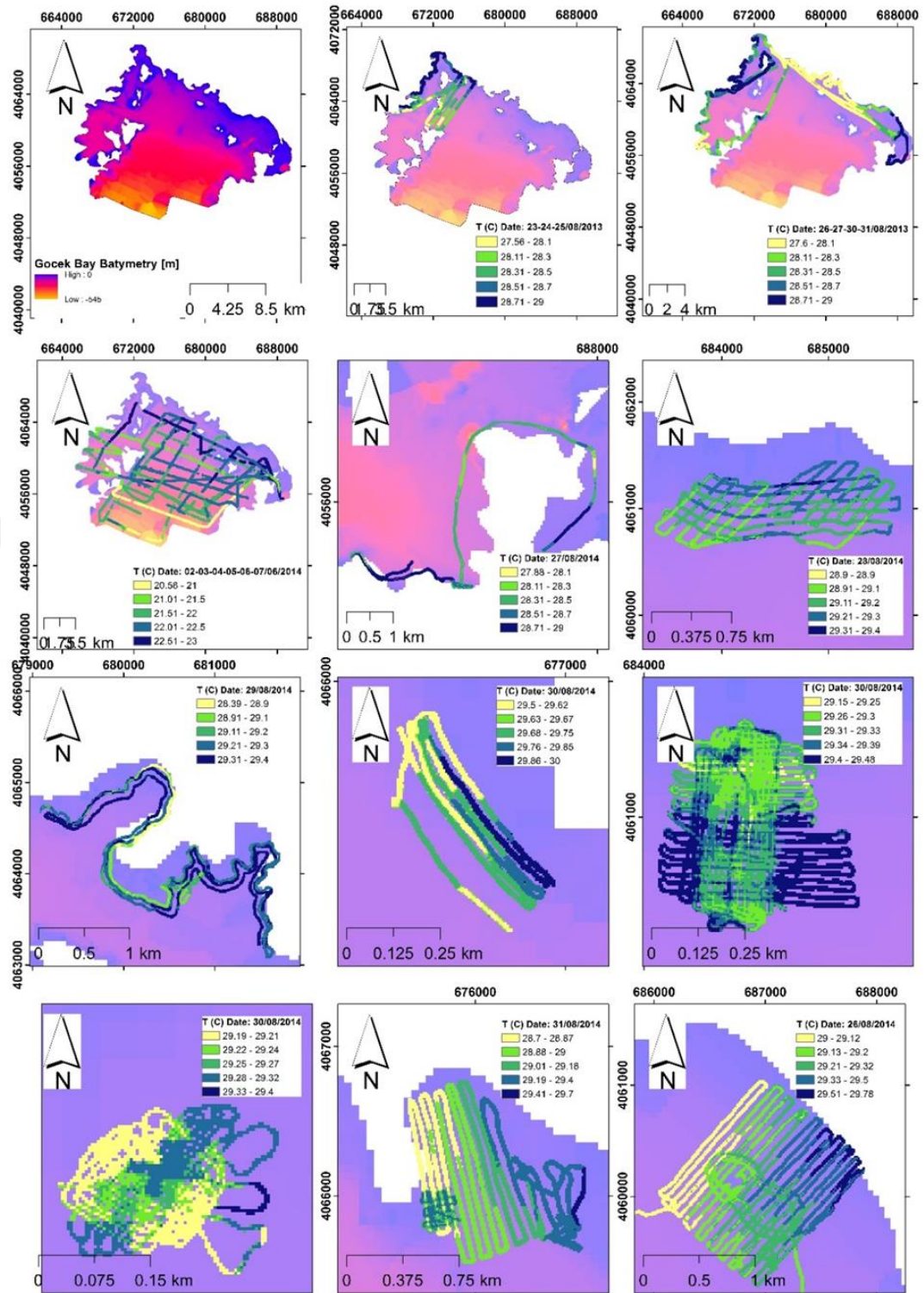


Figure 4 3.EBK interpolation for temperature at surface of Fethiye-Göcek Bay



4.2 Comparison of Landsat 8 OLI with in-situ temperature measurement

Landsat 8 TIR band10 images were compared with in-situ measurements (see table 3.3 above). Figure 4.5 and Fig 4.6 give correct Landsat thermal images according to the appropriate regression equation for Köyceğiz Lake. Fig. 4.7, Fig. 4.8 and Fig.4.9 give correct Landsat 8 thermal images according to the calculated regression equation for Fethiye-Göcek Bay.

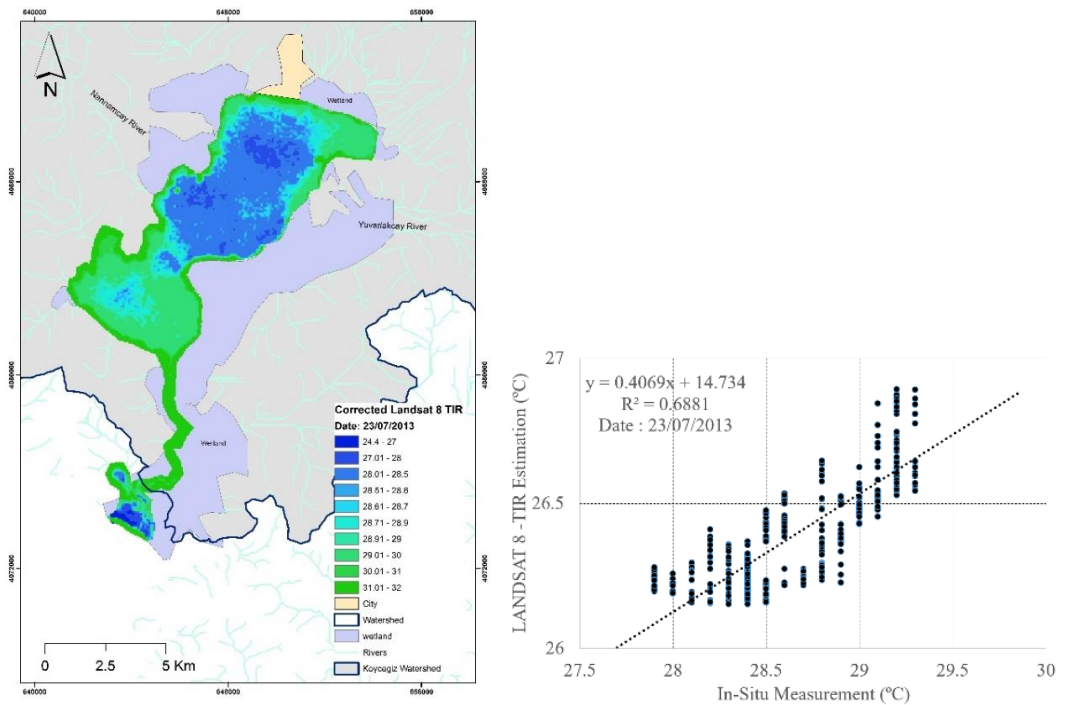
Table 4.2 present geostatistical summary to compare in-situ measurement and Landsat 8 TIR images.

Table 4.2 Geo-statistical evaluation of in-situ measurement, Landsat TIR images and corrected Landsat TIR images

In-Situ Measurement	Date				
	23.07.2013	30.07.2013	27.08.2014	7.06.2014	24.08.2013
Mean	28.68	29.91	28.63	22.22	28.30
Standard Deviation	0.39	0.37	0.25	0.29	0.20
Minimum	27.90	29.10	28.30	21.70	27.87
Maximum	29.30	30.50	29.20	22.97	28.75
Coefficient of Variation	0.01	0.01	0.01	0.01	0.01

Landsat 8	Date				
	23.07.2013	30.07.2013	27.08.2014	7.06.2014	24.08.2013
Mean	26.41	27.44	27.24	22.19	25.49
Standard Deviation	0.19	0.15	0.26	0.18	0.15
Minimum	26.15	27.10	26.84	21.85	25.25
Maximum	26.89	27.76	28.17	22.86	25.97
Coefficient of Variation	0.01	0.01	0.01	0.01	0.01

Landsat 8 corrected	Date				
	23.07.2013	30.07.2013	27.08.2014	7.06.2014	24.08.2013
Mean	28.68	26.34	28.63	22.22	28.30
Standard Deviation	0.47	0.07	0.35	0.39	0.24
Minimum	28.07	26.19	28.09	21.48	27.92
Maximum	29.88	26.48	29.90	23.68	29.07
Coefficient of Variation	0.02	0.00	0.01	0.02	0.01
R ² (coefficient of determination)	0.68	0.86	0.53	0.55	0.71



**Figure 4.5.Corrected Landsat 8 TIR image according to regression equation for Koycegiz Lake
(23/07/2013)**

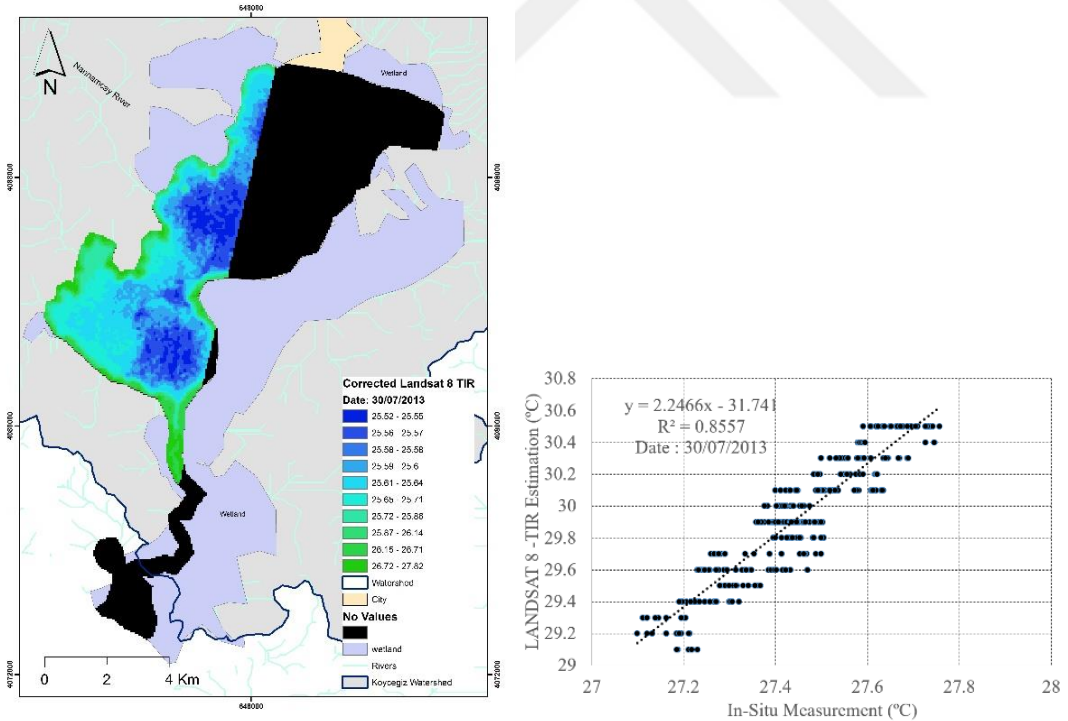


**Figure 4.6.Corrected Landsat 8 TIR image according to regression equation for Koycegiz Lake
(30/07/2013)**

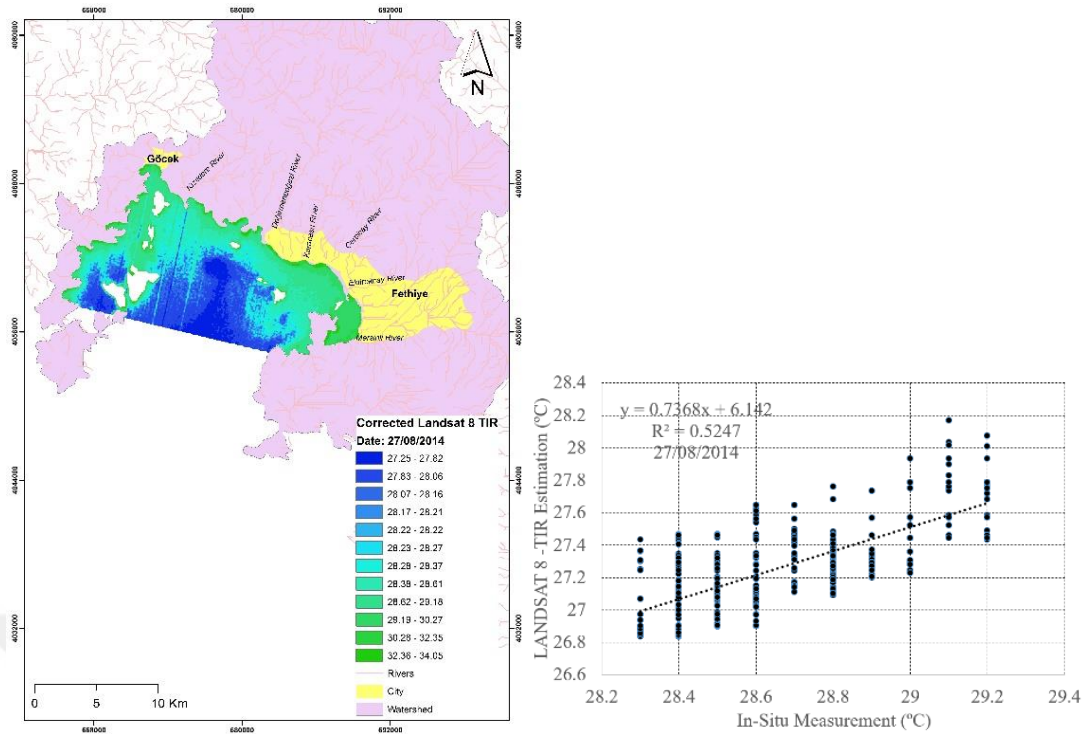


Figure 4.7.Corrected Landsat 8 TIR image according to regression equaiton for Göcek-Fethiye Bay (27/08/2014)

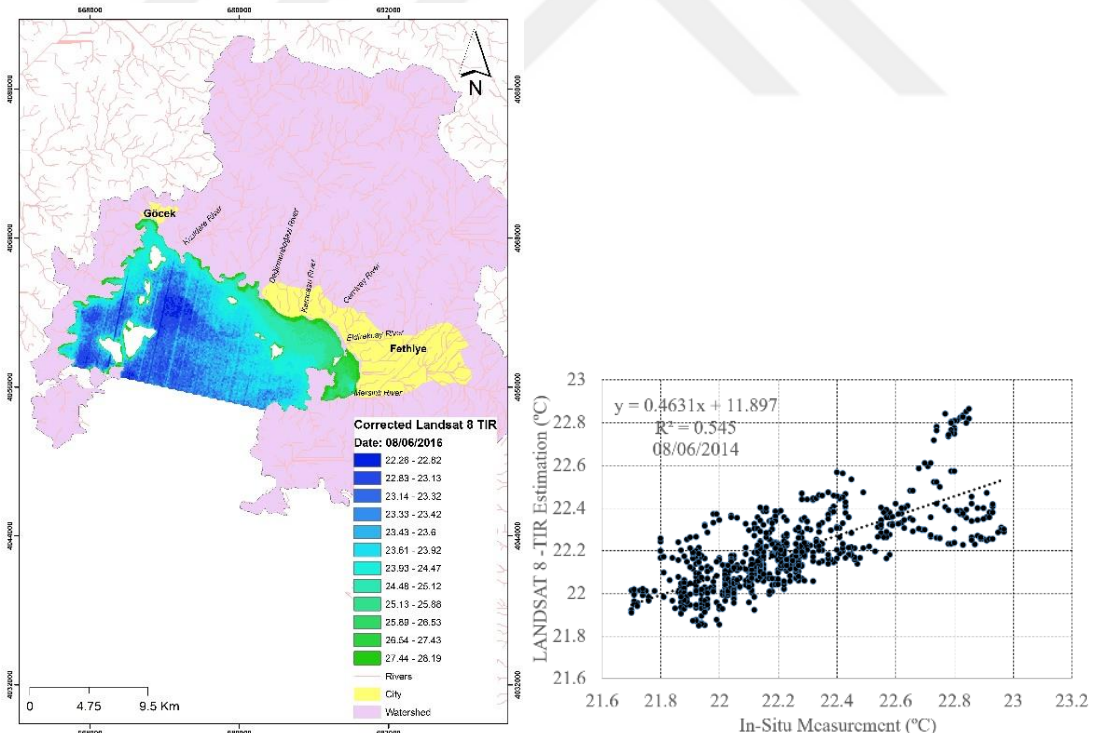


Figure 4.8.Corrected Landsat 8 TIR image according to regression equaiton for Göcek-Fethiye Bay (08/06/2014)

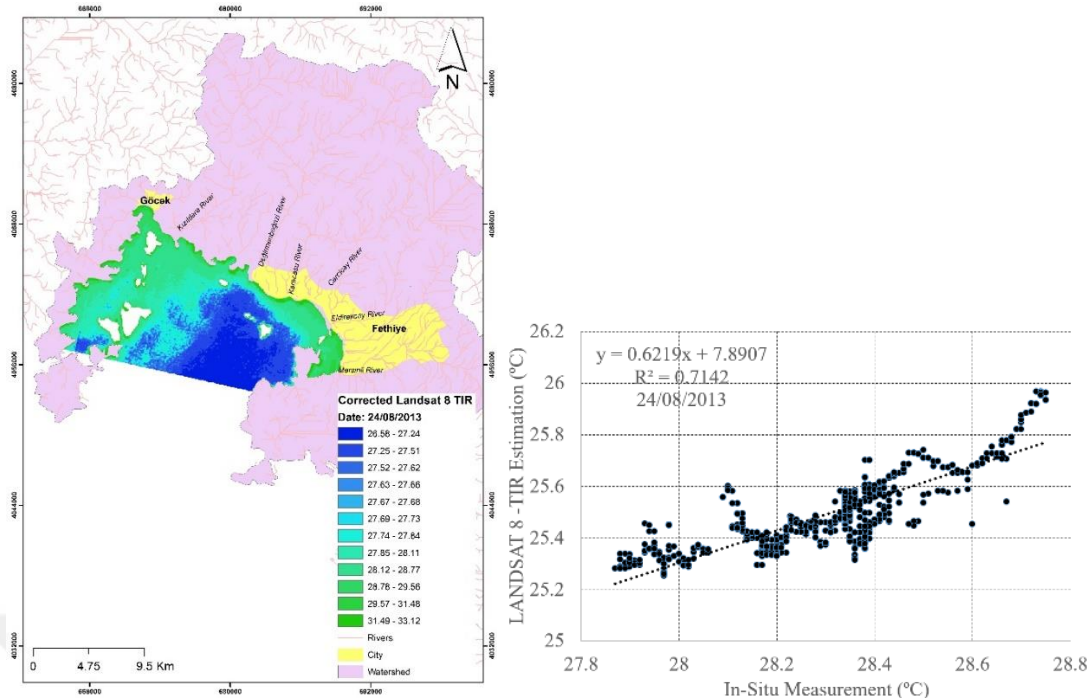


Figure 4.9. Corrected Landsat 8 TIR image according to regression equaiton for Göcek-Fethiye Bay (24/08/2013)

The south-west part of the lake can be seen hotter than the northeast part (Fig. 4.10, Fig. 4.11.). As well-known, there exist thermal springs at the south west part of the Köyceğiz lake (“Sultaniye Kaplıcaları”). This thermal source has significant effects on the south part of the lake. A thermal plume can be easily seen in Fig. 4.10 and Fig.4.11.

Near the coastal part of the Fethiye-Göcek Bay the water is hotter than the south part of the bay (Fig. 4.12, Fig. 4.13 and Fig. 4.14). There are also significant inputs of lakes which influence the thermal pattern.

4.3 Evidence of cold and hot spring results for Köyceğiz Lake and Fethiye-Göcek Bay

A detailed analysis is done also to determine the local cold and hot springs at Köyceğiz and Fethiye-Göcek Bay. Fig. 4.10 and Fig. 4.11 present the general temperature distribution for all grid patterns in Köyceğiz Lake and Fethiye-Göcek Bay. The maps show us that at the north east part of Köyceğiz lake surface temperature is significantly higher than south part of the lake. Namnamcay and

Yuvarlakcay River is feeding the Köyceğiz Lake at the middle part. The bathymetry and weather conditions also have an effect on the surface temperature of the Lake. At the corner of the lake the temperature is relatively higher than the other part because of the slightly lower thickness of the water mass body.

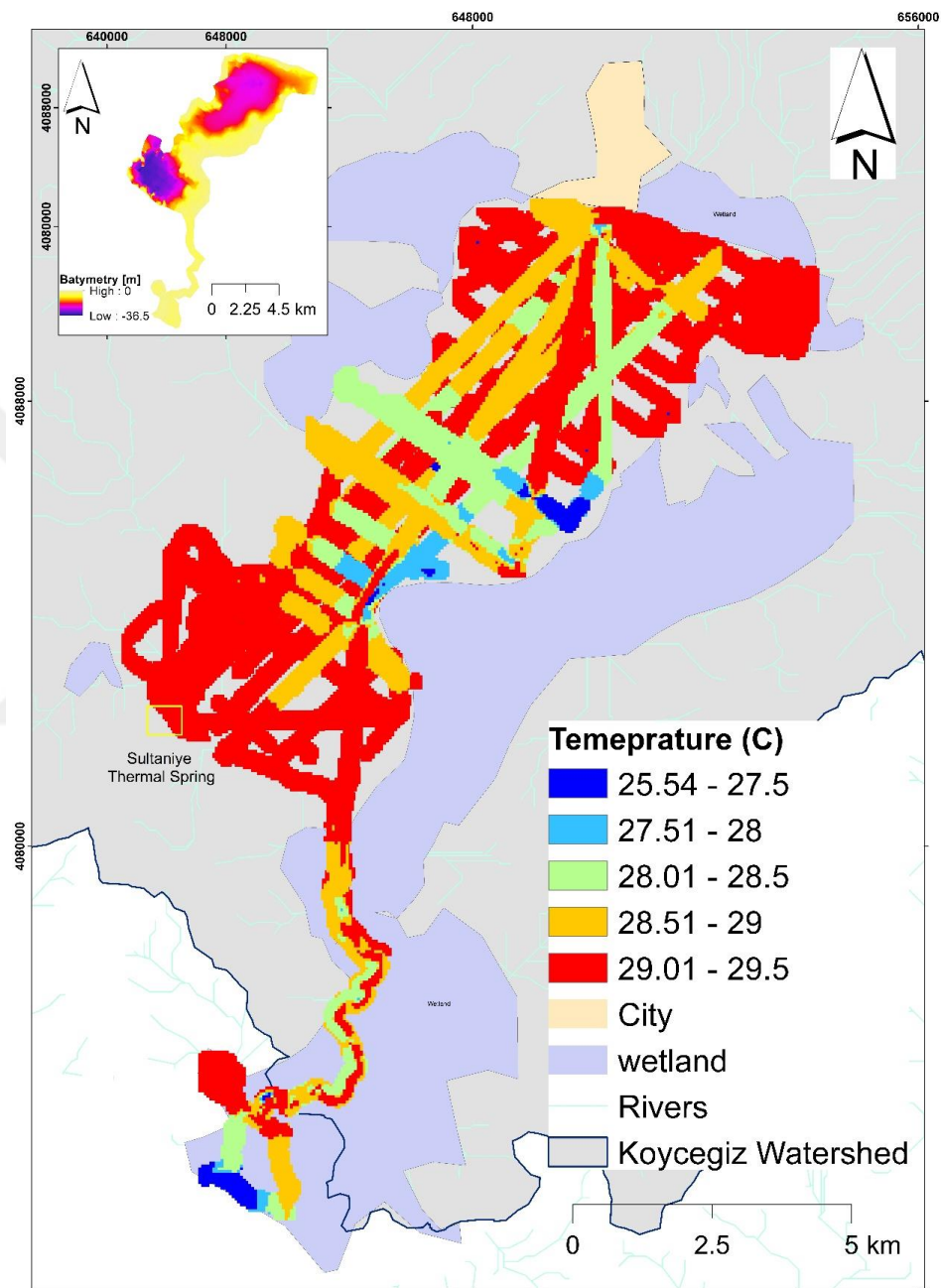


Figure 4 10.Surface Water Temperature interpolations for Köyceğiz Lake (July and August 2013).

For Fethiye-Göcek Bay, it is very difficult to assess the data due to the different several factors such as climatic conditions, different types of dry river inputs, wave effect etc... Especially at the south west part and southeast part of the bay, near the Göcek and Fethiye city center the surface water temperature is rising. After the Değirmenboğazı River to the Fethiye city due to the recharge of the several rivers the temperature is decreasing at the coastal site of the bay.

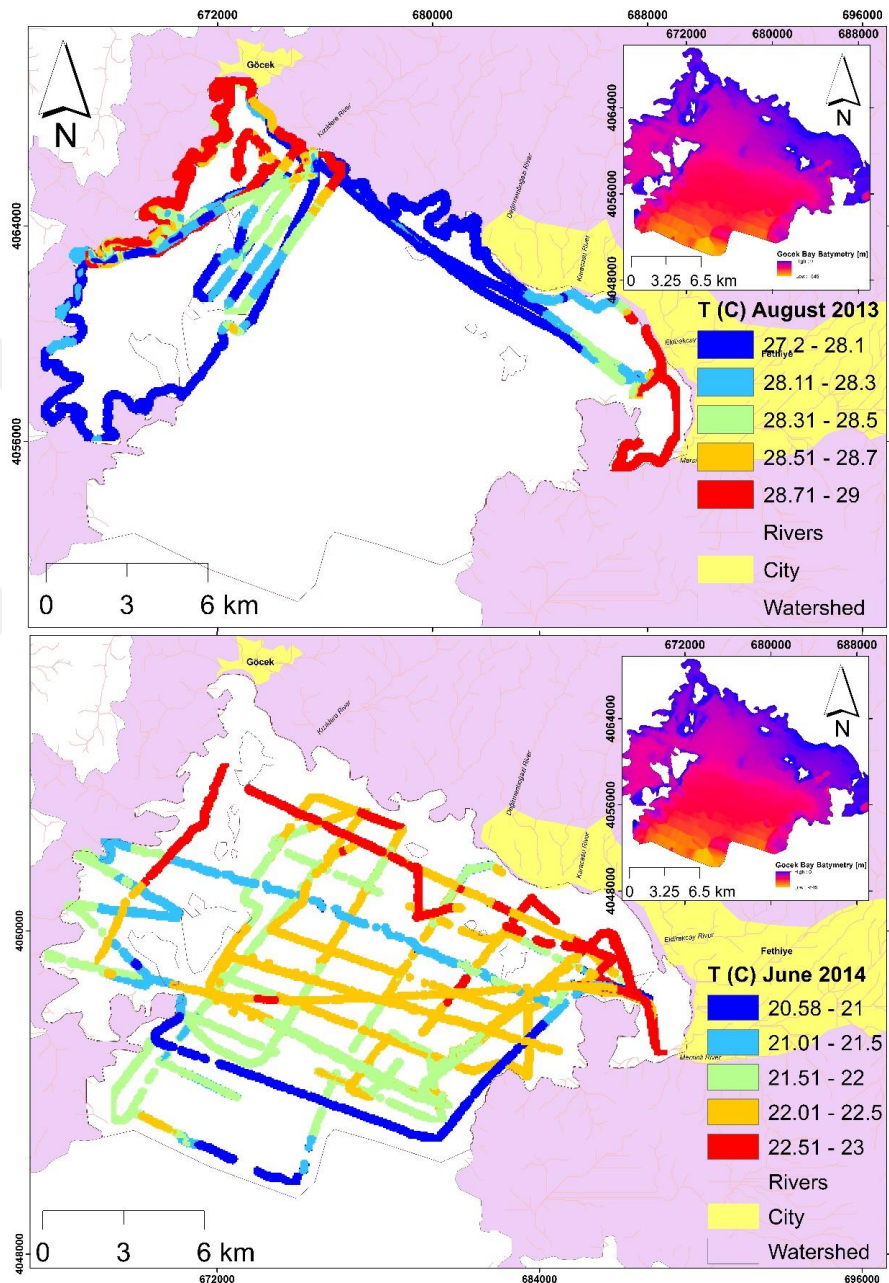


Figure 4 11.Surface Water Temperature interpolations for Fethiye-Göcek Bay (August 2013 and June 2014).

In order to find the local cold and hot spring each in-situ measurement at the depth of the Köycegiz Lake and Fethiye Göcek Bay are also analyzed one by one. According to a detailed analysis of depth temperature (DTK1 to DTK10 and DTG1 to DTG 9), local cold and hot springs are detected in Fig. 4.12 and Fig. 4.13. In order to better understand if there is an evidence of cold/hot springs or to find an anomaly the temperature data is divided by the bathymetry to normalize the data. The other validation method of the cold and hot springs at that region can be also seen with Specific conductivity, salinity and pH maps in Appendix I. The normalized temperature is defined as $(2 * (X-X_{min}) / (X_{max}-X_{min}) - 1$, where the X is the temperature values, and $(X_{max}-X_{min})$ is the amplitude of the temperature. The values will be a range between [-1 1].

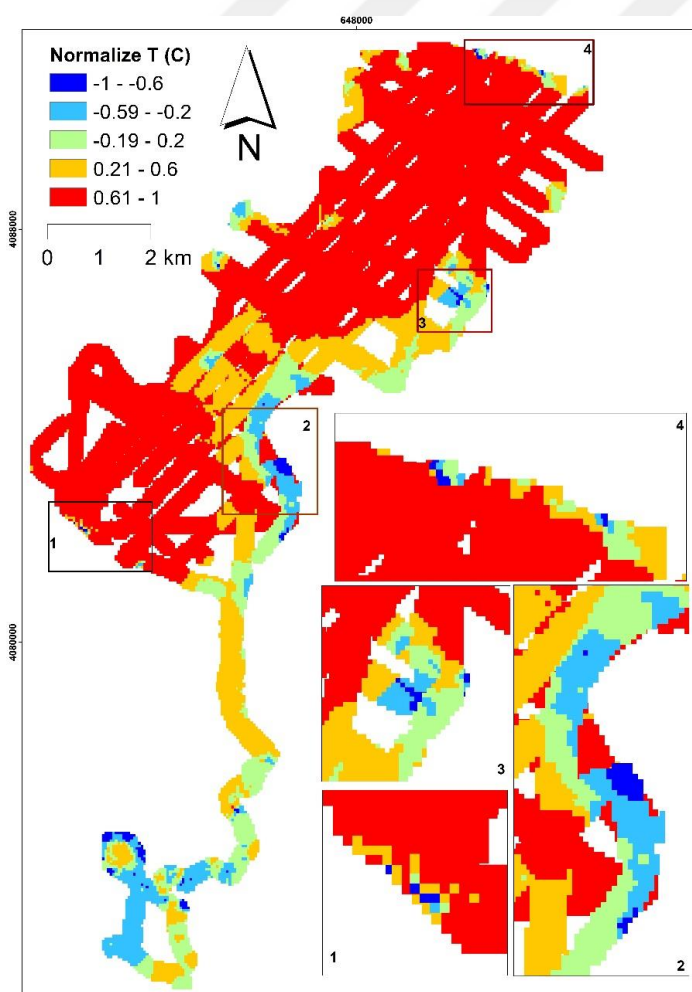
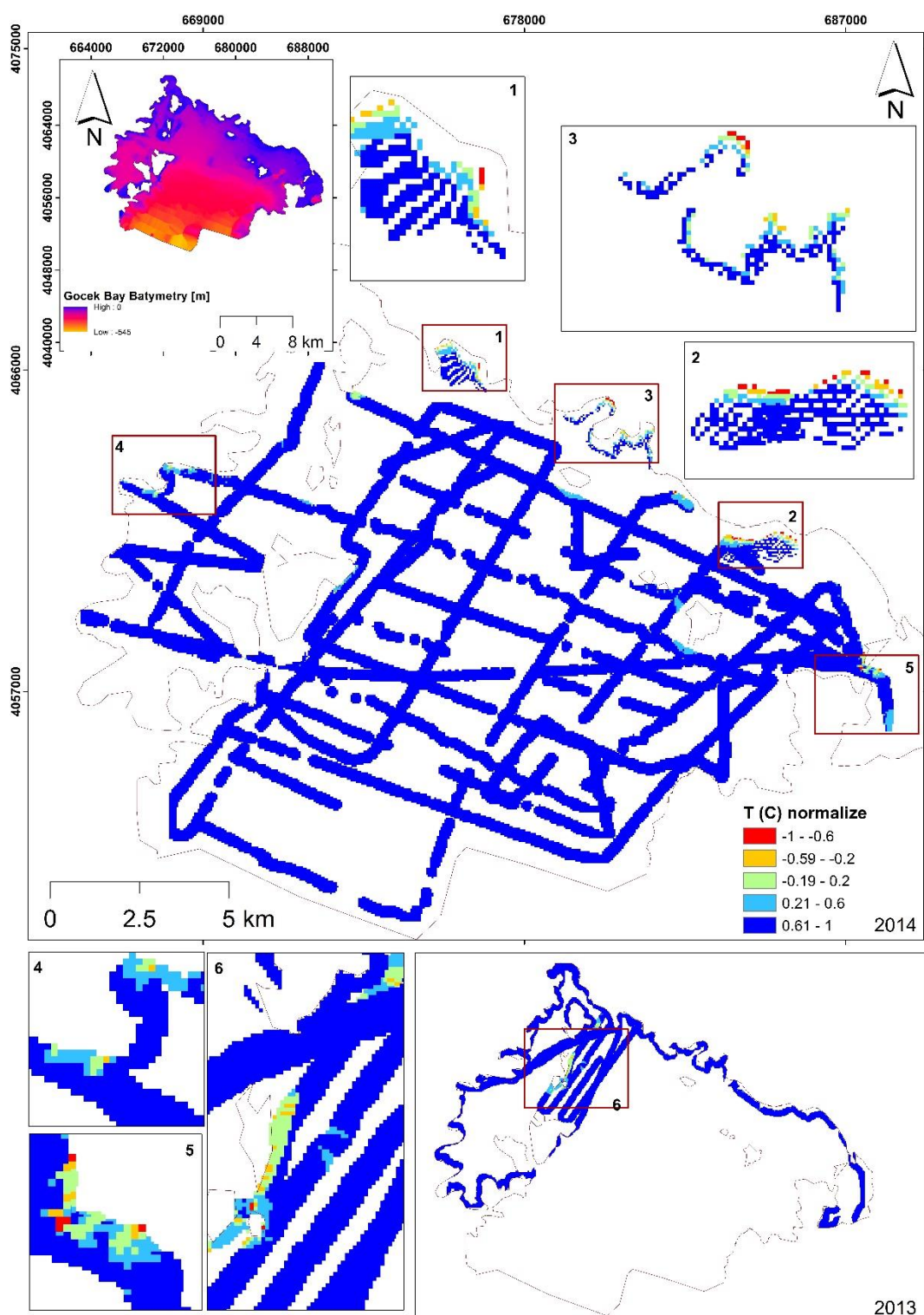


Figure 4 12. Normilize Depth Water Temperature Interpolation maps for Köycegiz Lake (July and August 2013)



**Figure 4 13. Normalize Depth water temperature Interpolations maps for Fethiye-Göcek Bay
(August 2013 and June 2014)**

4.4 Thermal Stratification (thermocline) of Köycegiz Lake

The thermal stratification of Köyceğiz lakes could also present the change in the temperature at different depths in the lake. This change is due to the change in water's density with temperature. The atmosphere force a temperature signal at the surface of the surface water body. As a consequence, thermal stratification can be observed during the warm season if a lake is sufficiently deep. In-situ measurement of temperature and specific electrical conductivity are plotted vs depth in Figure 4.14 for Köyceğiz Lake. Fig. 4.14 show clearly that there is a shift of thermal stratification at 7 m. The temperature vs depth plots for Fethiye-Göcek Bay are given in Appendix V. Fethiye-Göcek Bay temperature-depth profile give generally a decrease the temperature with increasing the depth. At the first 10m depth of the Fethiye Göcek Bay. There exist mixing water and the temperature has a mixing temperature level with depth (1m, 5m and 8m).

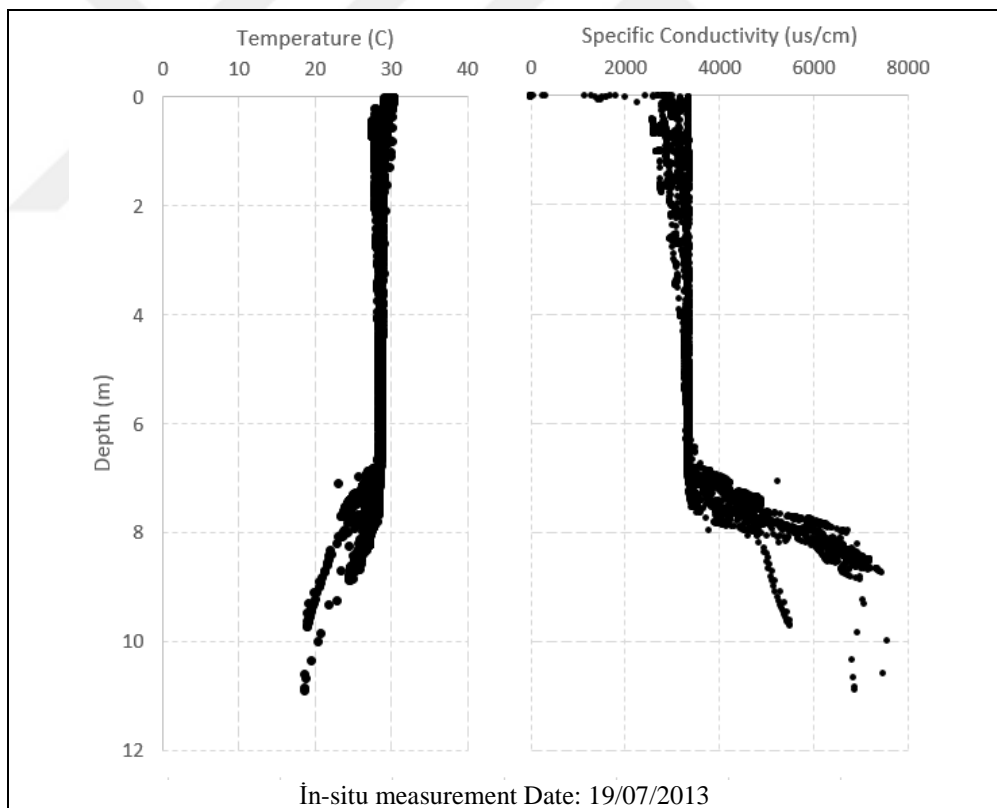


Figure 4.14.Temperature and Specific Conductivity vs Depth plots for Köycegiz Lake

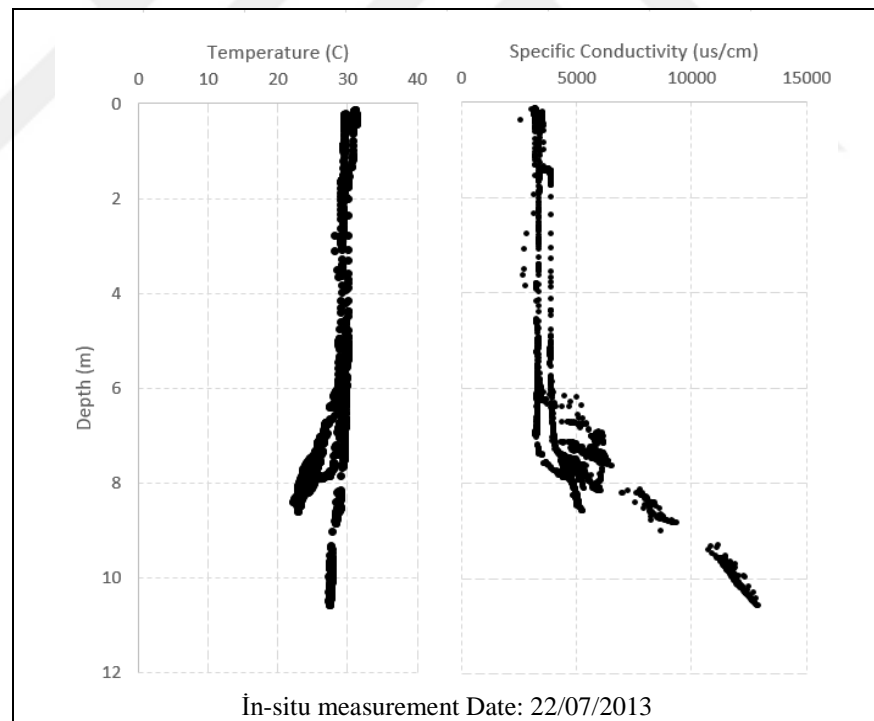
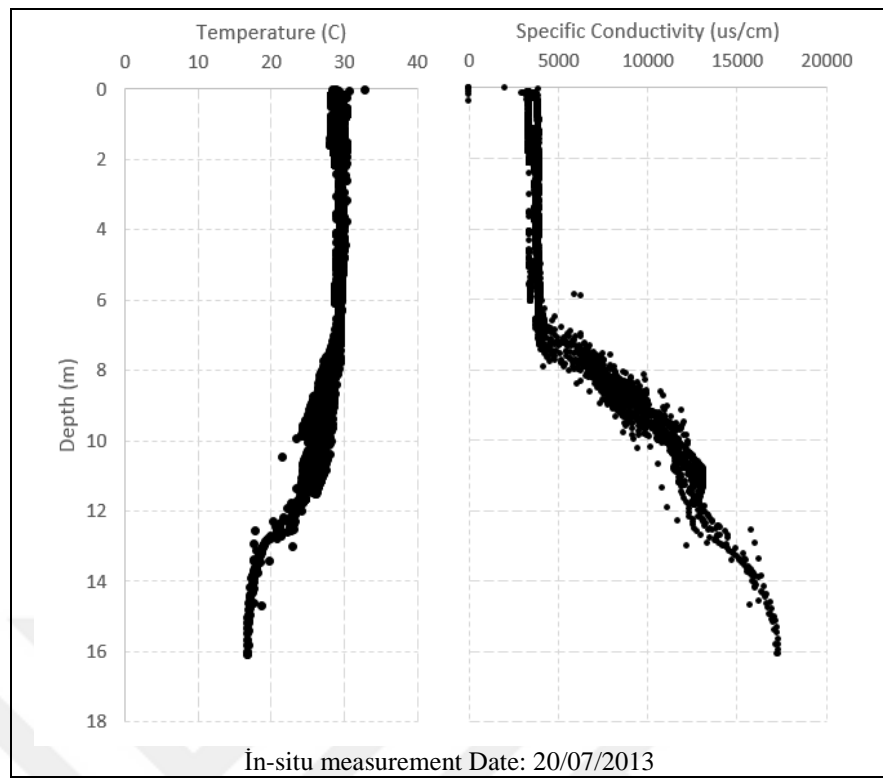


Figure 4 15.Temperature and Specific Conductivity vs Depth plots for Köyceğiz Lake (cont...)

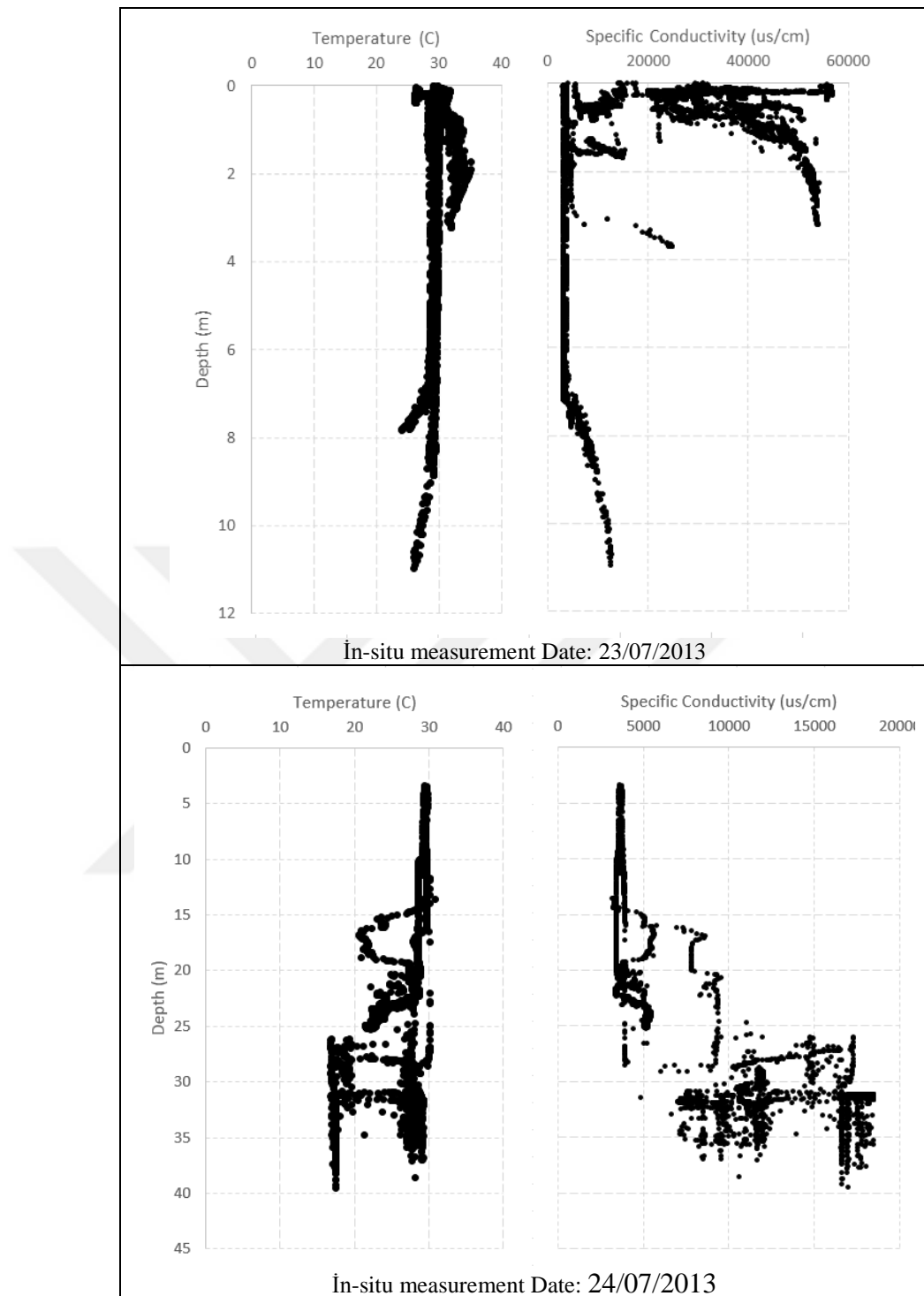


Figure 4 16.Temperature and Specific Conductivity vs Depth plots for Köyceğiz Lake (cont...)

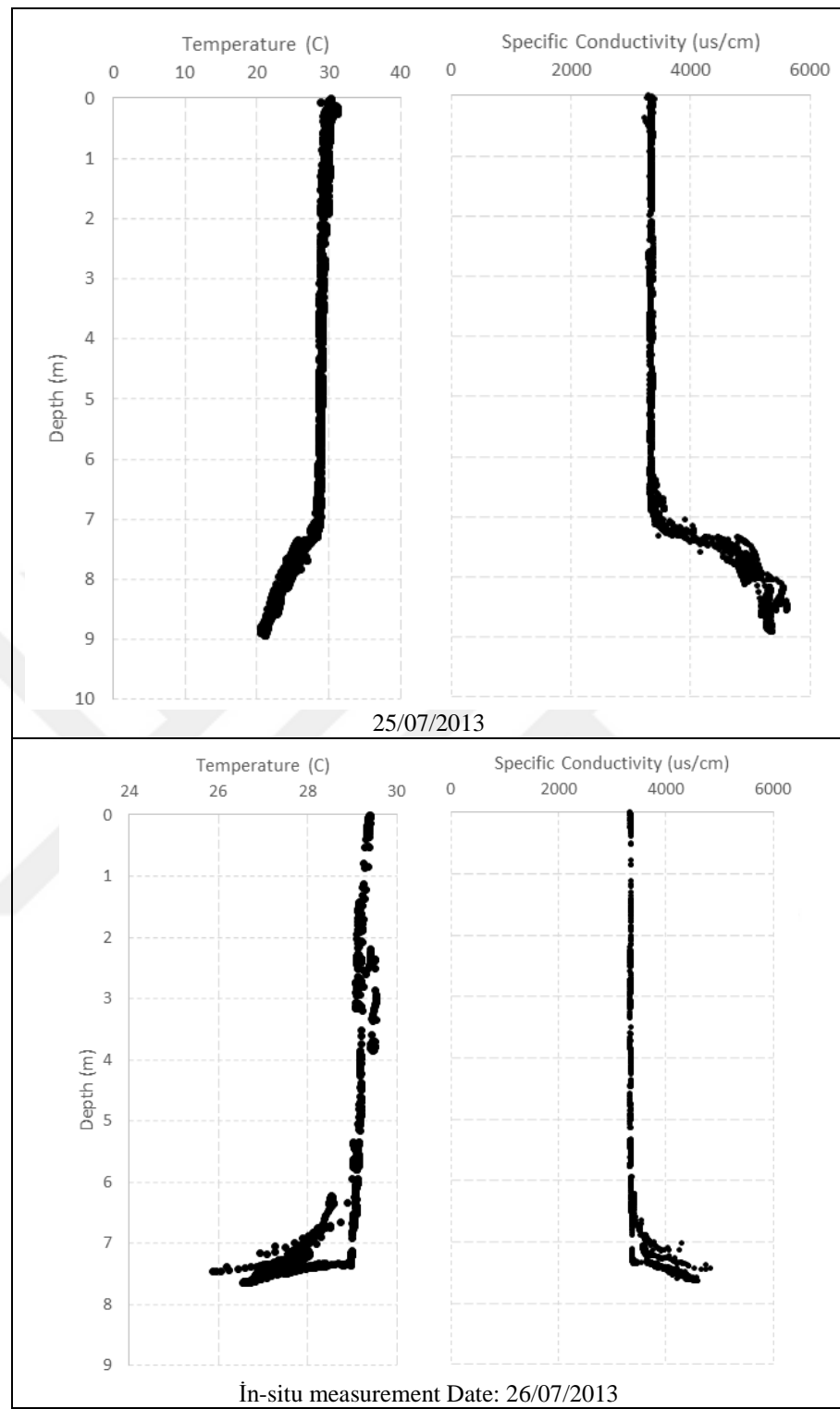


Figure 4 17.Temperature and Specific Conductivity vs Depth plots for Koycegiz Lake (cont...)

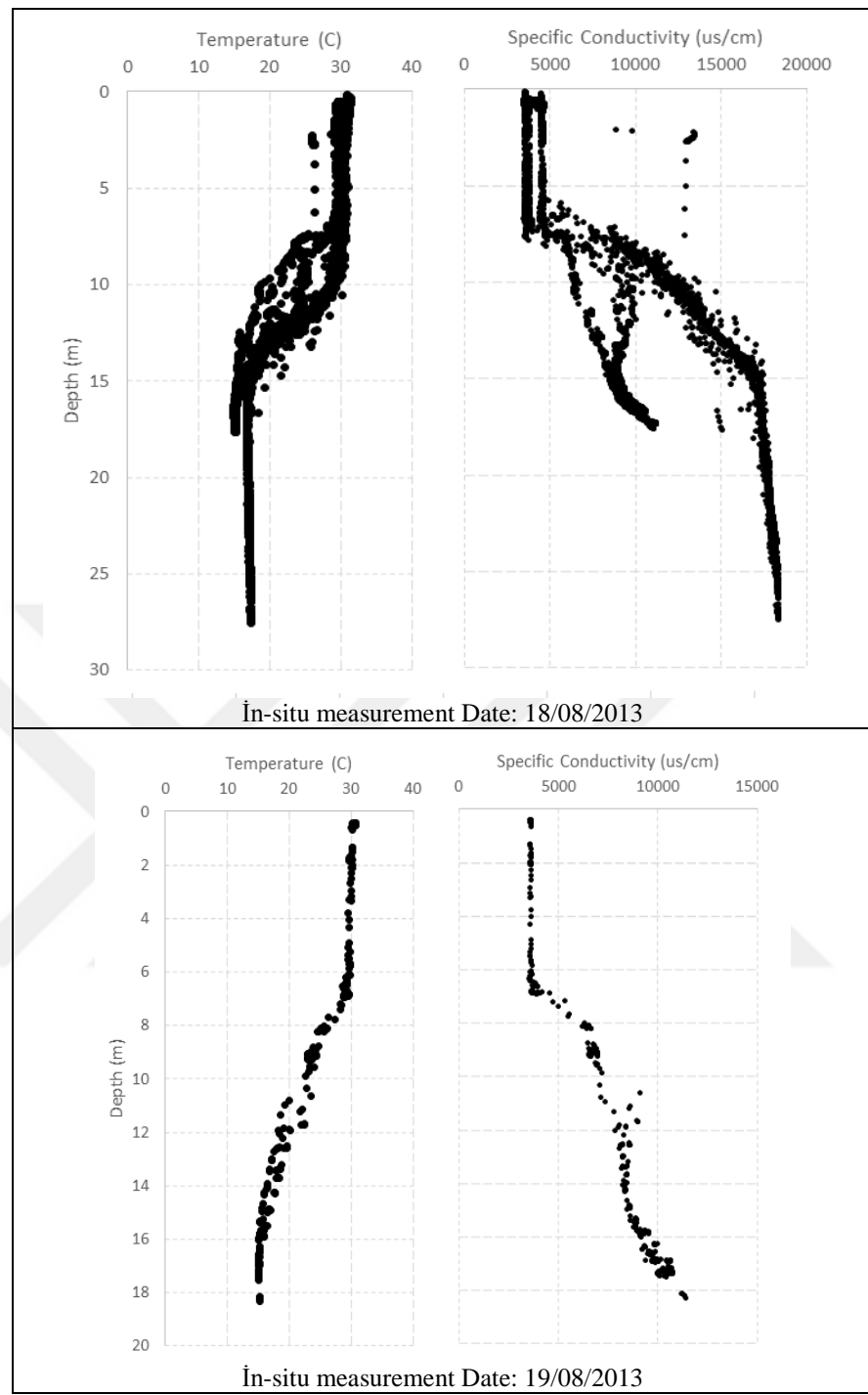


Figure 4 18.Temperature and Specific Conductivity vs Depth plots for Koycegiz Lake (cont...)

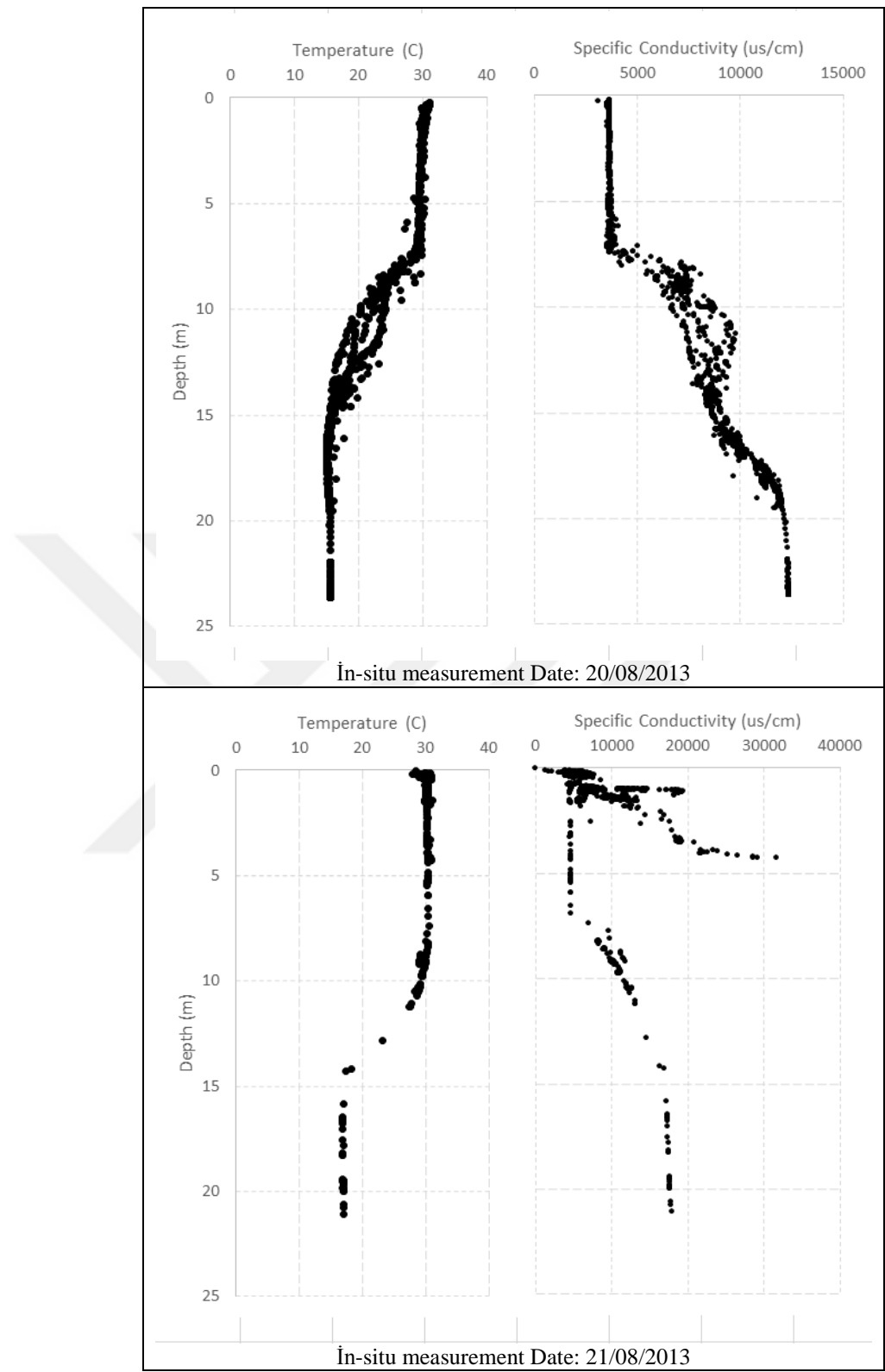


Figure 4 19.Temperature and Specific Conductivity vs Depth plots for Köyceğiz Lake (cont...)

5. CONCLUSION

In this study, thermal water (cold/hot) inputs were investigated for Köycegiz Lake and Fethiye-Göcek Bay. In order to find the evidence of springs in-situ measurement and satellite images was used. In situ measurement were done by data loggers. Landsat 8 thermal band was used for satellite measurement. At the depth of the Köyceğiz Lake and Fethiye-Göcek Bay, not only the temperature measurement are collected but also the electrical conductivity, pH and salinity measurement were made to validate the evidence of inputs. All maps were interpolated using a new methodology called as Empirical Bayesian Kriging (EBK). Vertical temperature profile of Köyceğiz Lake and Fethiye-Göcek Bay is also investigated to understand vertical stratification characteristics of the study areas. The following conclusions can be made according to obtained results:

- The combination of the different techniques such as in-situ measurements interpolation using EBK and Satellite estimation of temperature with Landsat 8 described in this study has proved very useful for the locating and quantifying the cold/hot spring at the Mediterranean Sea (Köyceğiz Lake, Fethiye-Göcek Bay).
- The comparison of Landsat 8 thermal image show a good correlation ($R^2>0.68$) with in-situ measurement. Hot thermal plume at Köyceğiz Lake was shown in Fig. 4.5 and Fig 4.6. For Fethiye-Göcek Bay, thermal satellite images also show a good correlation up to $R^2=0.71$. The thermal significance at the surface of the Fethiye-Göcek bay is more difficult to comment due to the several influence factor of the open sea (Fig 4.7, Fig 4.8 and Fig.4.9). However, it was also concluded that, using surface in-situ measurement near the Fethiye and Göcek village the temperature profile is rising to the surface. The inputs of the rivers decrease the temperature of the Sea between Fethiye and Göcek village (Fig 4.11). However, it must be also

mentioned that there is a significance difference of temperature up to 2°C between in-situ measurement and thermal image calculations.

- At the South West part of the Köceğiz Lake there a significant influence of Sultaniye hot spring, which were presented in the surface temperature interpolations maps (STK2, STK3, STK4, STK7, STK8, STK11). The cold spring and the influence of the rivers were located at the north part of the Lake. Fig. 10 present all temperatures in-situ measurement on the surface, it can be also seen that at the middle part of the lake (low depth) the water body has low temperature the other part of the lake.
- The normalization data of depth temperature (Fig.4.12) show also clear hot and cold inputs of the lake. There exist more than 5 evidence input at the bottom of the Lake Köyceğiz. Electrical conductivity, salinity and pH maps also validate the inputs of the Lake. The normalization temperature data at the bottom of the Fethiye-Göcek Bay show also some evidence of cold spring at the bottom near the coastal part of the Bay (Fig 4.13).
- The thermocline stratification of the lake was found using vertical temperature measurement. At 7m of the Lake there is a significant evidence of thermal stratifications. The temperature and electrical conductivity above 7m is approximately 29 °C and 4000 µS/cm respectively. Above 7m, the temperature is decreasing up to 15 °C and electrical conductivity can reach up to 15000 µS/cm.
- The stratification of the Fethiye - Göcek bay is not as clear as the Köyceğiz Lake. There exist mixing water at the surface water and the temperature at 1m, 5m and 8m depth varies between [28 °C 31 °C], [27.5 °C 29.5 °C], [25.5 °C 27.5 °C]. At 100m of depth the temperature can decrease up to 17 °C. The prediction of temperature at a depth of 200m according to observation at 23/08/2013 can be estimated 10 °C (Appendix V).

6. DISCUSSION AND RECOMMENDATION

It was very clear that the surface temperature can be estimated using Landsat 8 TIR images with a relatively medium uncertainty ($\pm 2^{\circ}\text{C}$). In order to have more accurate monitoring of temperature ($\pm 0.1^{\circ}\text{C}$), the resolution of the satellite images have to be increased or airborne thermal images must be done in the field. There exist also several atmospheric correction algorithm can be tested such as “split window algorithm” to reduce the uncertainty. If the weather conditions are also well known and measurement stations are close to the observation points, some error causing parameters (the flow condition, air temperature, wind velocity effects etc..) can be estimated and the errors could be reduced. We recommend also that the water temperature estimation can be used in calibration and validation of models in a coarse scale. Another recommendation is that water temperature can be used also in ecological works, hydrological studies for water quality monitoring and climate change.

REFERENCES

- Abedini, M., Nasseri, M. and Ansari, A. (2008) Cluster-based ordinary kriging of piezometric head in West Texas/New Mexico- testing of hypothesis, *J Hydrol*, 351(3-4):360-367.
- Abrahart, R., Kneale, P. and See, L. (2004) *Neural Networks for hydrological modeling*, New York City, 316 p.
- Anonymous, *Su Kirliliği Kontrolü Yönetmeliği*, Republic of Turkey, Ministry of Forest and Water, Ankara, 2004, 51 p.
- Anonymous, *2012 edition of the Drinking Water Standards and Health Advisories*, Office of Water U.S. Environmental Protection Agency, Washington, DC, 2012, 12 p.
- Ayvaz, M. T., Karahan, H. and Aral, M. M. (2007) Aquifer parameter and zone structure estimation using kernel-based fuzzy c-means clustering and genetic algorithm, *J Hydrol*, 343:240-253.
- Aziz, A.R. and Wong, K.F.V. (1992) A neural network approach to the determination of aquifer parameters, *Ground Water*, 30(2):164-166.
- Baratti, R., Cannas, B., Fanni, A., Pintus, M., Sechi, G.M. and Toreno, N. (2003) River flow forecast for reservoir management through neural networks, *Neurocomputing*, 55:421-437.
- Billen, G., Garnier, J., Mouchel, J.M. and Silvestre, M., (2007) The Seine system: Introduction to a multidisciplinary approach of the functioning of a regional river system, *Sci Total Environ*, 375:1-12.
- Brochu, Y. and Marcotte, D. (2003) A simple approach to account for radial flow and boundary conditions when Kriging hydraulic head fields for confined aquifers, *Math Geol*, 35(2):11-139.
- Buchanan, S. and Triantafyllis, J. (2009) Mapping water table depth using geophysical and environmental variables, *Ground Water*, 47(1):80-96.

- Chang, F.J., Chiang, Y.M., Tsai, M.J., Shieh, M.C., Hsu, L.K. and Sorooshian, S. (2014) Watershed rainfall forecasting using neuro-fuzzy networks with the assimilation of multi-sensor information, *J Hydrol*, 508:374-384.
- Chen, J. and Adams, B.J. (2006) Integration of artificial neural networks with conceptual models in rainfall-runoff modelling, *J Hydrol*, 318:232-249.
- Cigizoglu, H.K. (2005) Generalized regression neural network in monthly flow forecasting, *Civ Eng Environ Syst*, 22(2):71-84.
- Corsini, A., Cervi, F. and Ronchetti, F. (2009) Weight of evidence and artificial neural networks for potential groundwater spring mapping: an application to the Mt. Modino area (Northern Apennines, Italy), *Geomorphology*, 111:79-87.
- Flipo, N., Jeannée, N., Poulin, M., Even, S. and Ledoux, E. (2007) Assessment of nitrate pollution in the Grand Morin aquifers (France): combined use of geostatistics and physically-based modeling, *Environ Pollut*, 146(1):241-256.
- French, M., Krajewski, W. and Cuykendall, R. (1992) Rainfall forecasting in space and time using a neural network, *J Hydrol*, 137:1-31.
- Garcia, L. and Shigidib, A. (2006) Using neural networks for parameter estimation in ground water, *J Hydrol*, 318:215-231.
- Goswami, M. and O'Connor, K.M. (2007) Real-time flow forecasting in the absence of quantitative precipitation forecasts: A multi-model approach, *J Hydrol*, 334(1-2):125-145.
- Halff, A.H., Halff, H.M. and Azmoodeh, M. (1993) Predicting runoff from rainfall using neural networks, *Proc Eng Hydrol*, ASCE, New York, 768-775.
- Hong, Y.S.T. and White, A.P. (2009) Hydrological modelling using a dynamic neuro-fuzzy system with on-line and local learning algorithm, *Adv Water Resour*, 32:110-119.
- Hsu, K., Gupta, H.V. and Sorooshian, S. (1995) Artificial neural network modelling of the rainfall-runoff process, *Water Resour Res*, 31(10):2517-2530.

- Imrie, C.E., Durucan, S. and Korre, A. (2000) River flow prediction using artificial neural networks: generalization beyond the calibration range, *J Hydrol*, 233:138-153.
- Jang, R. (1996) Neuro-Fuzzy and Soft Computing, a tutorial given at the Asian Fuzzy Systems Symposium.
- Johannet, A., Ayral, P. and Vayssade, B. (2007) Modelling non measurable process by neural networks: Forecasting underground flow case study of the Ceze basin (Gard-France), 53-58, Elleithy, K. (editor), *Advances and innovation in Systems, Computing Sciences and Software Engineering*, Springer, 578 p.
- Karahan, H. and Ayvaz, M.T. (2008) Simultaneous parameter identification of a heterogeneous aquifer system using artificial neural networks, *Hydrogeol J*, 16:817-827.
- Kazemi, S.M. and Hosseini, S.M. (2011) Comparison of spatial interpolation methods for estimating heavy metals in sediments of Caspian Sea, *Expert Syst Appl*, 38:1632-1649.
- Kholghi, M. Hosseini, S.M. (2008) Comparison of groundwater level estimation using neuro-fuzzy and ordinary kriging, *Environ Model Assess*, 14:729-737.
- Kuo, Y.M., Liu, C.W. and Lin, K.H. (2004) Evaluation of the ability of an artificial neural network model to assess the variation of groundwater quality in an area of blackfoot disease in Taiwan, *Water Res*, 38:148-158.
- Kurtulus, B. and Razack, M. (2006) Evaluation of the ability of an artificial neural network model to simulate the input-output responses of a large karstic aquifer: the La Rochefoucauld aquifer (Charante, France), *Hydrogeol J*, 15:241-254.
- Kurtulus, B., Flipo, N., Vilain, G., Tournebize, J., Tallec, G. and Goblet, P. (2009) Comparison of ANFIS and ordinary kriging to assess hydraulic head distribution: the Orgeval case study, *Proceedings of the International Joint Conference on Computational Intelligence*, October 5-7, Maderia, 371-378.
- Kurtulus, B. and Razack, M. (2010) Modeling daily discharge responses of a large karstic aquifer using soft computing methods: Artificial neural network and neuro-fuzzy, *J Hydrol*, 381:101-111.

Kurtulus B. and Flipo, N. (2012) Hydraulic head interpolation using ANFIS – model selection and sensitivity analysis, *Comput Geosci*, 38:43-51.

Lallaheem, S. and Mania, J. (2003) A nonlinear rainfall-runoff model using neural network technique: example in fractured porous media, *Math Comput Model*, 37(9-10):1047-1061.

Ledoux, E., Gomez, E., Monget, J., Viavattene, C., Viennot, P., Ducharne, A., Benoit, M., Mignolet, C., Schott, C. and Mary, B. (2007) Agriculture and Groundwater nitrate contamination in the Seine basin, The STICS-MODCOU modelling chain, *Sci Total Environ*, 375:33-47.

Lin, G.F. and Chen, L.H. (2004) A spatial interpolation method based on radial basis function networks incorporating a semivariogram model, *J Hydrol*, 288(3-4):288-298.

Liu, Z., Peng, C., Xiang, W., Deng, X., Tian, D. and Zhao, M. (2012) Simulations of runoff and evapotranspiration in Chinese fir plantation ecosystems using artificial neural networks, *Ecol Model*, 226:71-76.

Lyon, S., Seibert, J., Lembo, A., Walter, M. and Steenhuis, T. (2006) Geostatistical investigation into the temporal evolution of spatial structure in a shallow water table, *Hydrol Earth Syst Sc*, 10(1):113-125.

Makkeasorn, A., Chang, N.B. and Zhou, X. (2008) Short-term streamflow forecasting with global climate change implications – A comparative study between genetic programming and neural network models, *J Hydrol*, 352:336-354.

Minns, A.W. and Hall, M.J. (1996) Artificial neural networks as rainfall runoff models, *Hydrolog Sci J*, 41(3):399-417.

Morshed, J. and Kaluarachchi, J.J. (1998) Application of artificial neural network and genetic algorithm in flow and transport simulations, *Adv Water Resour*, 22(2):145-158.

Pardo-Iguzquiza, E., Chica-Olmo, M., Garcia-Soldado, M. and Luque-Espinar, J.A. (2009) Using semivariogram parameter uncertainty in hydrogeological applications, *Ground Water*, 47(1):25-34.

- Rajurkar, M.P., Kothyari, U.C. and Chaube, U.C. (2004) Modeling of the daily rainfall-runoff relationship with artificial neural network, *J Hydrol*, 285:96-113.
- Rampone, S. (2013) Three-and-six-month-before forecast of water resources in a karst aquifer in the Terminia massif (Southern Italy), *Appl Soft Comput*, 13:4077-4086.
- Ranjithan, R.S., Eheart, D.E. and Garrett, J.H. (1995) Application of neural network in groundwater remediation under conditions of uncertainty, 133-144, Kundzewicz (editor), *New uncertainty concepts in hydrology and water resources*, Cambridge University Press, New York, 322.
- Renard, F. and Jeannee, N. (2008) Estimating transmissivity fields and their influence on flow and transport: The case of Champagne Mounts, *Water Resour Res*, 44:1-12.
- Rogers, L.L., Dowla, F.U. and Johnson, V.M. (1995) Optimal field scale groundwater remediation using neural networks and the genetic algorithm, *Environ Sci Technol*, 29(5):1145-1155.
- Sajikumar, N. and Thandaveswara, B.S. (1999) A nonlinear rainfall-runoff model using an artificial neural network, *J Hydrol*, 216:32-55.
- Samani, N., Gohari-Moghadam, M. and Safavi, A. (2007) A simple neural network model for the determination of aquifer parameters, *J Hydrol*, 340:1-11.
- Shamseldin, A.Y. (1997) Application of a neural technique to rainfall-runoff modelling, *J Hydrol*, 199:272-294.
- Siou, L.K.A., Cros, K., Johannet, A., Borrell-Estudina, V. and Pistre, S. (2013) Knox method, or Knowledge eXtraction from neural network model. Case study on the Lez karst aquifer (southern France), *J Hydrol*, 507:19-32.
- Sun, Y., Kang, S., Li, F. and Zhang, L. (2009) Comparison of interpolation methods for depth to groundwater and its temporal and spatial variations in the Minqin Oasis of Northwest China, *Environ Model Softw*, 24(10):1163-1170.

Taormina, R., Chau, K.W. and Sethi, R. (2012) Artificial neural network simulation of hourly groundwater levels in a coastal aquifer system of the Venice lagoon, *Eng Appl Artif Intel*, 25:1670-1676.

Theodosiou, N. and Latinopoulos, P. (2006) Evaluation and optimisation of groundwater observation networks using the kriging methodology, *Environ Modell Softw*, 21(7):991-1000.

Tutmez, B., Hatipoglu, Z. and Kaymak, U. (2009) Modelling electrical conductivity of groundwater using an adaptive neuro-fuzzy inference system, *Comput Geosci*, 32(4):421-433.

Yan, S. and Minsker, B. (2006) Optimal groundwater remediation design using an adaptive neural network genetic algorithm, *Water Resour Res*, 42(5):W05407.

APPENDICES

Appendix A. EBK Interpolation For Salinity and Specific Conductance For Köyceğiz Lake

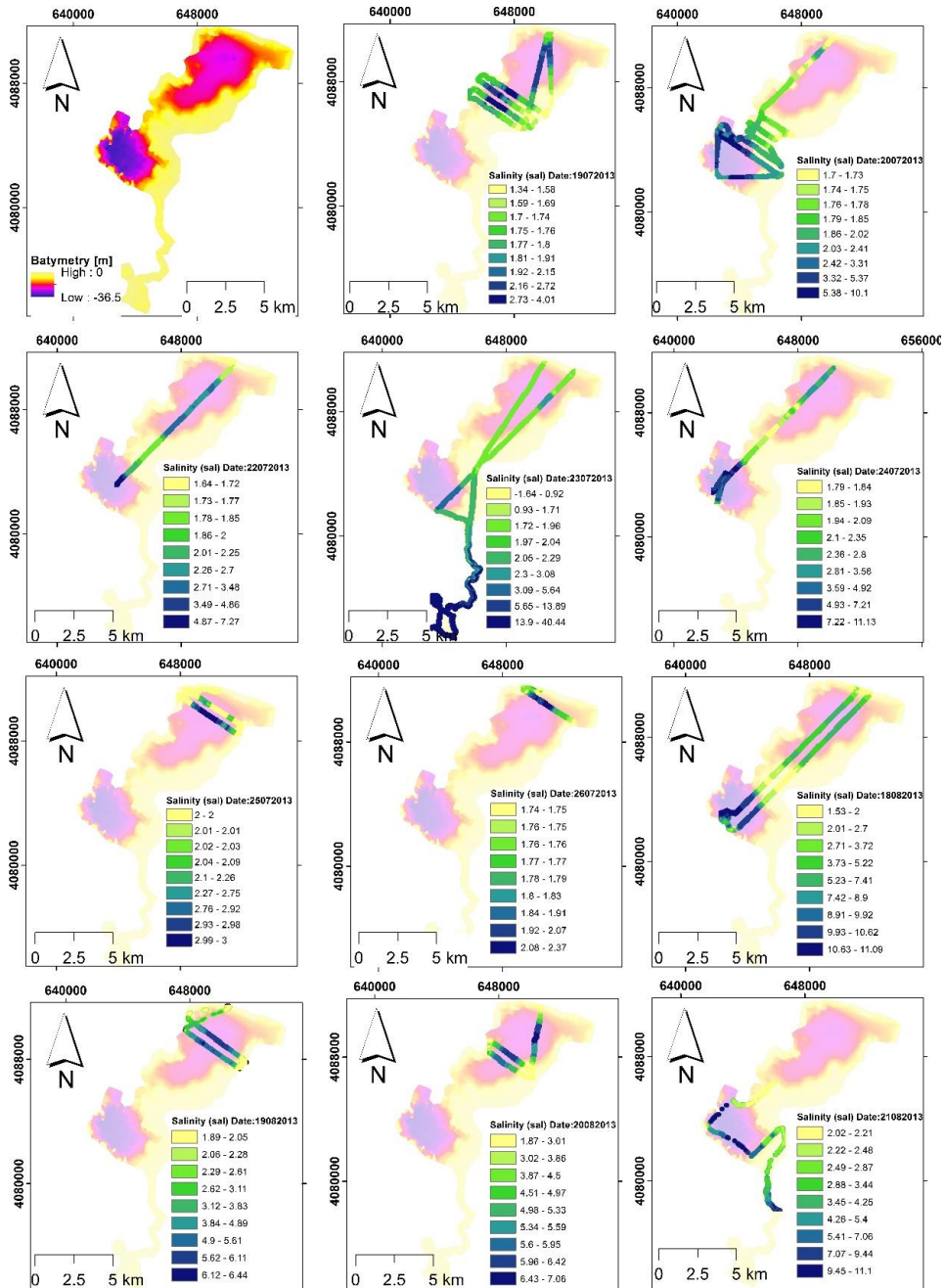


Figure A 1.EBK interpolation for salinity at depth of Köyceğiz Lake

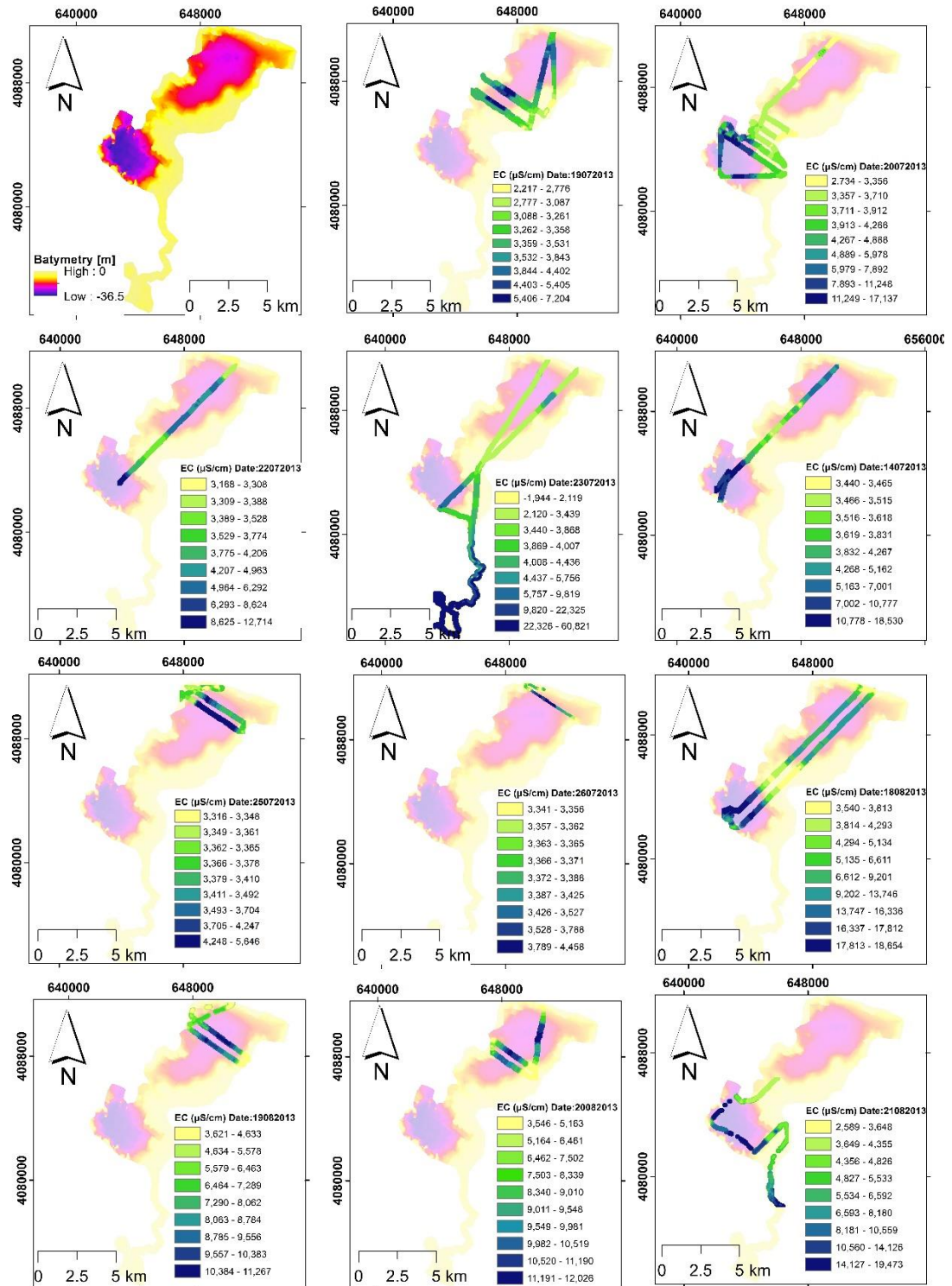


Figure A 2.EBK interpolation for Specific Conductivity at depth of Köyceğiz Lake

Appendix B. EBK Interpolations Maps for Specific Conductance, pH and salinity for Fethiye-Göcek Bay

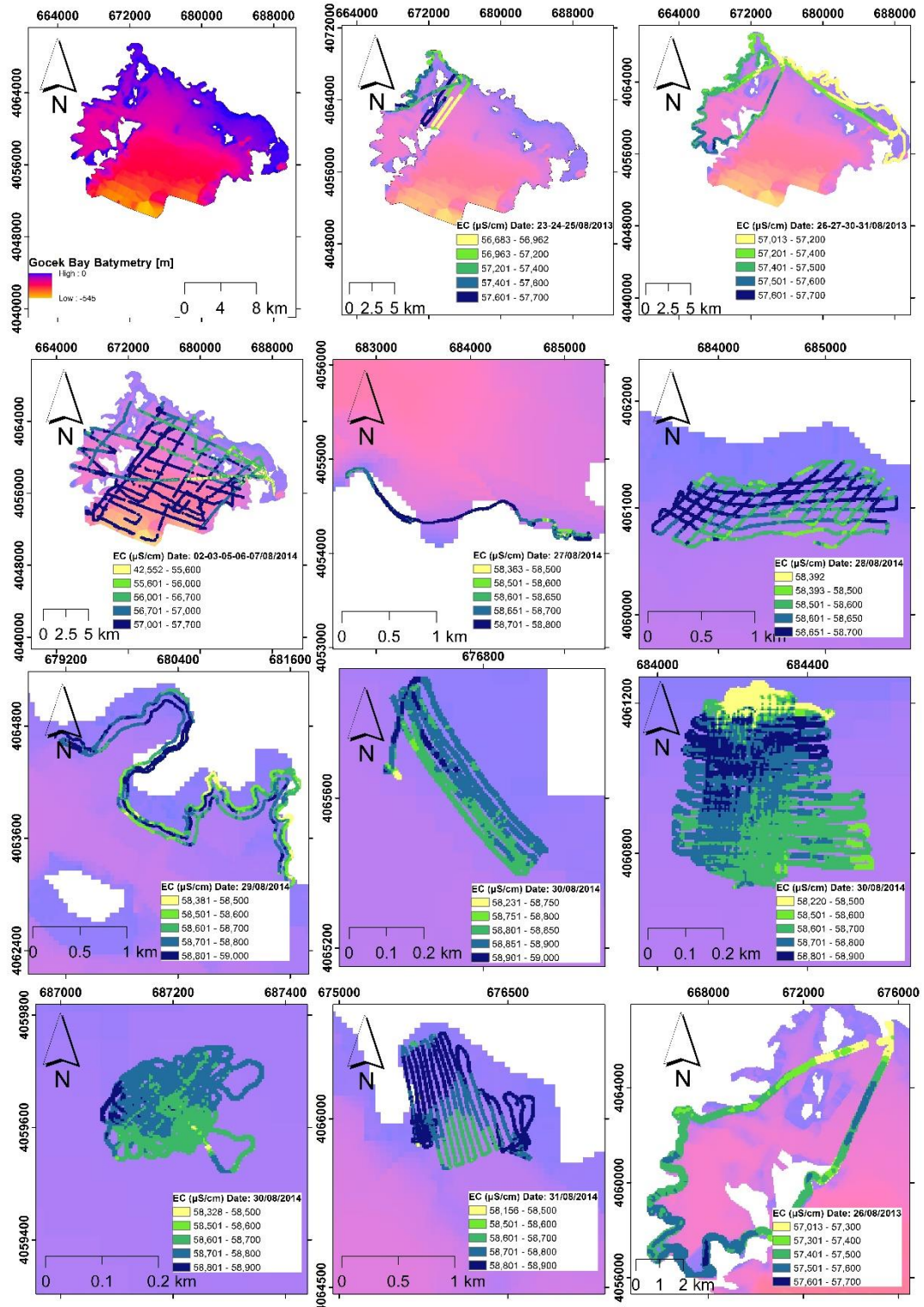


Figure B 1.EBK interpolation for Specific Conductivity at depth of Fethiye-Göcek Bay

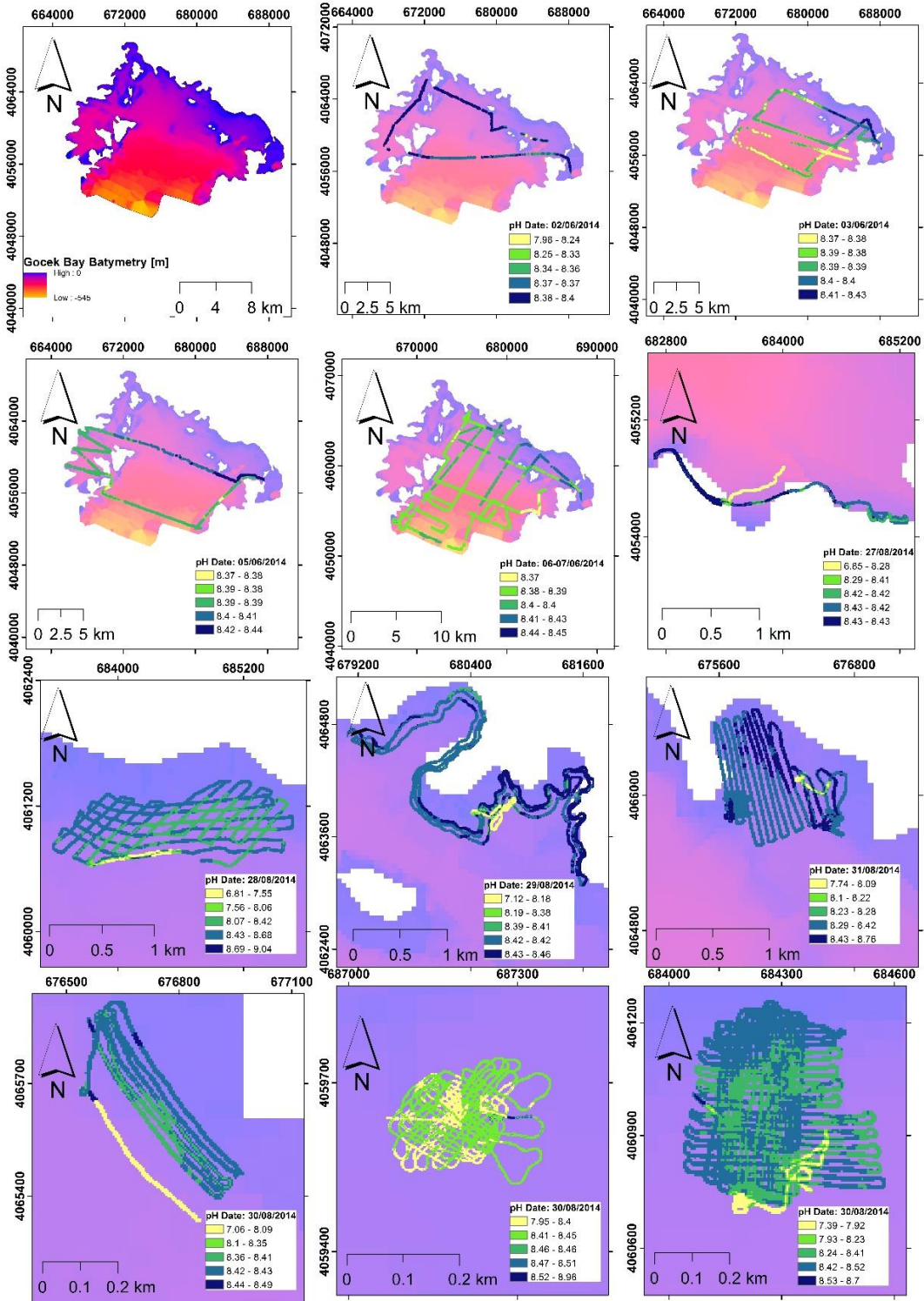


Figure B 2.EBK interpolation for pH at depth of Fethiye-Göcek Bay

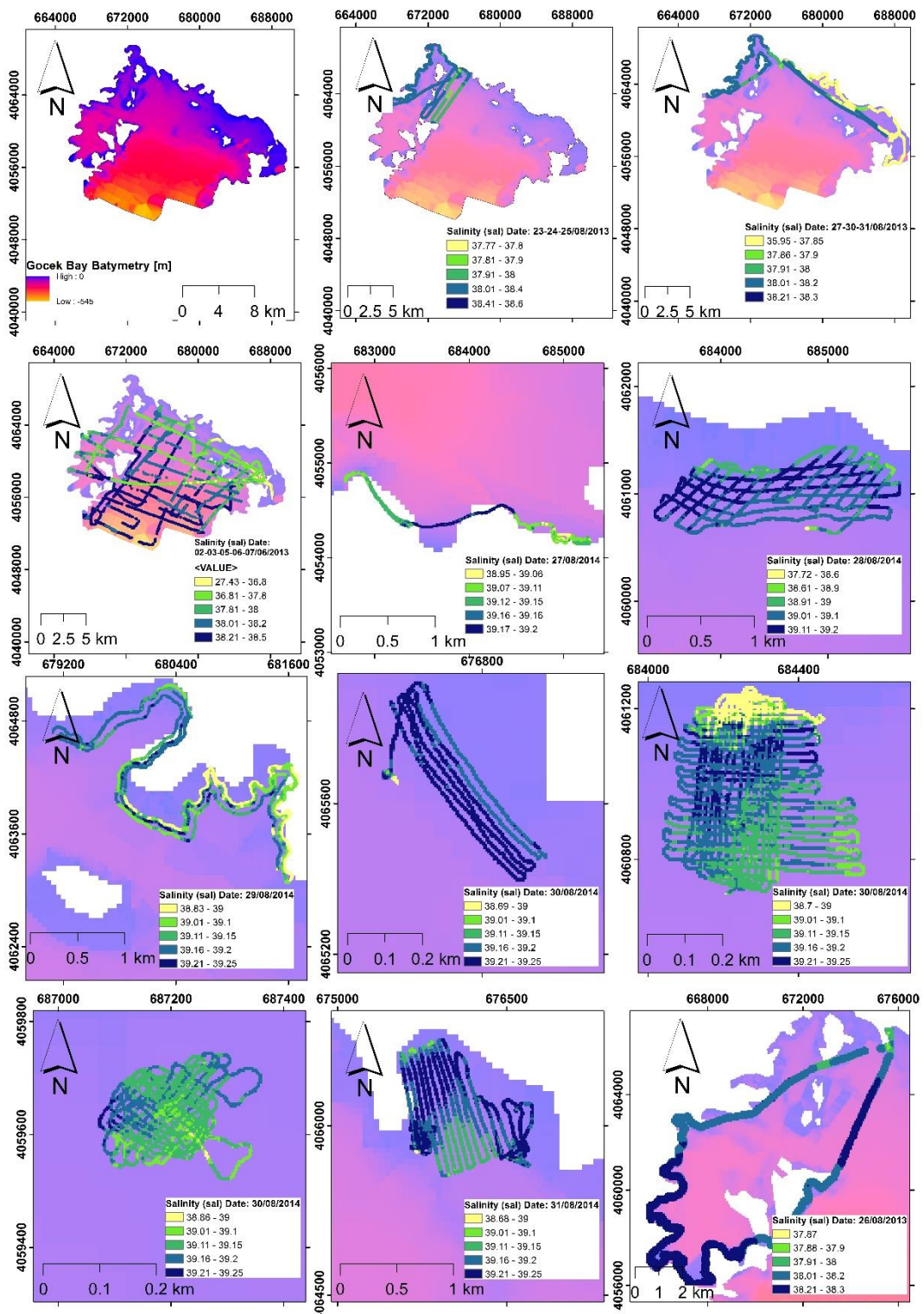


Figure B 3.EBK interpolation for salinity at depth of Fethiye- Göcek Bay

Appendix C. EBK Error Maps and Variograms for Köyceğiz Lake

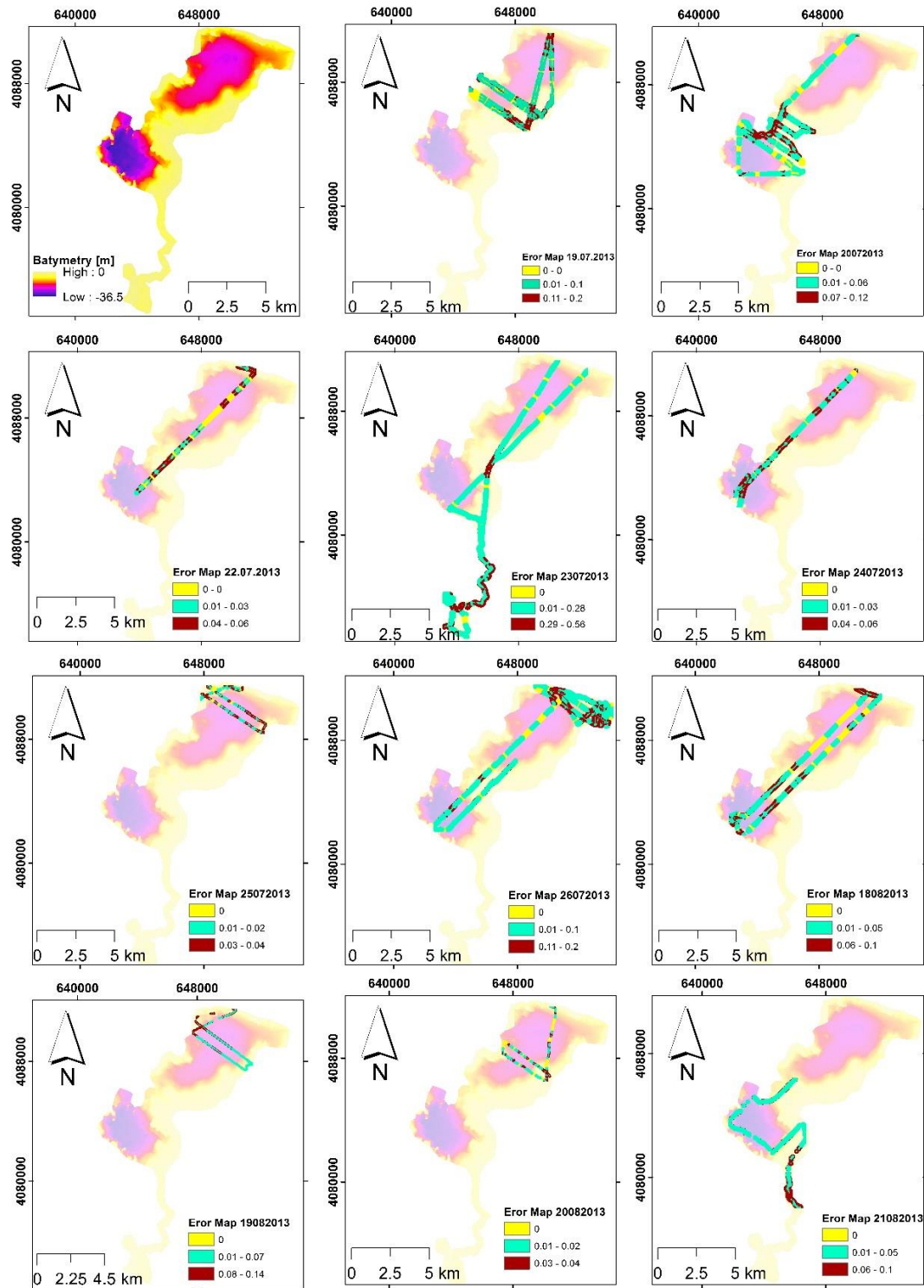


Figure C 1.The surface temperature error map of Köyceğiz Lake

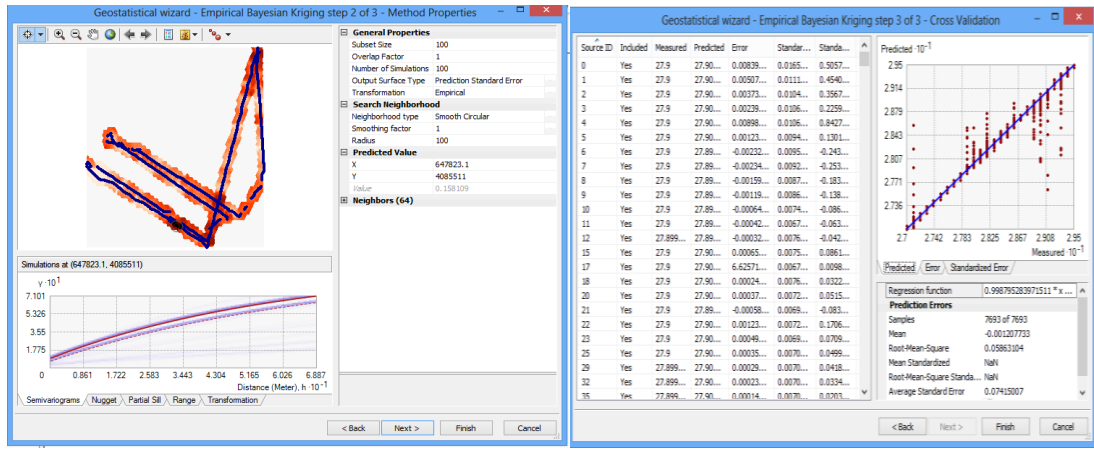


Figure C 2.The surface temperature variogram of Köyceğiz Lake in 19.07.2013

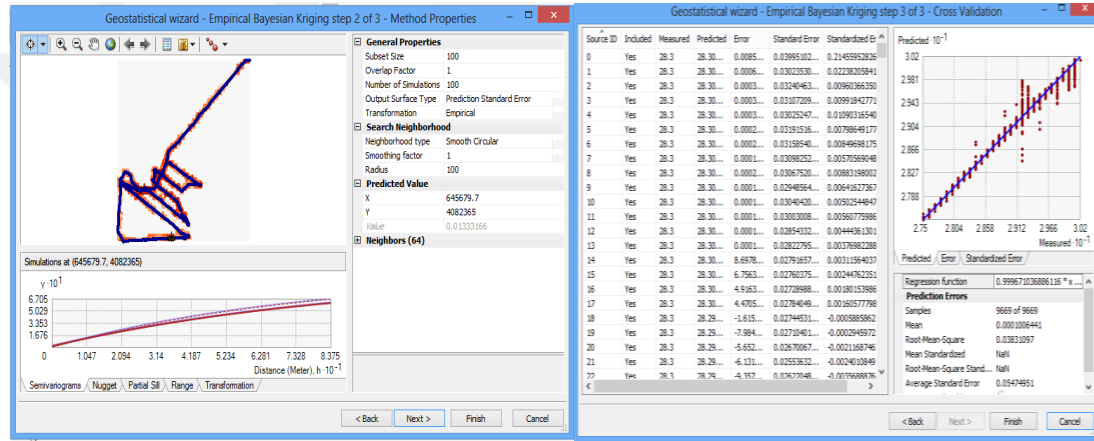


Figure C 3.The surface temperature variogram of Köyceğiz Lake in 20.07.2013

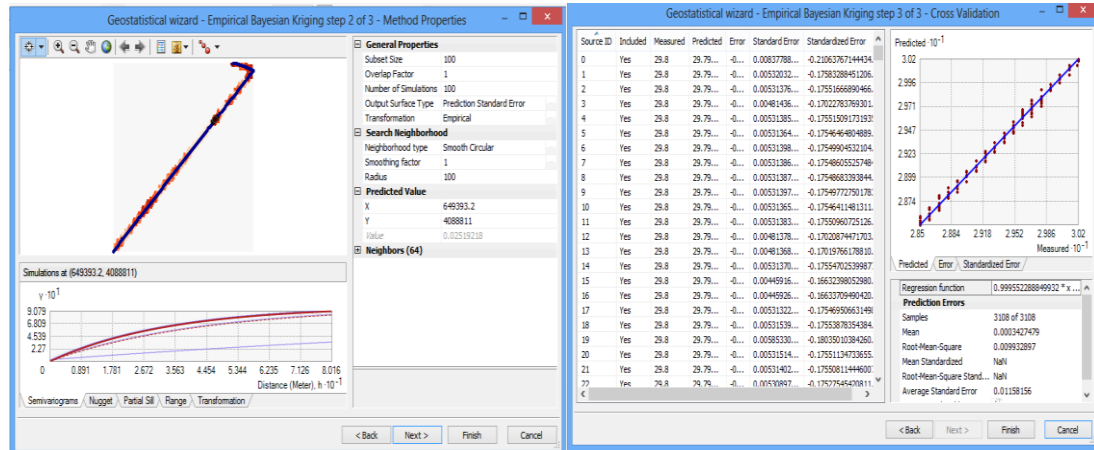


Figure C 4.The surface temperature variogram of Köyceğiz Lake in 22.07.2013

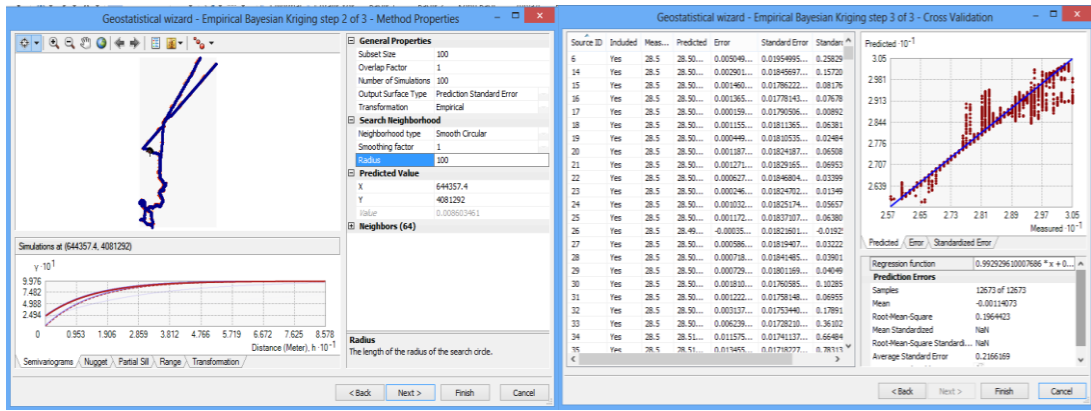


Figure C 5.The surface temperature variogram of Köyceğiz Lake in 23.07.2013

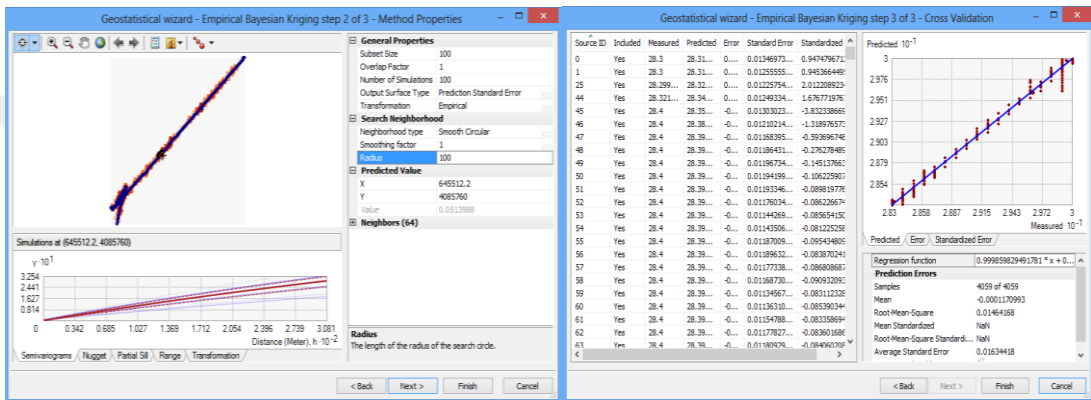


Figure C 6.The surface temperature variogram of Köyceğiz Lake in 24.07.2013

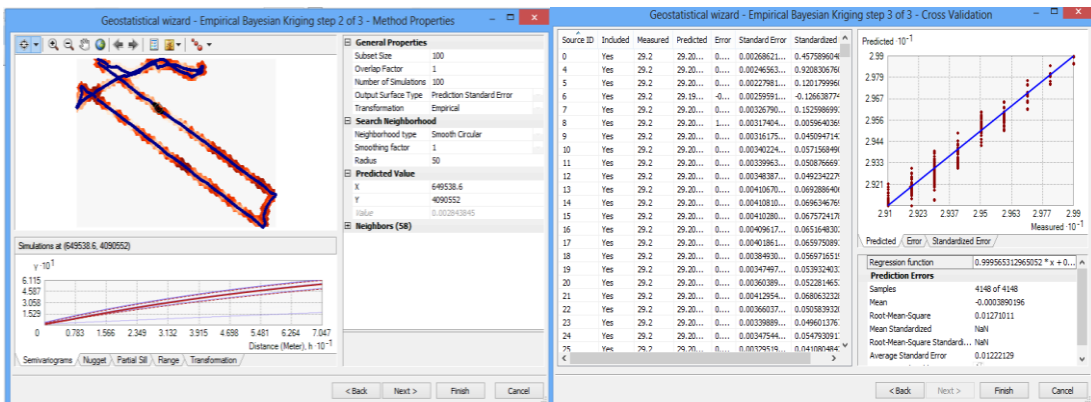


Figure C 7.The surface temperature variogram of Köyceğiz Lake in 25.07.2013

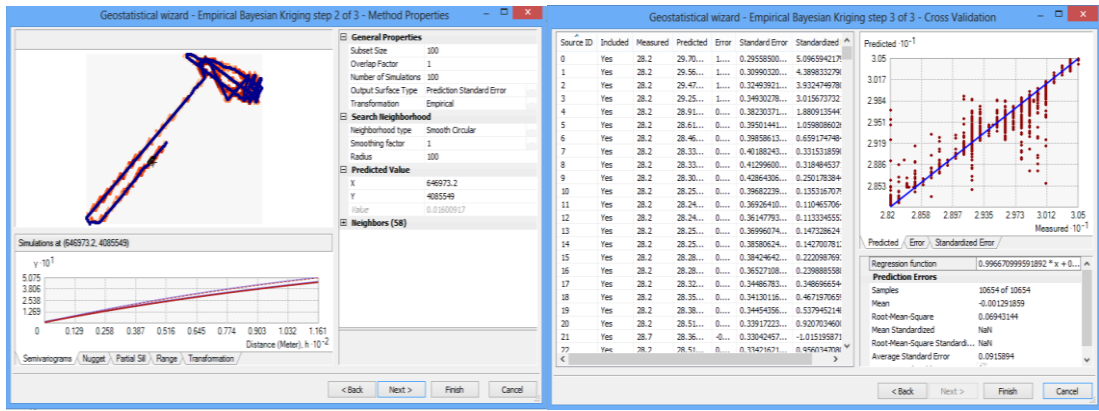


Figure C 8.The surface temperature variogram of Köyceğiz Lake in 26.07.2013

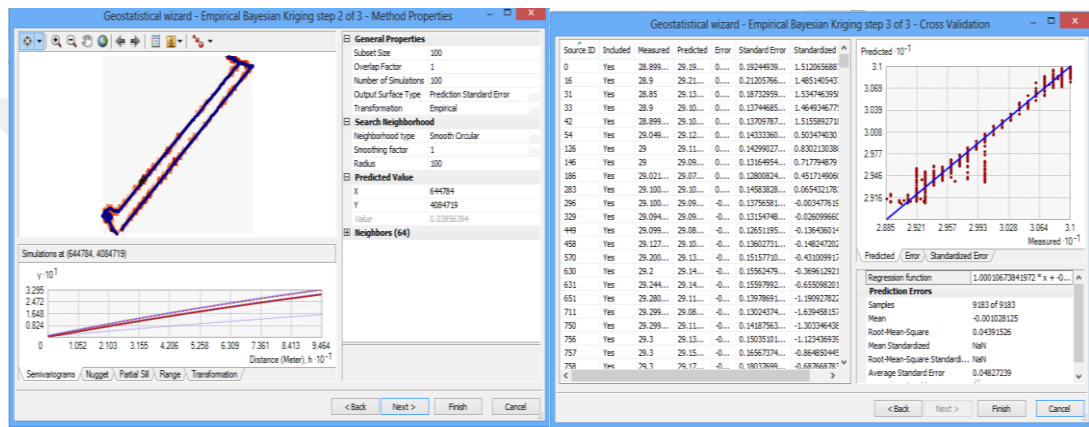


Figure C 9.The surface temperature variogram of Köyceğiz Lake in 18.08.2013

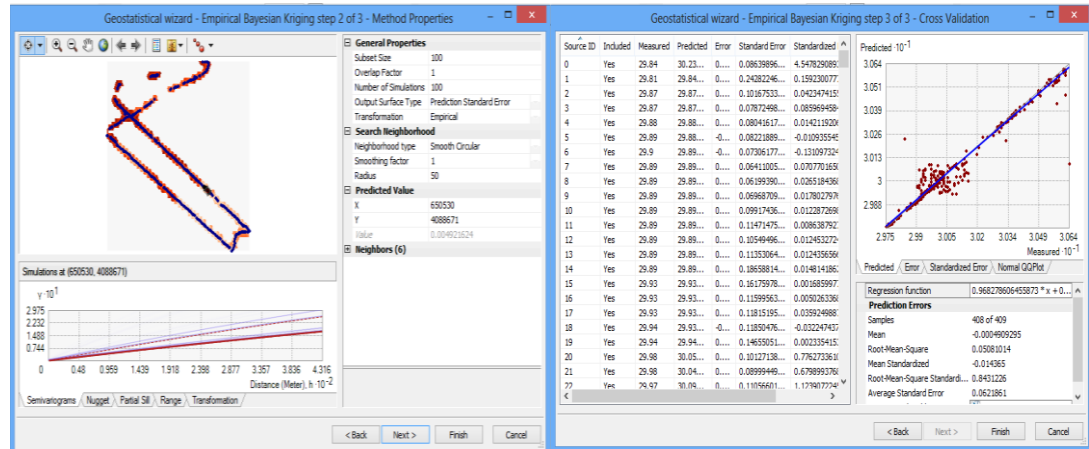


Figure C 10.The surface temperature variogram of Köyceğiz Lake in 19.08.2013

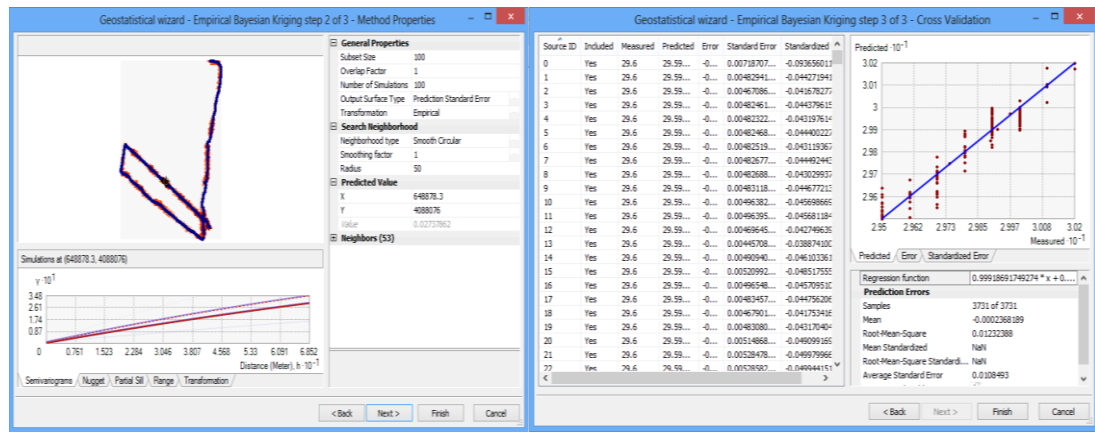


Figure C 11.The surface temperature variogram of Köyceğiz Lake in 20.08.2013

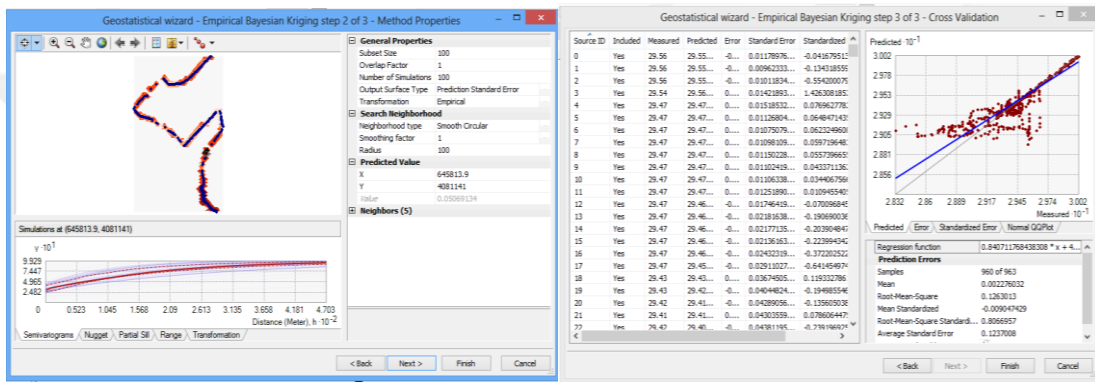


Figure C 12.The surface temperature variogram of Köyceğiz Lake in 21.08.2013

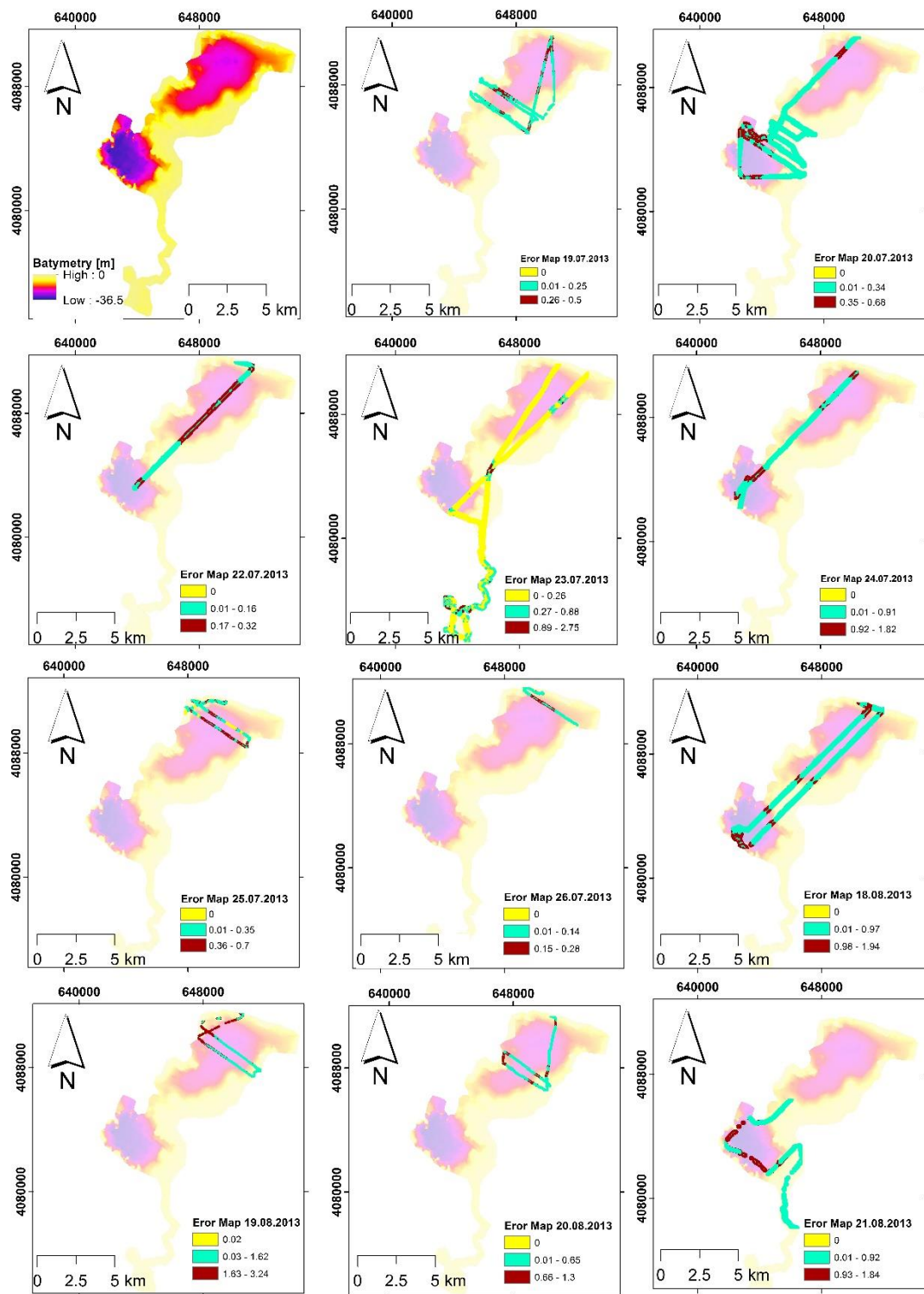


Figure C 13.The depth temperature eror map of Köyceğiz Lake

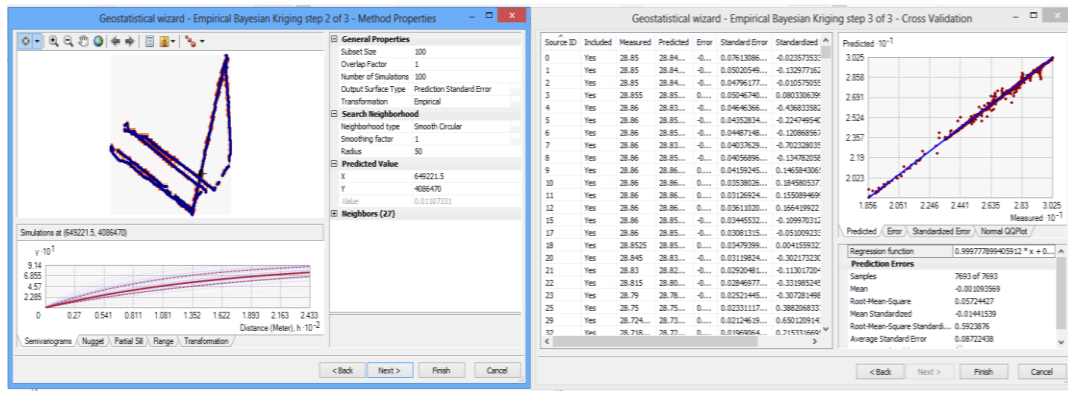


Figure C 14.The depth temperature variogram of Köyceğiz Lake in 19.07.2013

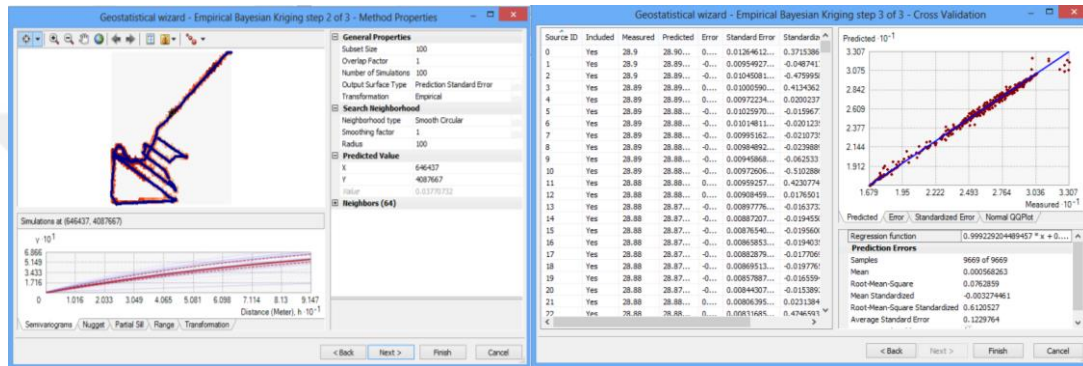


Figure C 15.The depth temperature variogram of Köyceğiz Lake in 20.07.2013

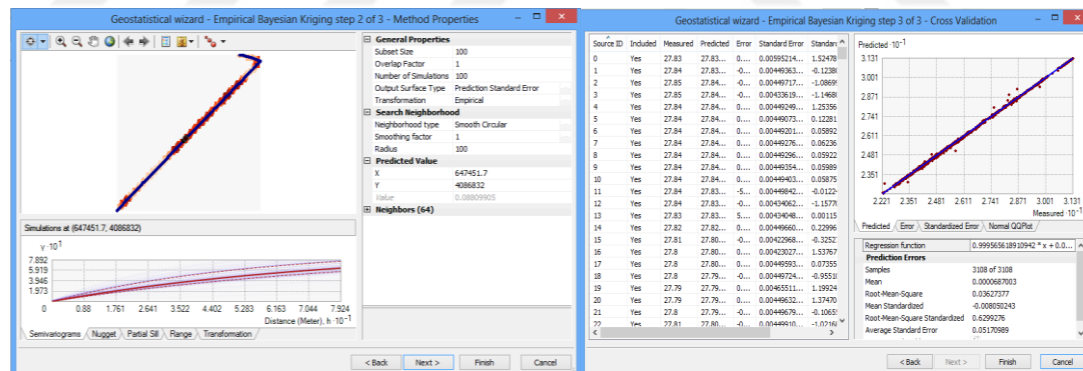


Figure C 16.The depth temperature variogram of Köyceğiz Lake in 22.07.2013

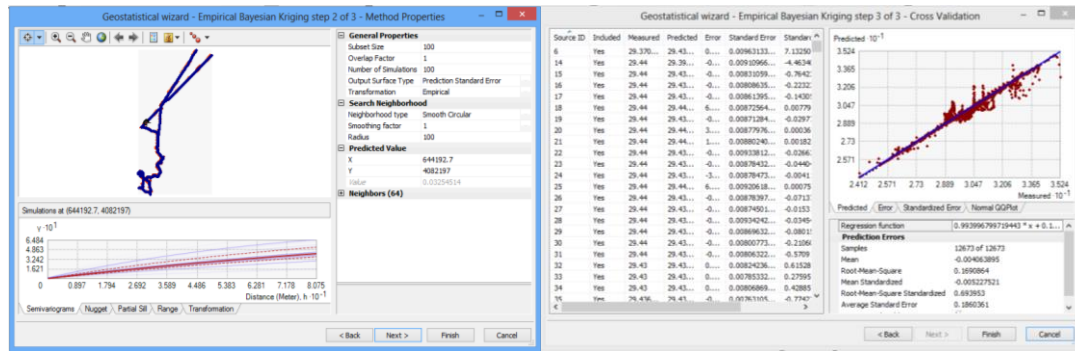


Figure C 17.The depth temperature variogram of Köyceğiz Lake in 23.07.2013

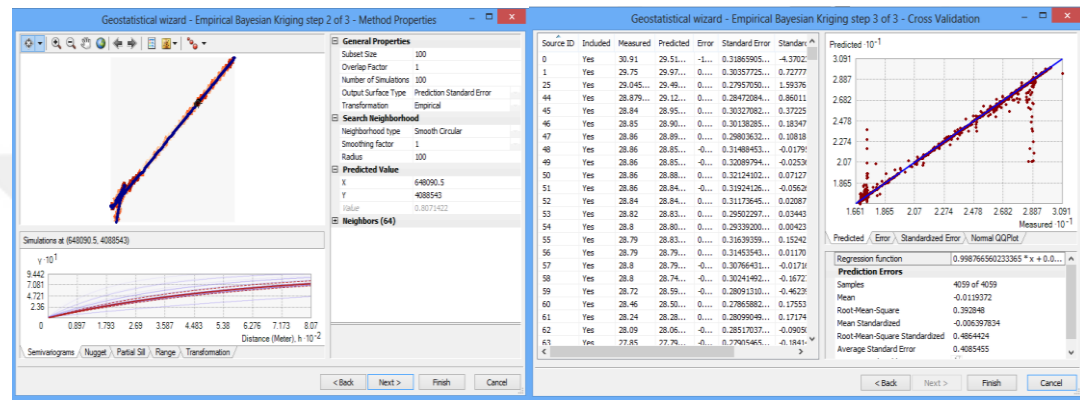


Figure C 18.The depth temperature variogram of Köyceğiz Lake in 24.07.2013

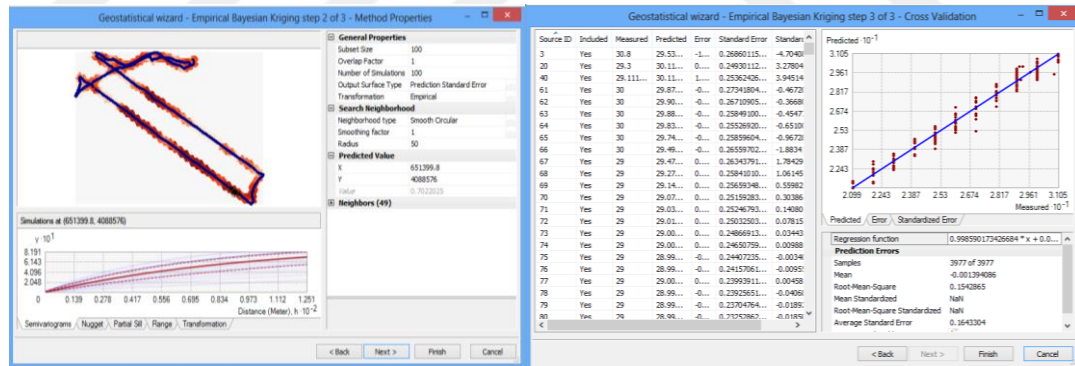


Figure C 19.The depth temperature variogram of Köyceğiz Lake in 25.07.2013

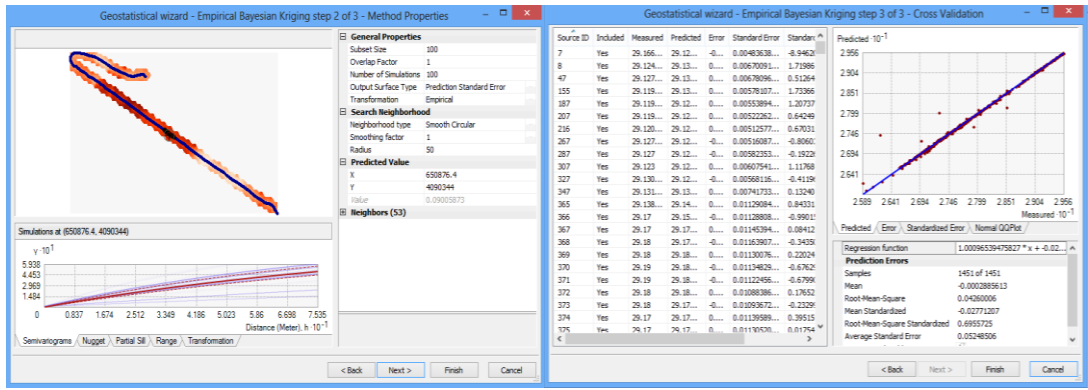


Figure C 20.The depth temperature variogram of Köyceğiz Lake in 26.07.2013

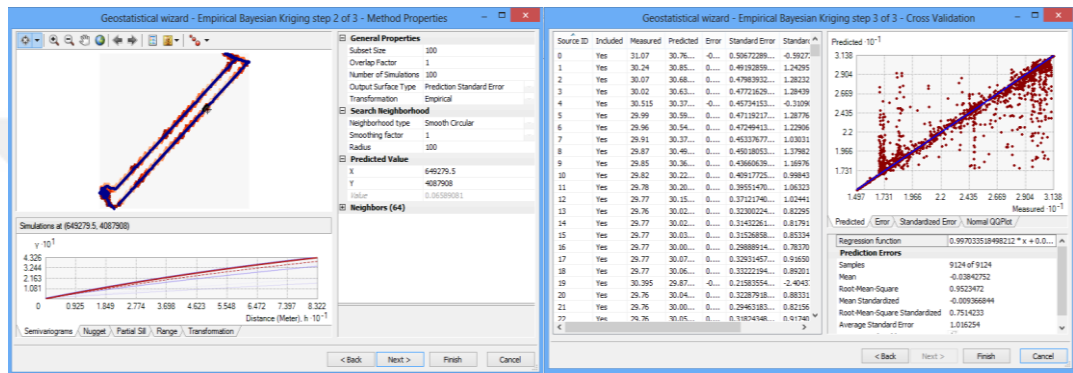


Figure C 21.The depth temperature variogram of Köyceğiz Lake in 18.08.2013

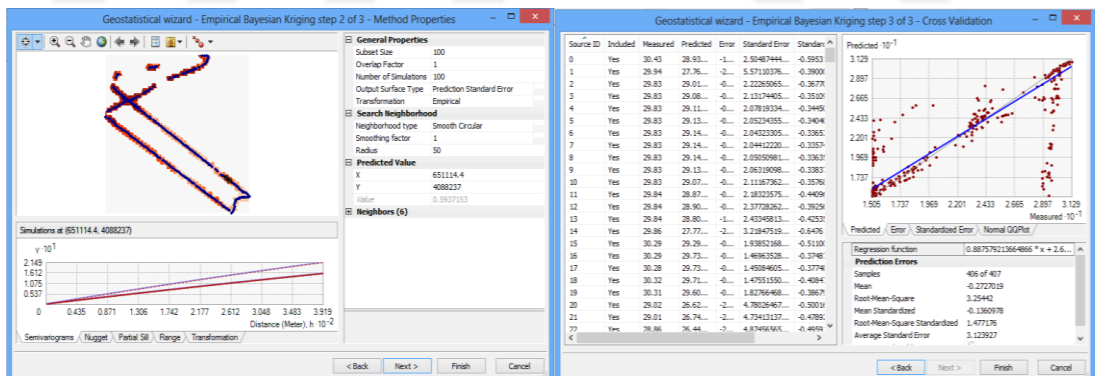


Figure C 22.The depth temperature variogram of Köyceğiz Lake in 19.08.2013

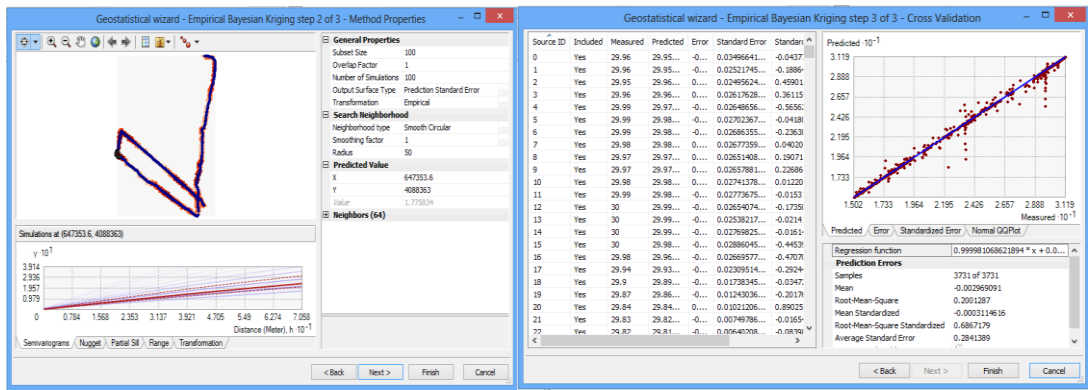


Figure C 23.The depth temperature variogram of Köyceğiz Lake in 20.08.2013

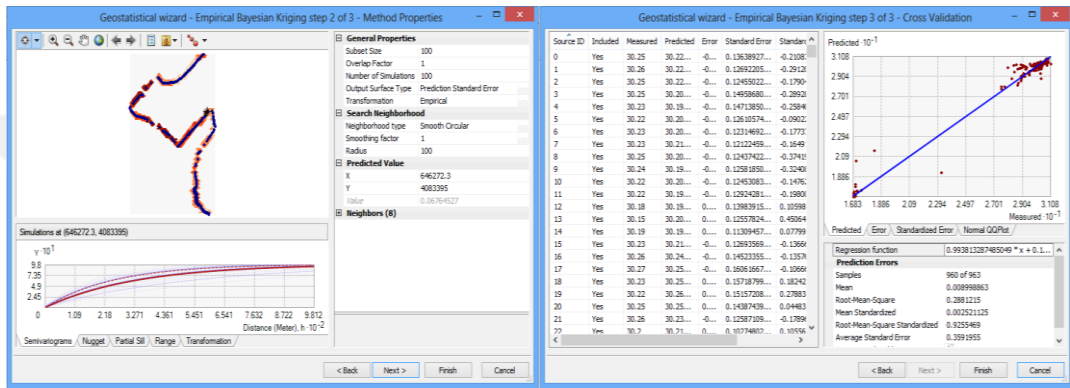


Figure C 24.The depth temperature variogram of Köyceğiz Lake in 21.08.2013

Appendix D. EBK error maps and variograms for Fethiye-Göcek Bay

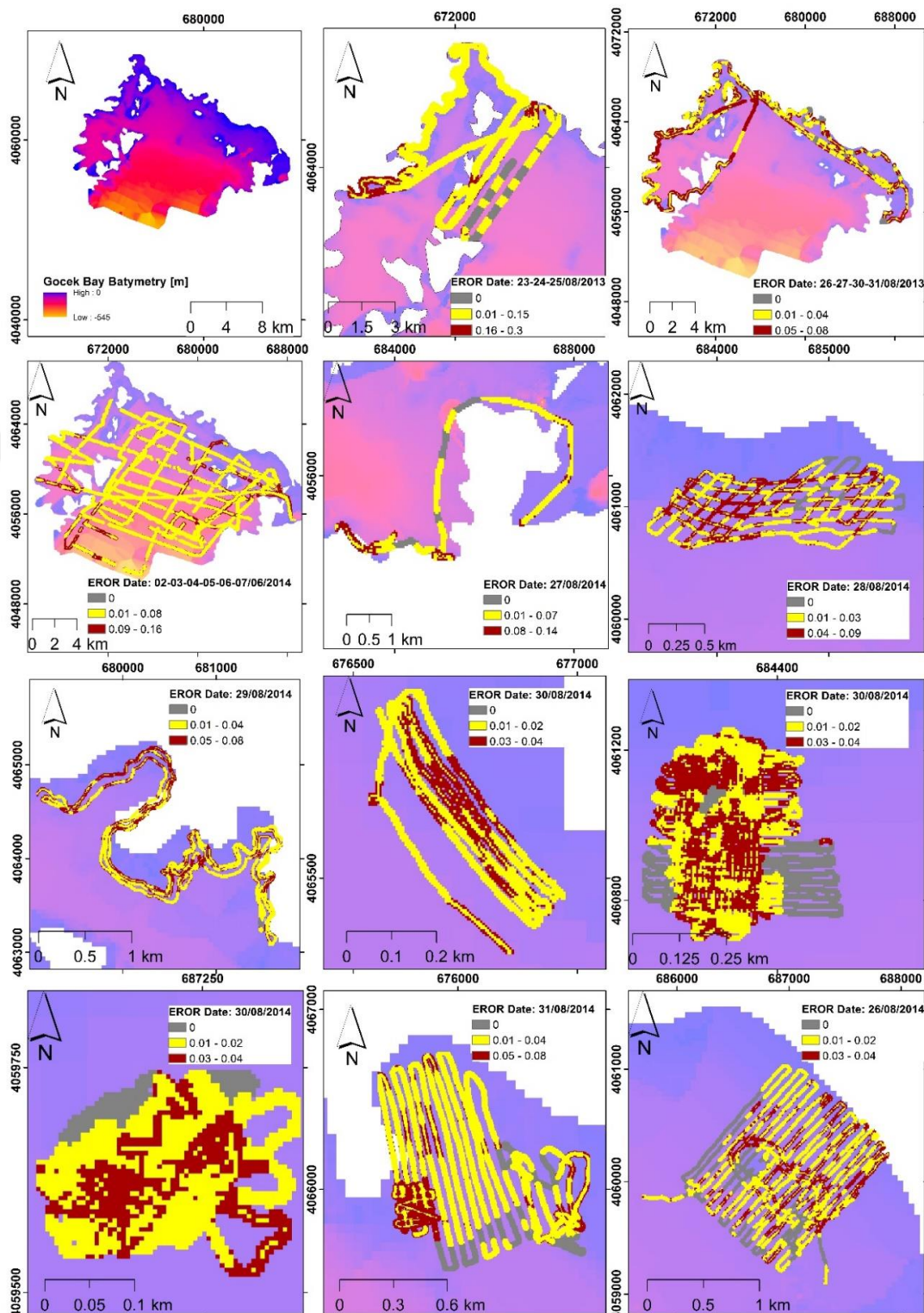


Figure D 1.The surface temperature eror map of Fethiye-Göcek Bay

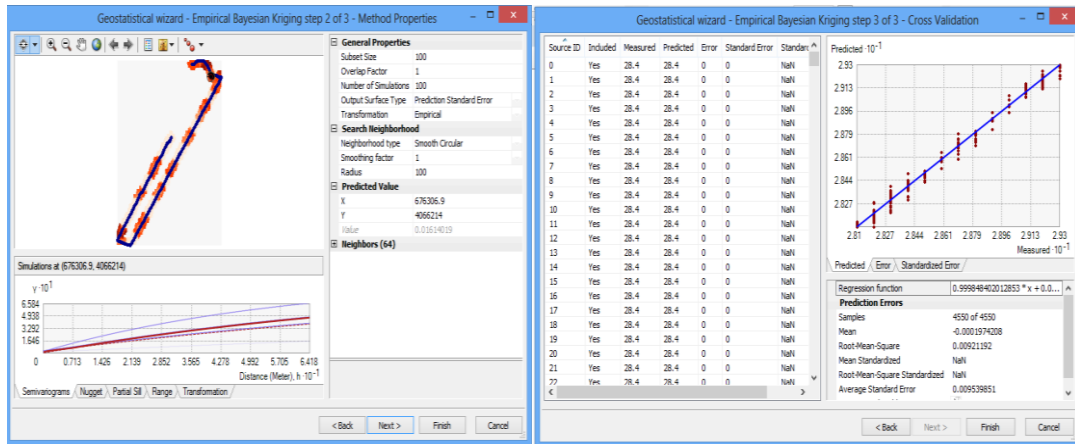


Figure D 2.The surface temperature variogram of Fethiye-Göcek Lake in 23.08.2013

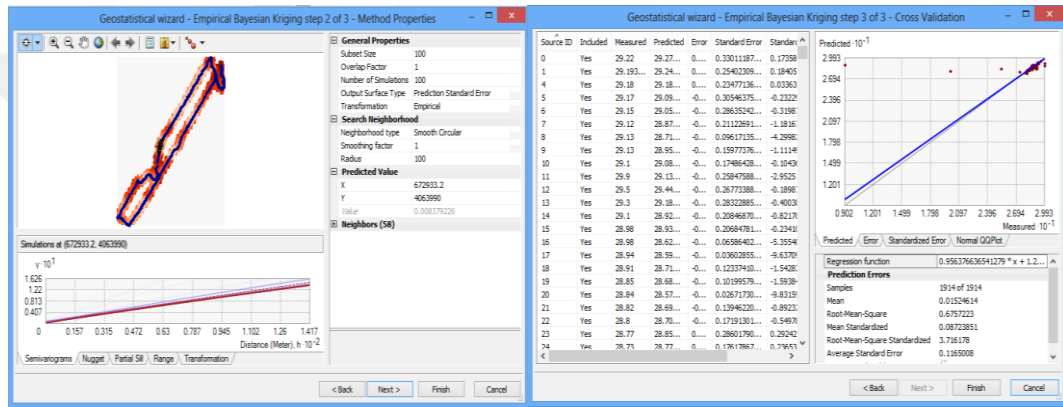


Figure D 3.The surface temperature variogram of Fethiye-Göcek Lake in 24.08.2013

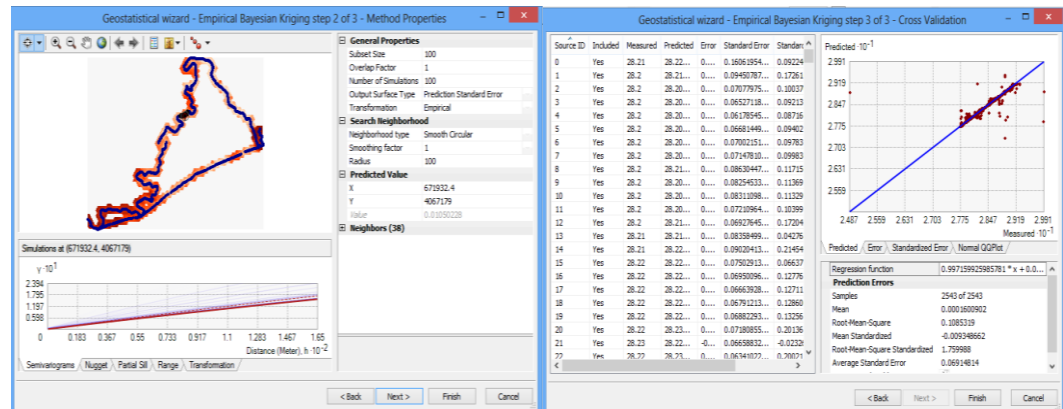


Figure D 4.The surface temperature variogram of Fethiye-Göcek Lake in 25.08.2013

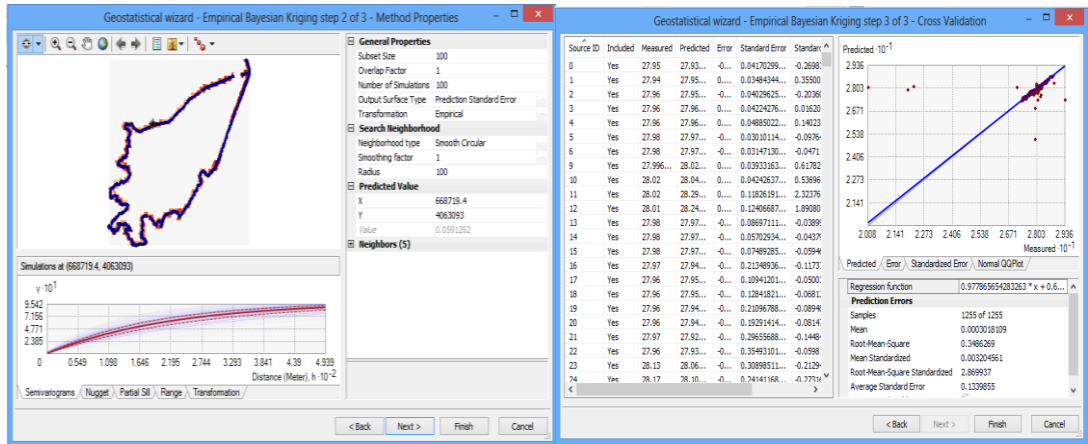


Figure D 5.The surface temperature variogram of Fethiye-Göcek Lake in 26.08.2013

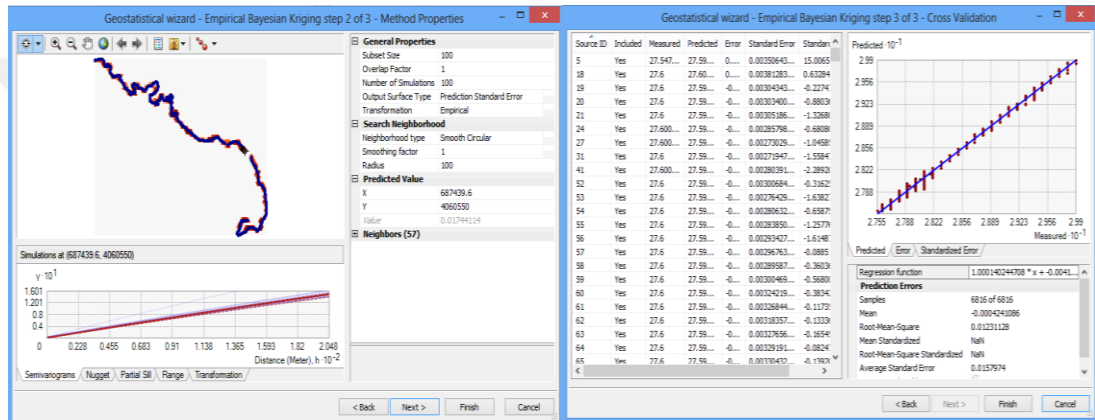


Figure D 6.The surface temperature variogram of Fethiye-Göcek Lake in 27.08.2013

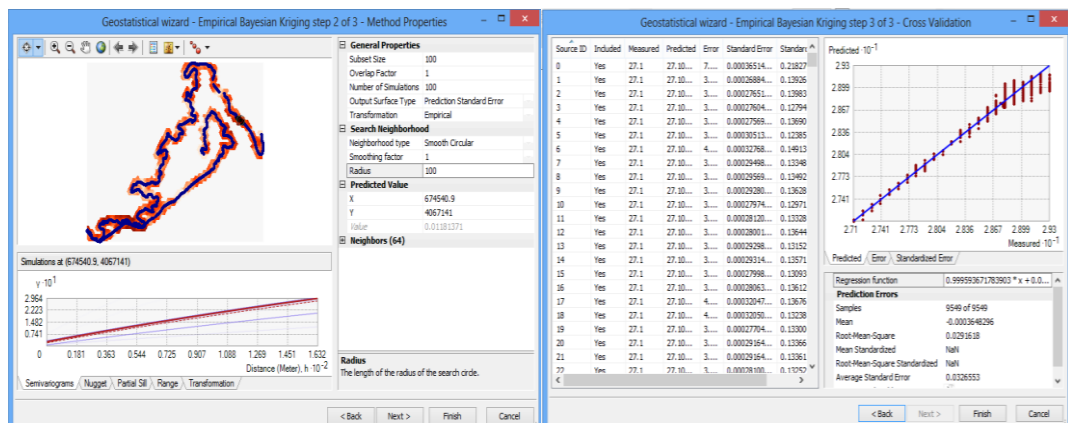


Figure D 7.The surface temperature variogram of Fethiye-Göcek Lake in 30.08.2013

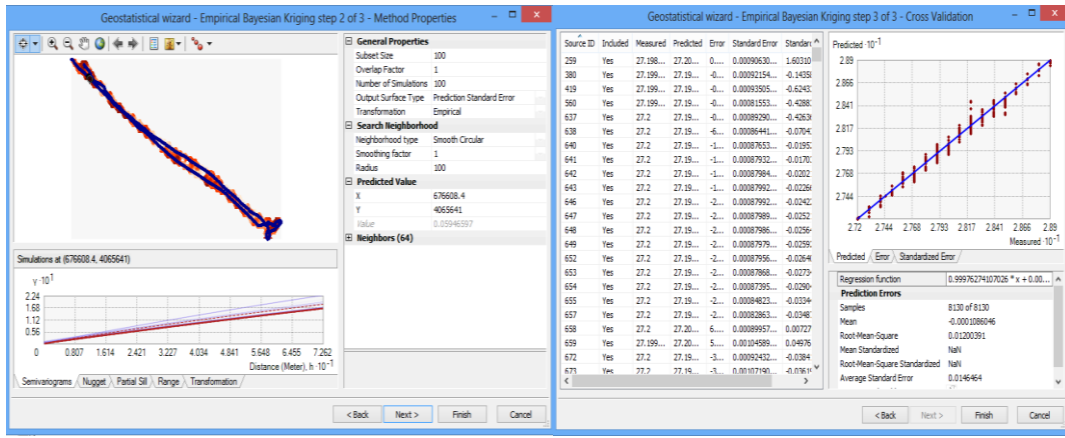


Figure D 8.The surface temperature variogram of Fethiye-Göcek Lake in 31.08.2013

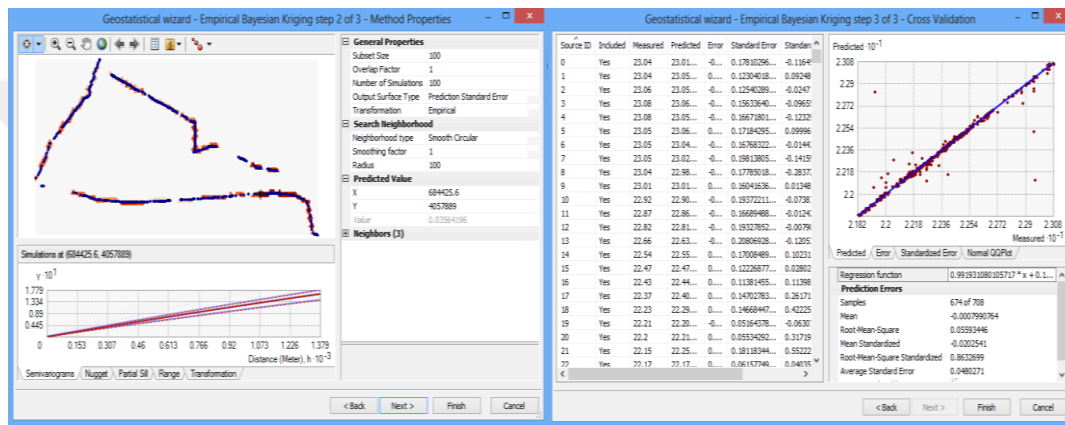


Figure D 9.The surface temperature variogram of Fethiye-Göcek Lake in 03.06.2014

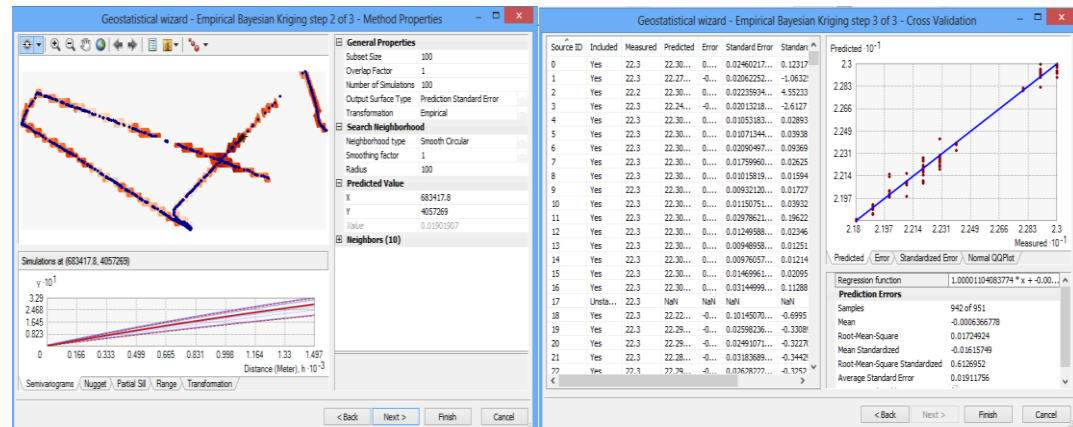


Figure D 10.The surface temperature variogram of Fethiye-Göcek Lake in 04.06.2014

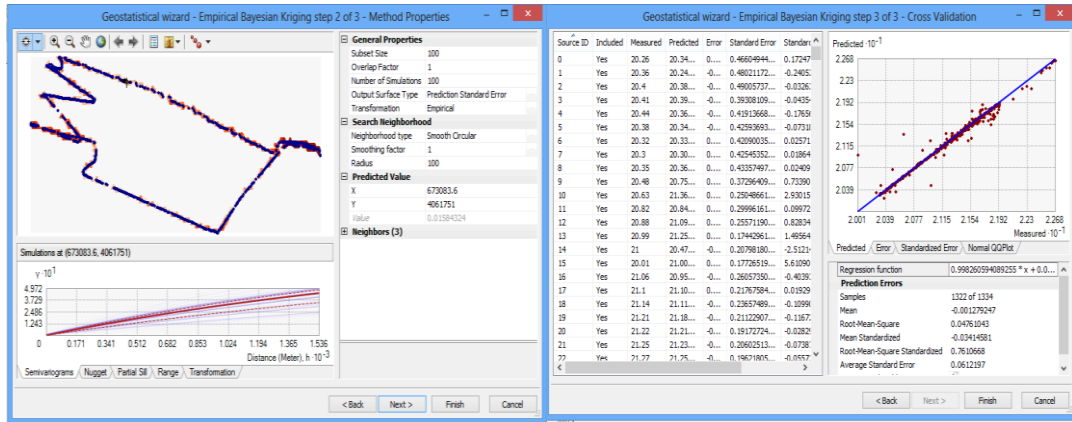


Figure D 11.The surface temperature variogram of Fethiye-Göcek Lake in 05.06.2014

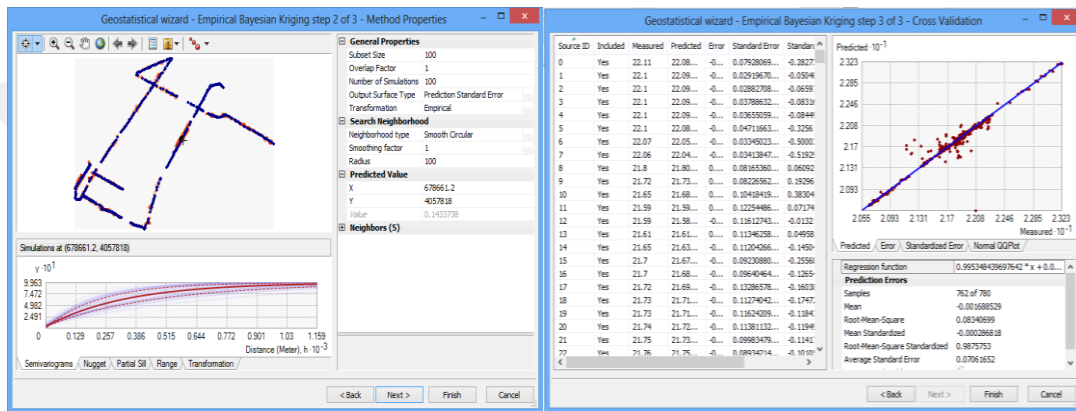


Figure D 12.The surface temperature variogram of Fethiye-Göcek Lake in 06.06.2014

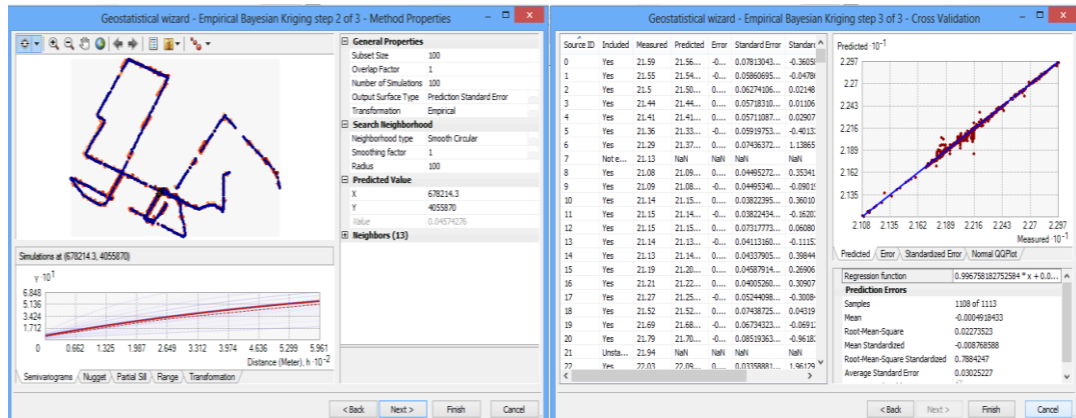


Figure D 13.The surface temperature variogram of Fethiye-Göcek Lake in 07.06.2014

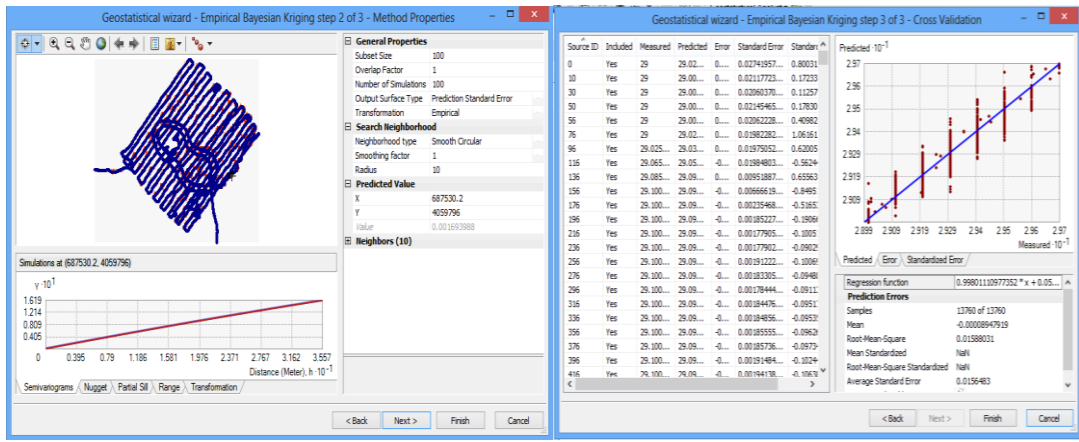


Figure D 14.The surface temperature variogram of Fethiye-Göcek Lake in 26.08.2014

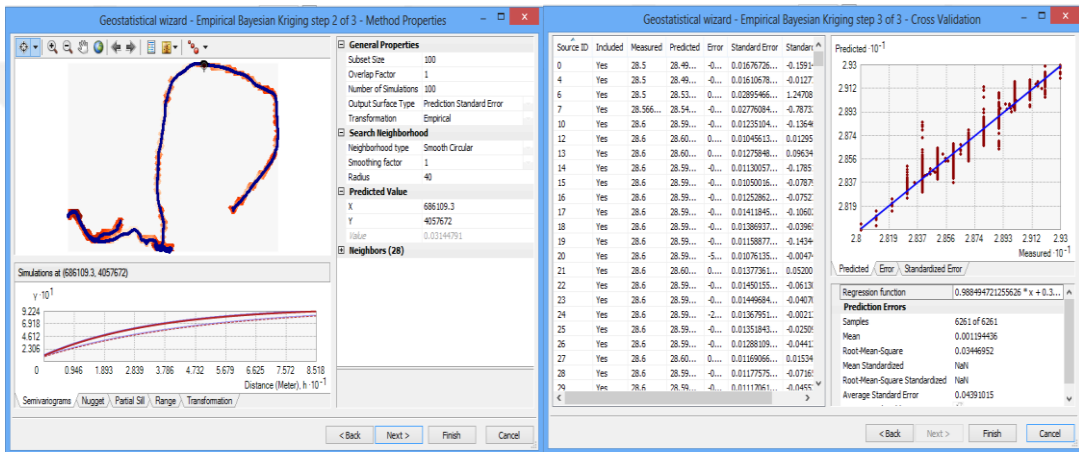


Figure D 15.The surface temperature variogram of Fethiye-Göcek Lake in 27.08.2014

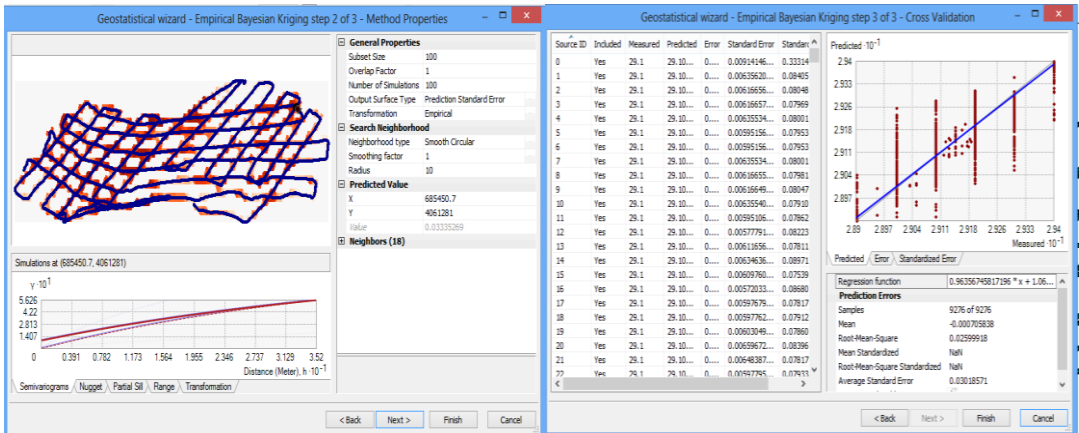


Figure D 16.The surface temperature variogram of Fethiye-Göcek Lake in 28.08.2014

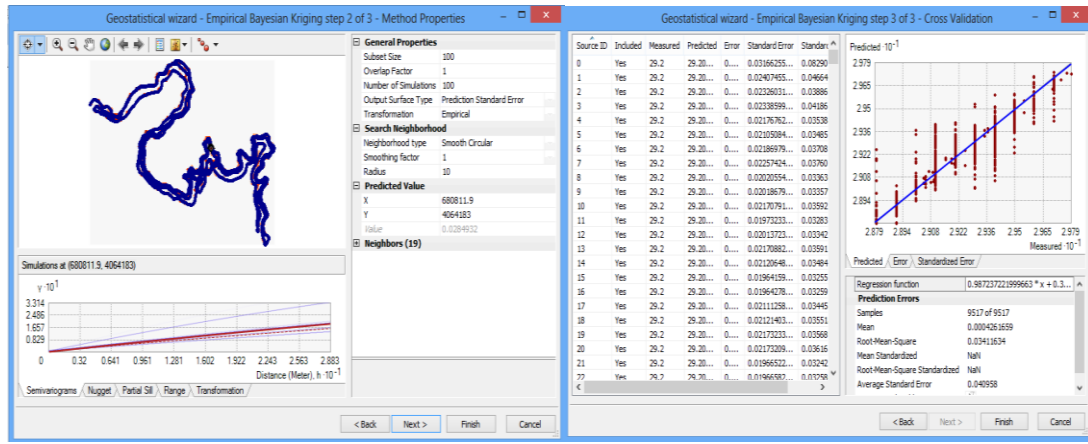


Figure D 17.The surface temperature variogram of Fethiye-Göcek Lake in 29.08.2014

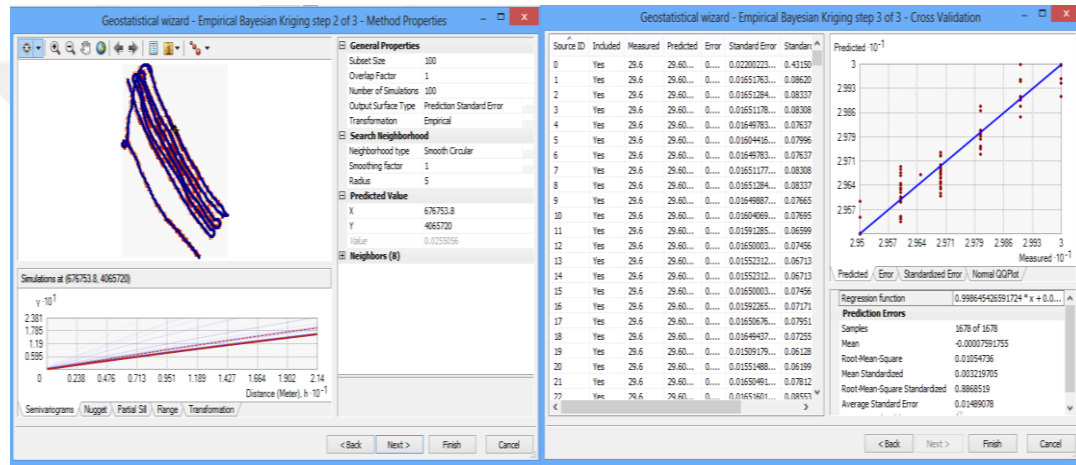


Figure D 18.The surface temperature variogram of Fethiye-Göcek Lake in 30.08.2014

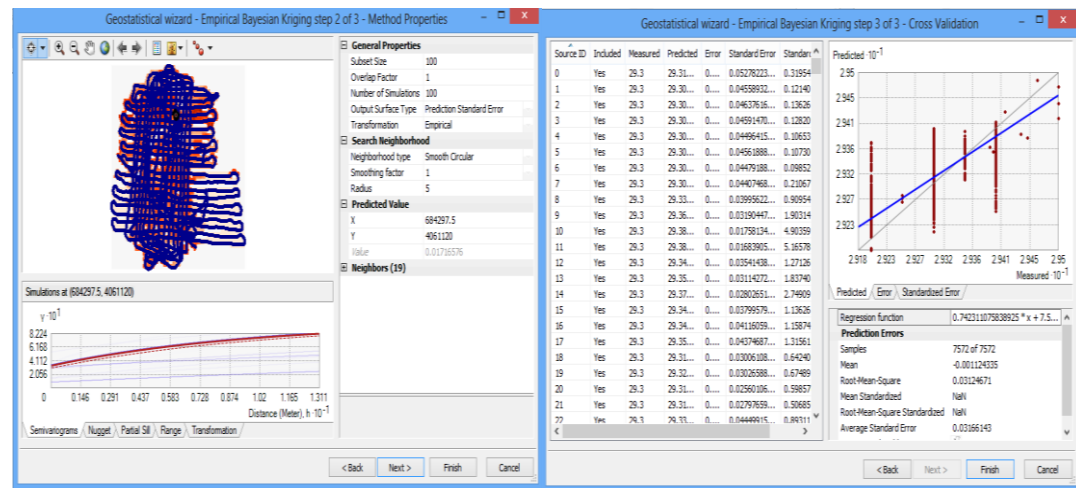


Figure D 19.The surface temperature variogram of Fethiye-Göcek Lake in 30.08.2014

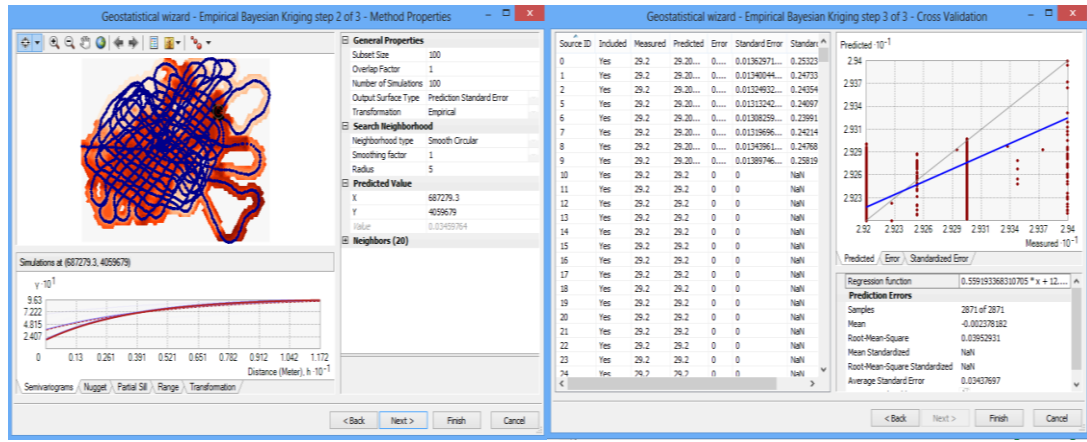


Figure D 20.The surface temperature variogram of Fethiye-Göcek Lake in 30.08.2014

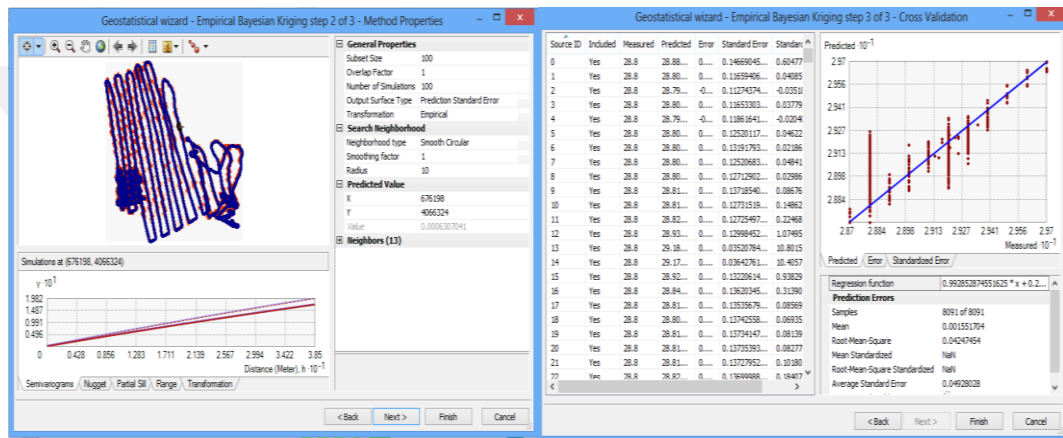


Figure D 21.The surface temperature variogram of Fethiye-Göcek Lake in 31.08.2014

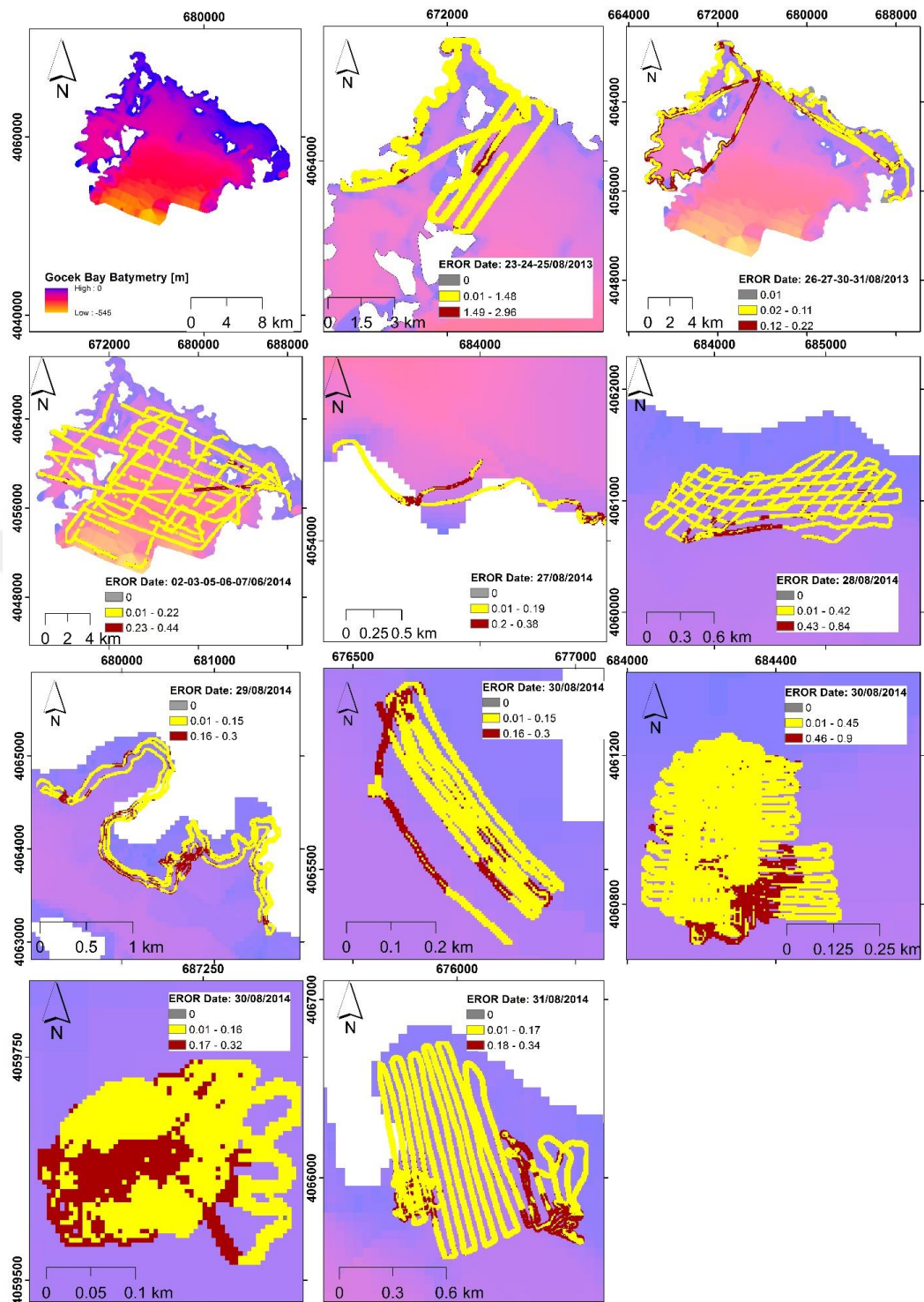


Figure D 22.The depth temperature eror map of Fethiye-Göcek Bay

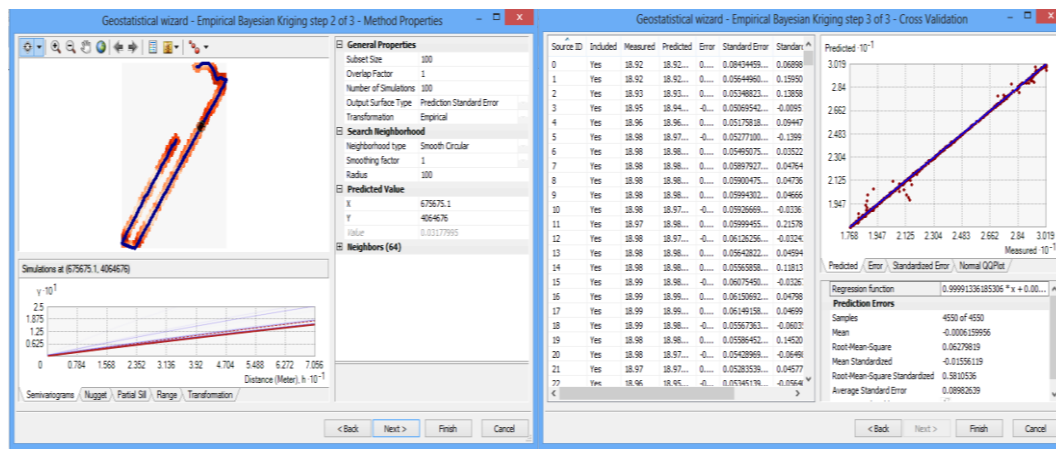


Figure D 23.The depth temperature variogram of Fethiye-Göcek Lake in 23.08.2013

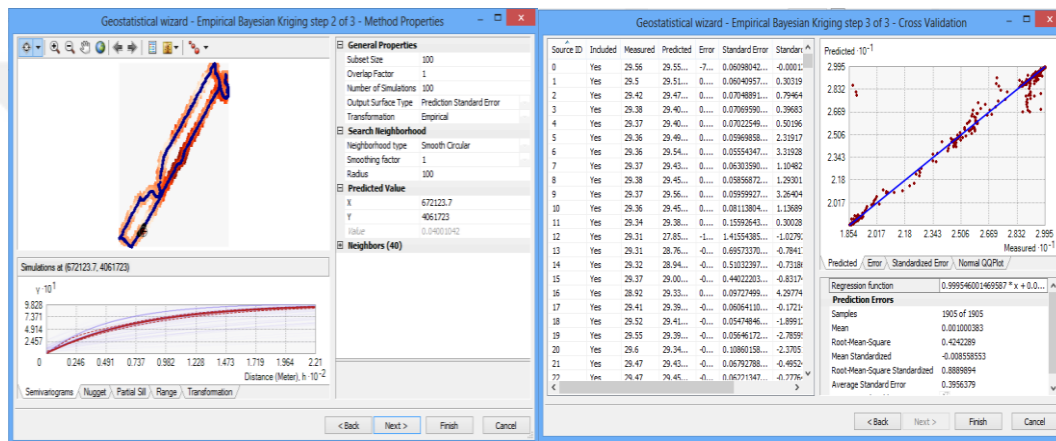


Figure D 24.The depth temperature variogram of Fethiye-Göcek Lake in 24.08.2013

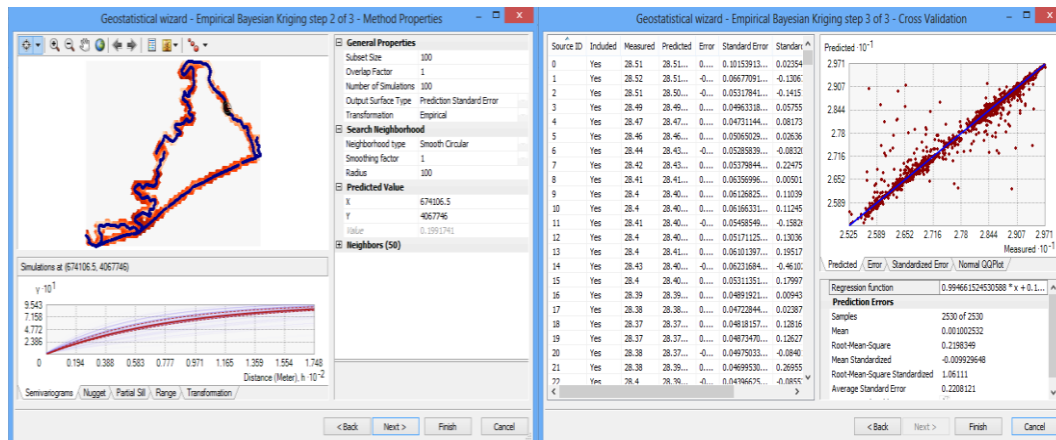


Figure D 25.The depth temperature variogram of Fethiye-Göcek Lake in 25.08.2013

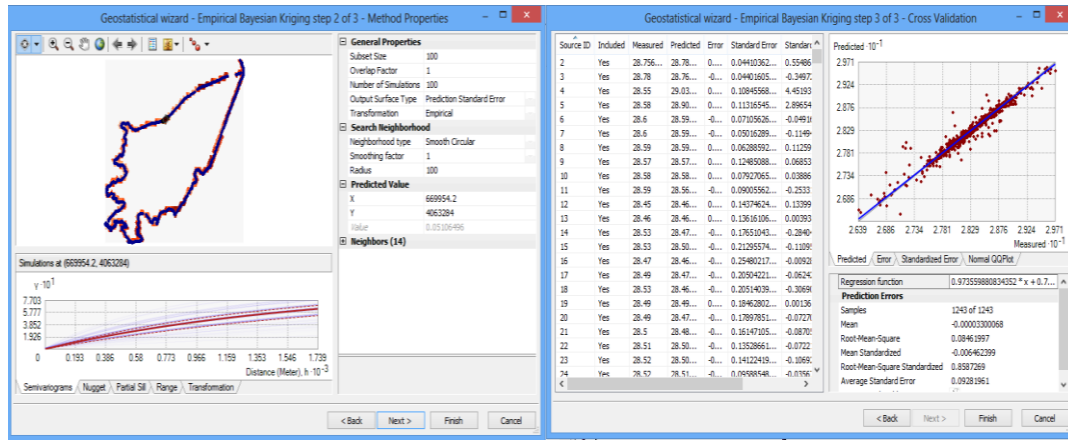


Figure D 26.The depth temperature variogram of Fethiye-Göcek Lake in 26.08.2013

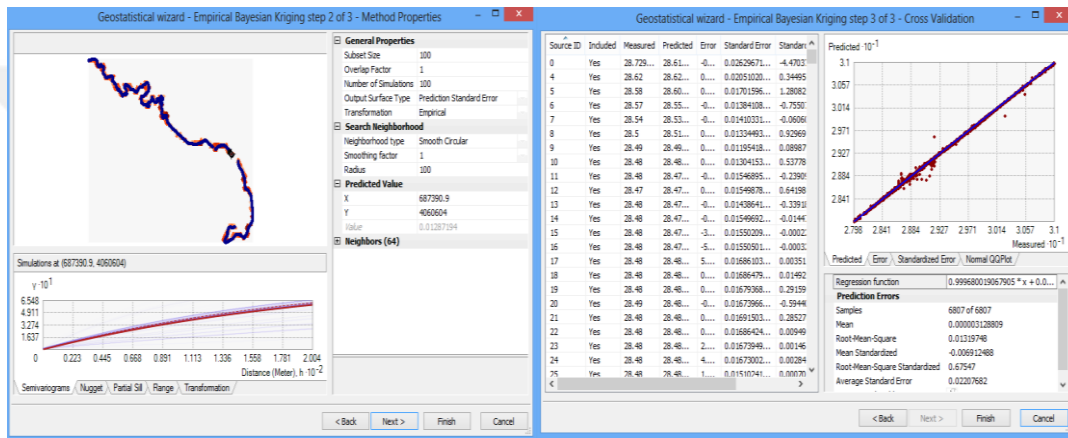


Figure D 27.The depth temperature variogram of Fethiye-Göcek Lake in 27.08.2013

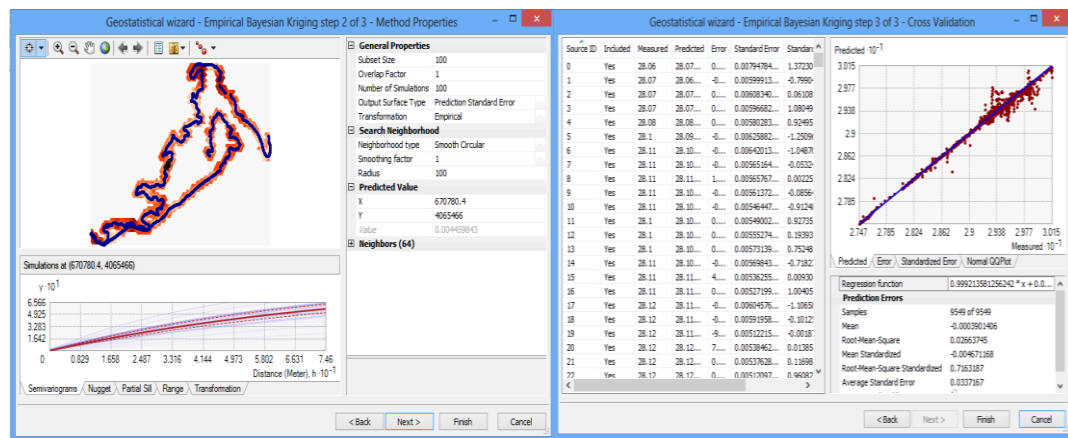


Figure D 28.The depth temperature variogram of Fethiye-Göcek Lake in 30.08.2013

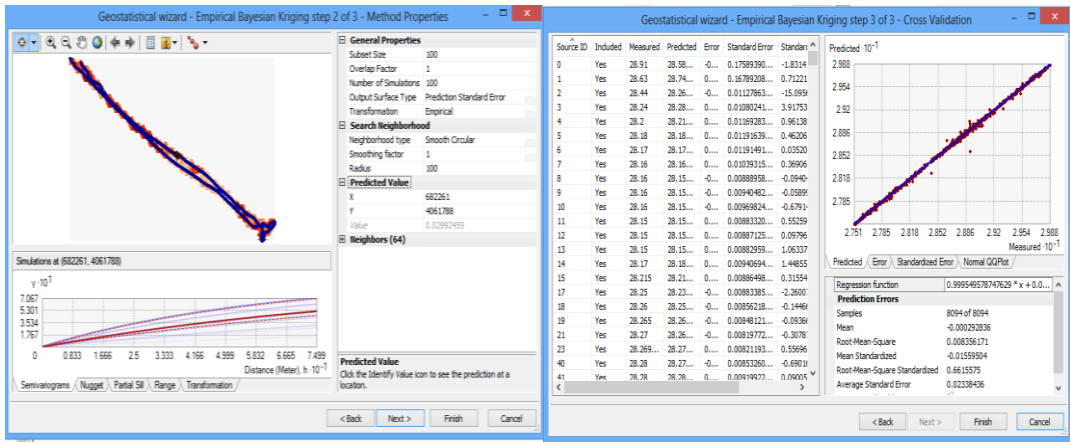


Figure D 29.The depth temperature variogram of Fethiye-Göcek Lake in 31.08.2013

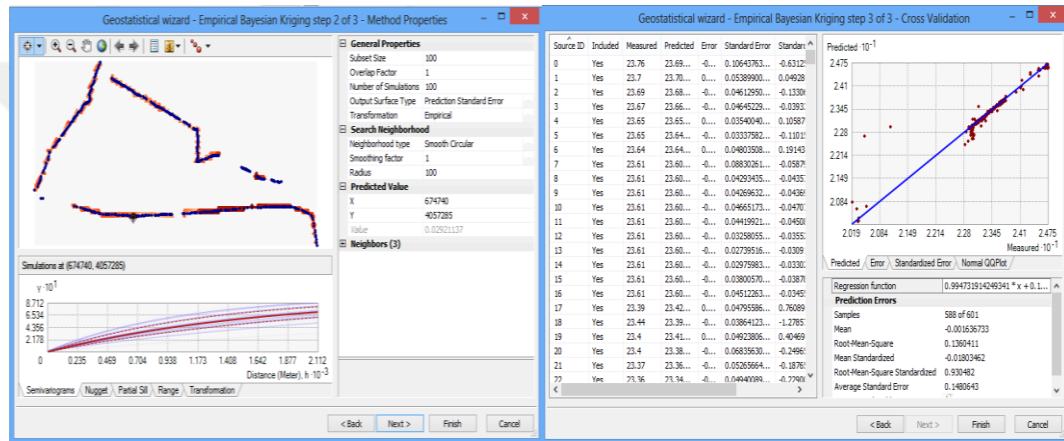


Figure D 30.The depth temperature variogram of Fethiye-Göcek Lake in 02.06.2014

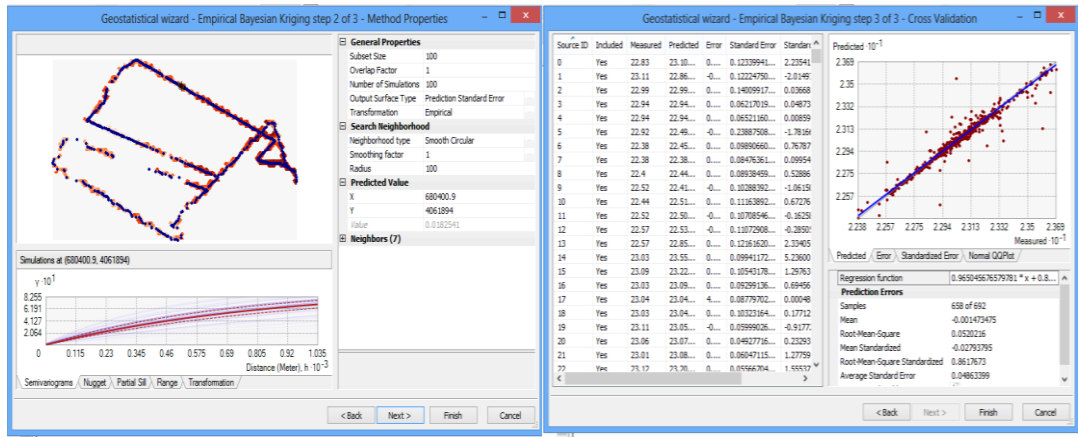


Figure D 31.The depth temperature variogram of Fethiye-Göcek Lake in 03.06.2014

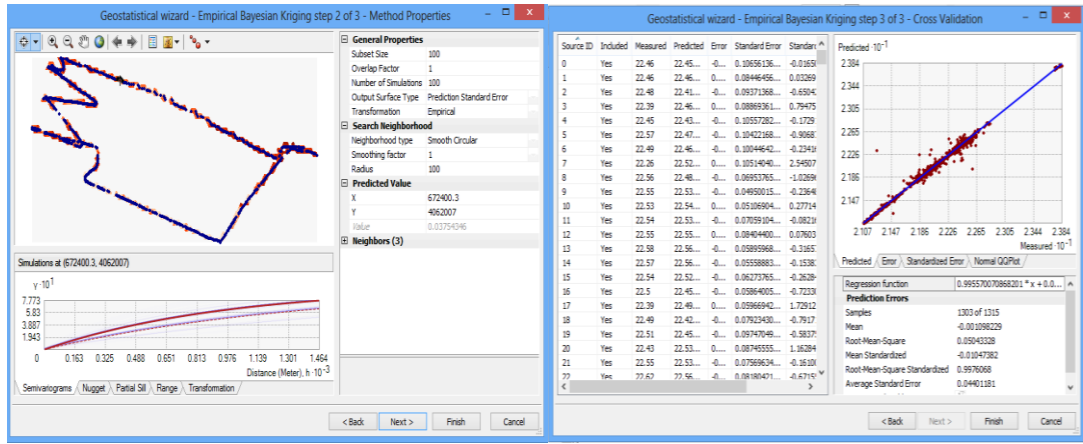


Figure D 32.The depth temperature variogram of Fethiye-Göcek Lake in 05.06.2014

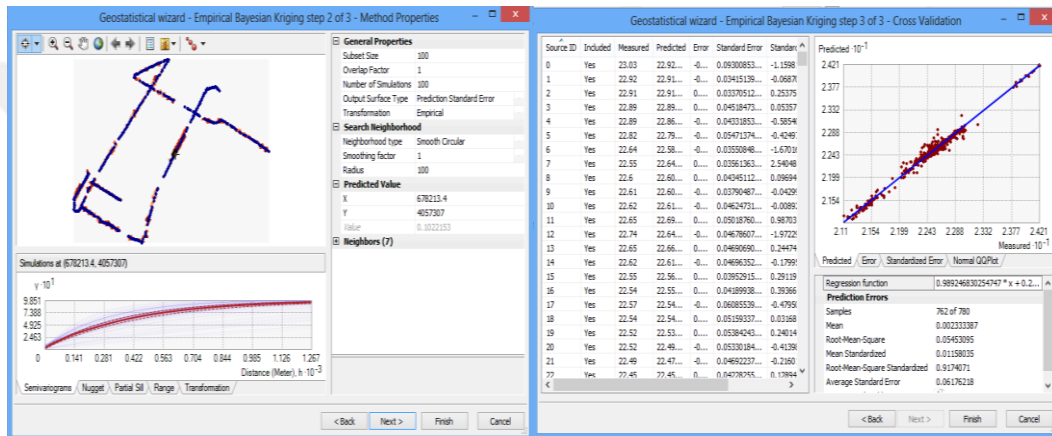


Figure D 33.The depth temperature variogram of Fethiye-Göcek Lake in 06.06.2014

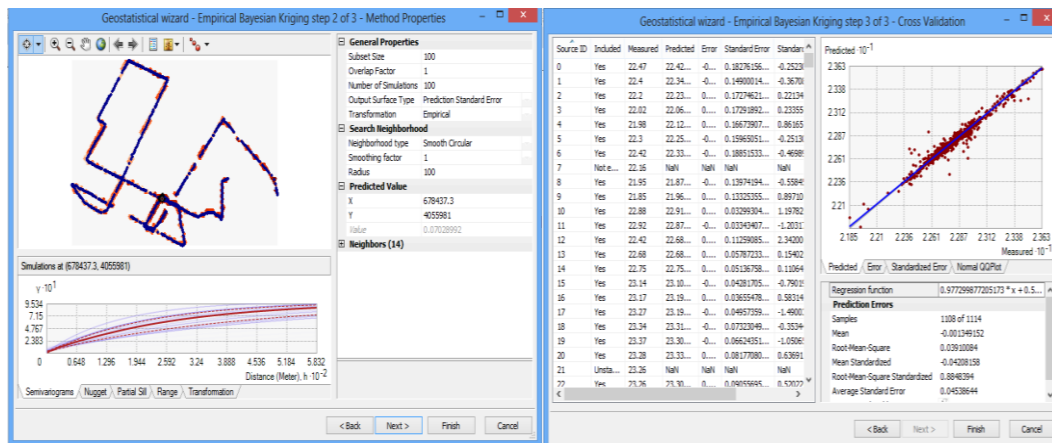


Figure D 34.The depth temperature variogram of Fethiye-Göcek Lake in 07.06.2014

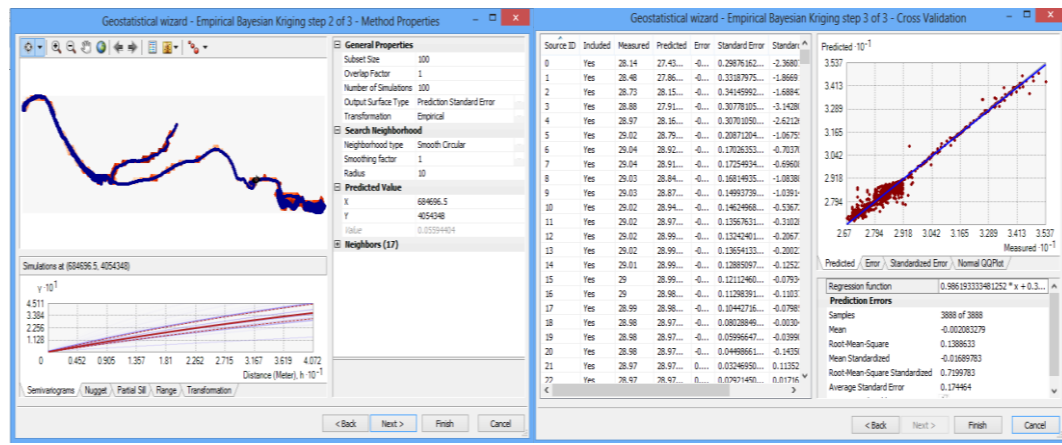


Figure D 35.The depth temperature variogram of Fethiye-Göcek Lake in 27.08.2014

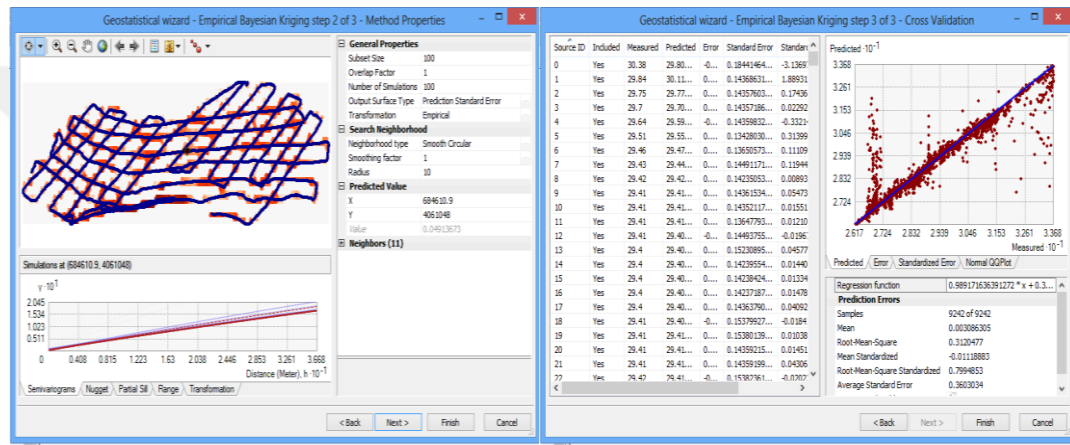


Figure D 36.The depth temperature variogram of Fethiye-Göcek Lake in 28.08.2014

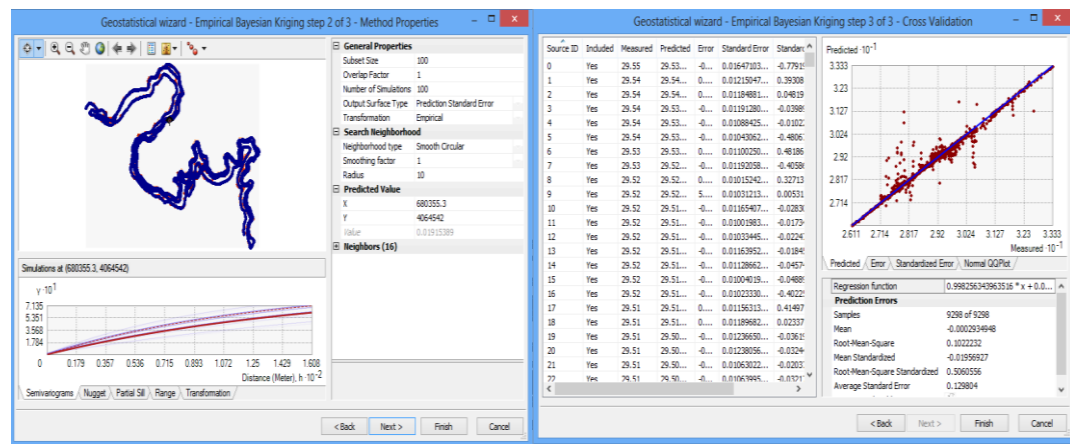


Figure D 37.The depth temperature variogram of Fethiye-Göcek Lake in 29.08.2014

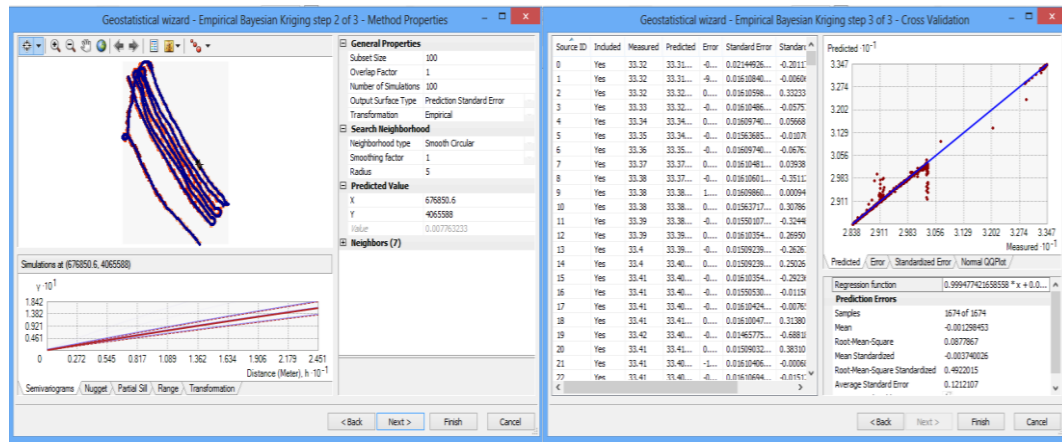


Figure D 38.The depth temperature variogram of Fethiye-Göcek Lake in 30.08.2014

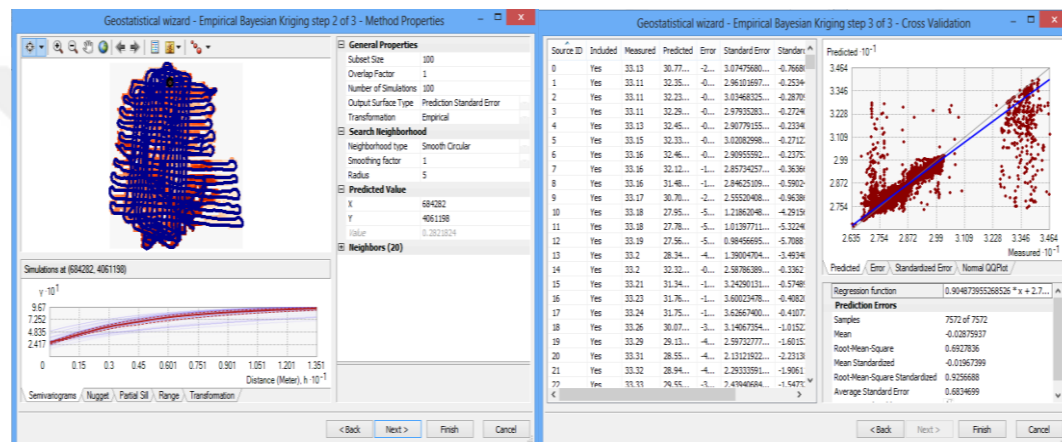


Figure D 39.The depth temperature variogram of Fethiye-Göcek Lake in 30.08.2014

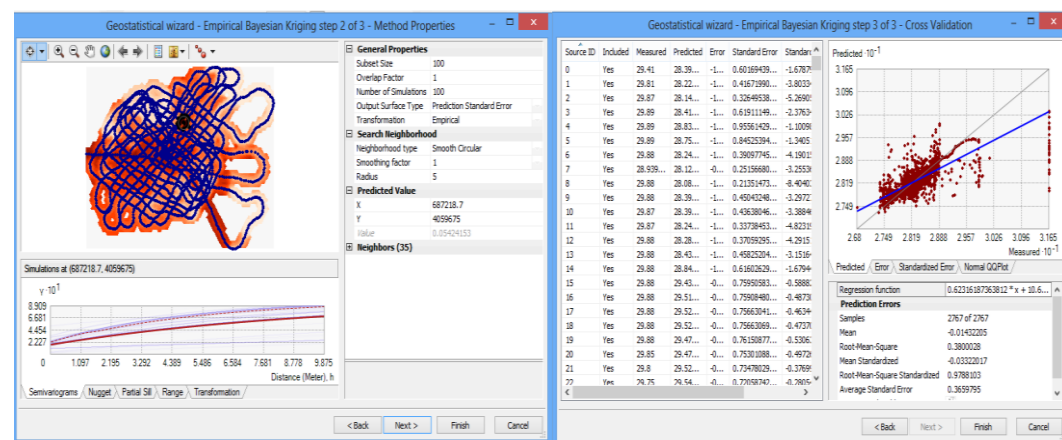


Figure D 40.The depth temperature variogram of Fethiye-Göcek Lake in 30.08.2014

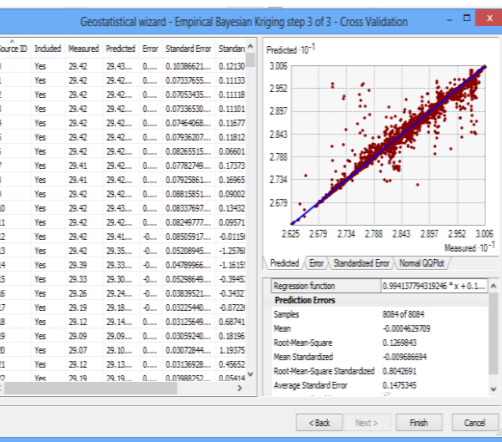
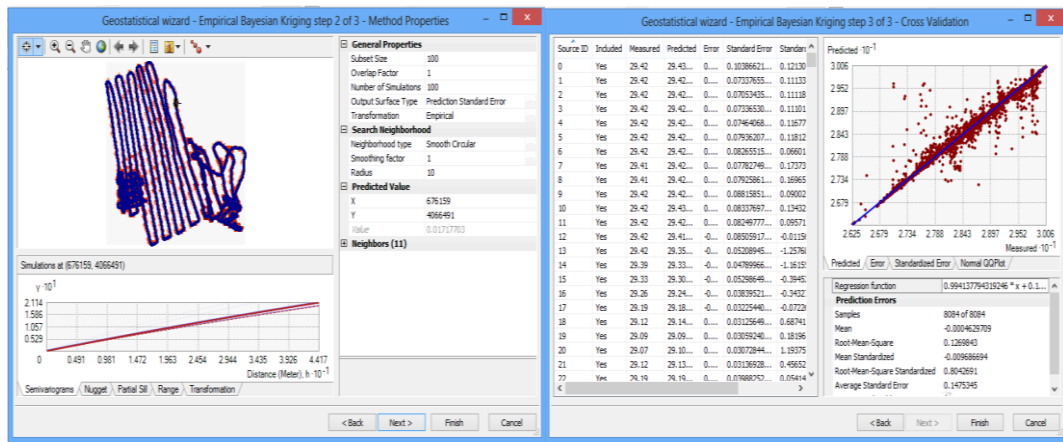


Figure D 41.The depth temperature variogram of Fethiye-Göcek Lake in 31.08.2014

Appendix E. Temperature vs. Depth Graphs for Fethiye-Göcek Bay

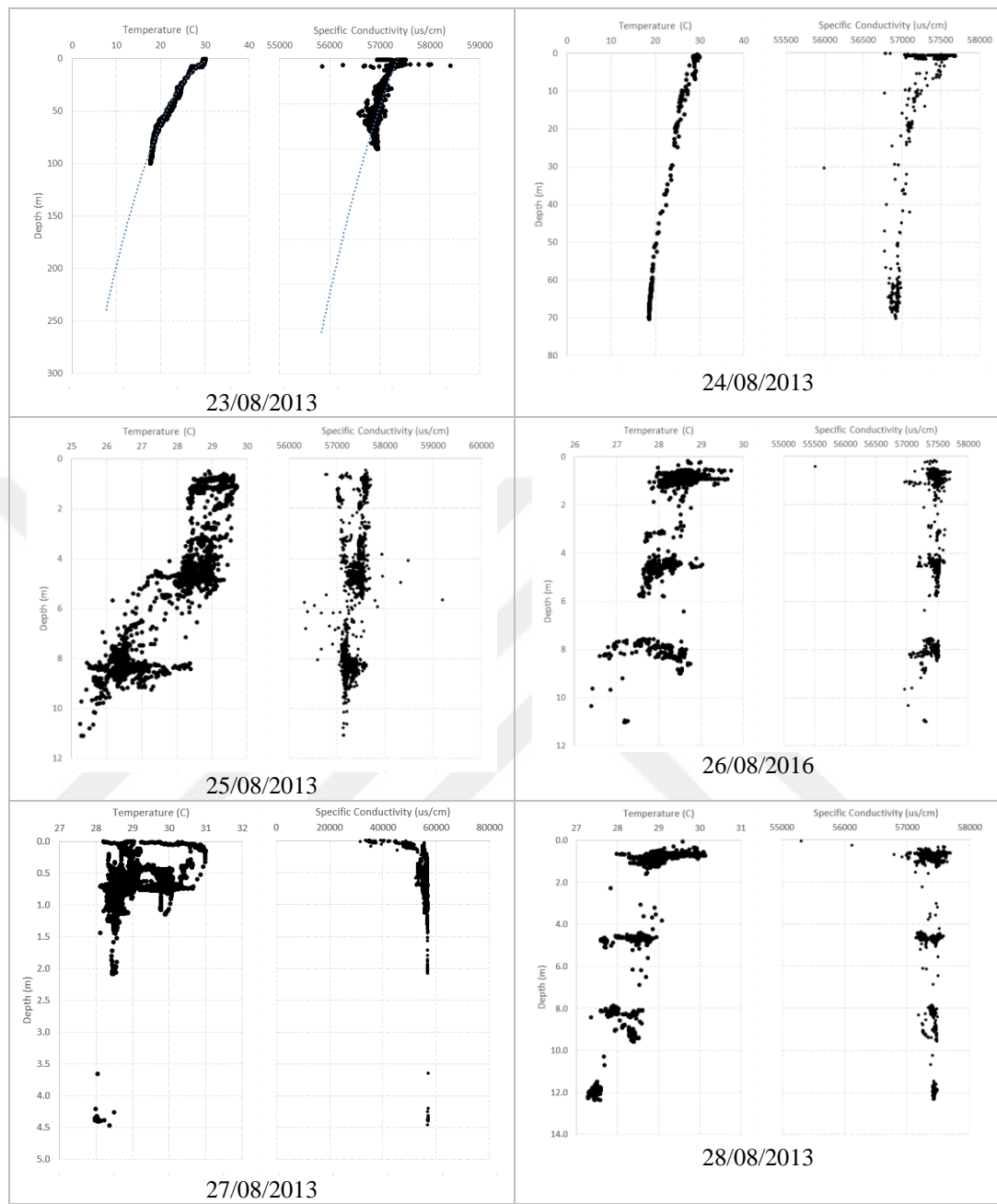
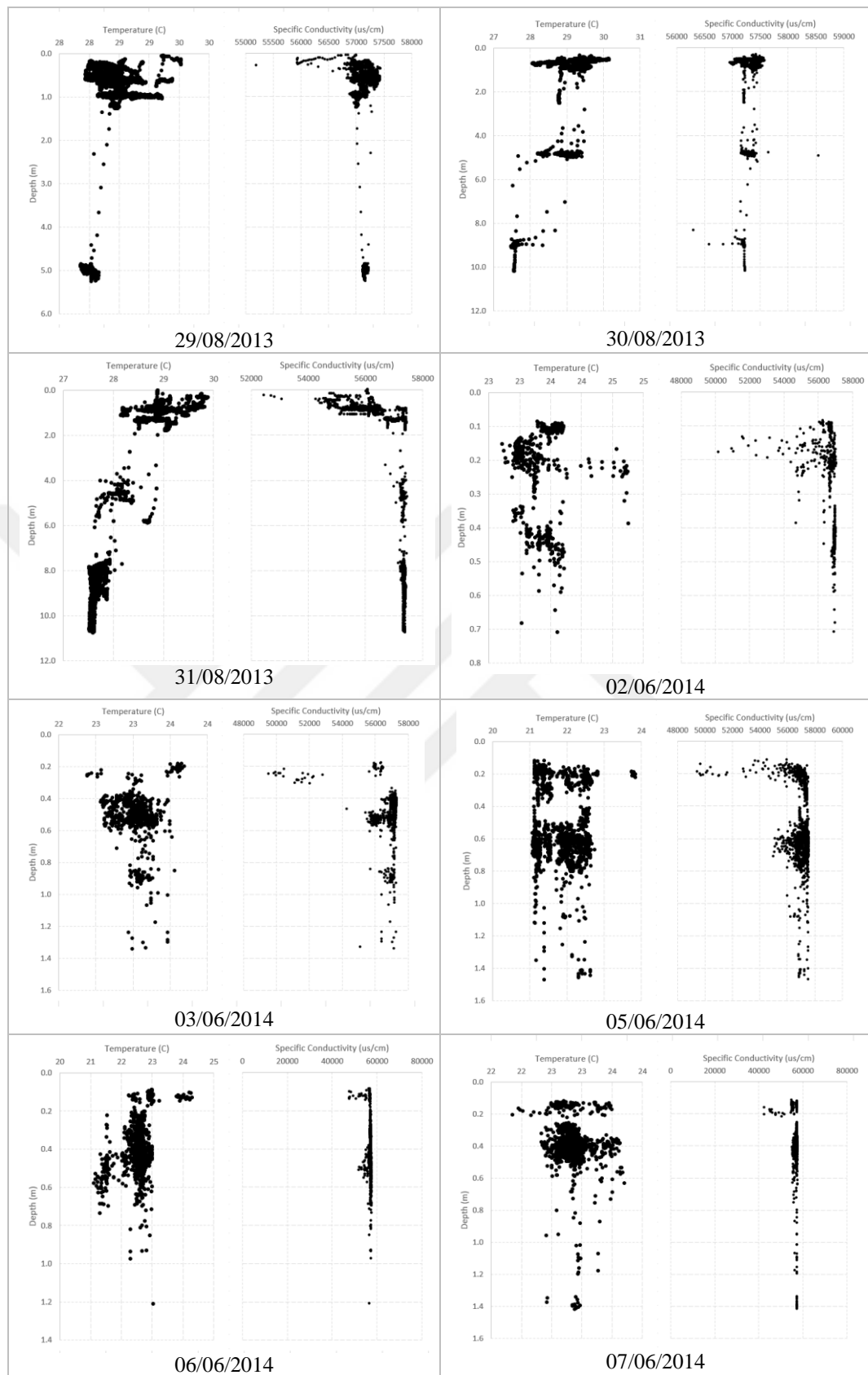
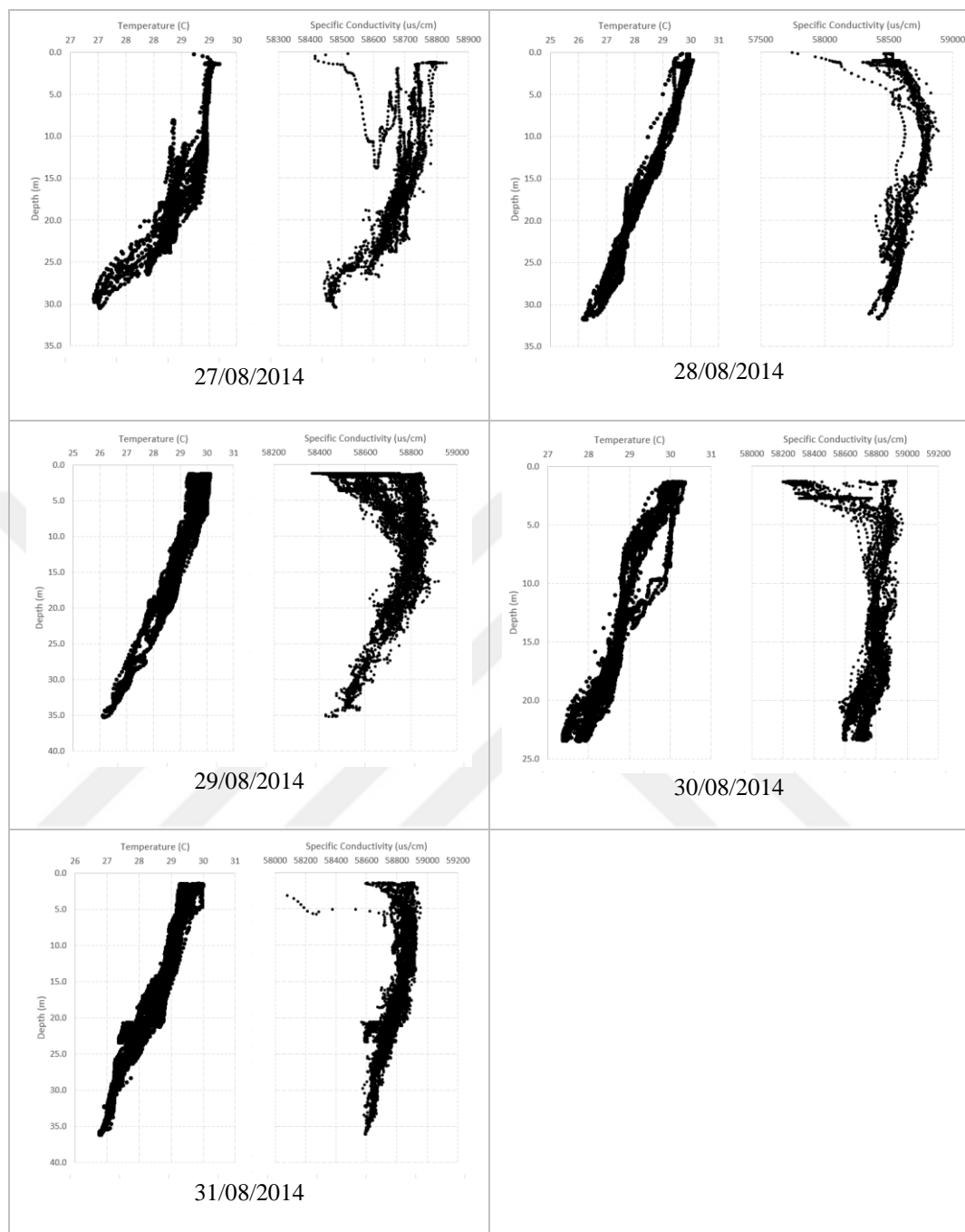


Figure E 1.Temperature and Specific Conductivity vs Depth plots for Fethiye-Göcek Bay



**Figure E 2.Temperature and Specific Conductivity vs Depth plots for Fethiye-Göcek Bay
(cont...)**



**Figure E 3.Temperature and Specific Conductivity vs Depth plots for Fethiye-Göcek Bay
(cont...)**

CURRICULUM VITAE

PERSONAL INFORMATION

Name Surname : Tugba Gurcan

Birth of Date : 22.05.1989

Nationality : Turkey

Email Address : gurcan.tugba26@gmail.com

Phone Number : +90 5415262826

EDUCATION

- 2015-2016 : Joint M2 (Master 2) Student Hydrogeology and Associated Transfers, University of Poitiers, Poitiers/France & Geological Engineering (Hydrogeology Laboratory), Mugla Sitki Kocman University, Mugla/Turkey (CGPA 3.71/4).
- 2015 (Sum) : St.Giles International English School Brighton- UK
- 2014-2015 : M1 (Master 1) Geological Engineering (Hydrogeology Laboratory), Mugla Sitki Kocman University, Mugla, Turkey
- 2013-2014 : Sıtkı Koçman School of Foreign Languages, Mugla Sitki Kocman University/Turkey
- 2008-2012 : Bachelor of Science in Geological Engineering, University of Firat, Elazig, Turkey
- 2003-2007 : Yalova Foreign Language Intensive High School/ Yalova/ Turkey

SKILLS

- OS: Windows Operating System (Windows 8, 7, Vista), Mac OS X, Linux
- Software: Groundwater Vistas, Groundwater Modeling Software (GMS), Suffer, Rockworks 14, ARCGIS 10.2-10.3, Jchess, MODFLOW, MT3D, SPSS, Global Mapper, MS Office (Word, Excel, Power Point)
- Languages: Matlab 2014b

SCHOLARSHIPS

French Government Master Fellowship (2015-2016)

Sıtkı Koçman Foundation Master Fellowship (2015-2016)

PUBLICATIONS

Gürçan T., Kurtulus B., Avsar U., and Avsar Ö., Evaluating the thermal stratification of Köyceğiz Lake (SW Turkey) using in-situ and remote sensing observation. (Under review in Limnology and Oceanography)

Gürçan T., Kurtulus B., Amphibious Unmanned Air Vehicle Based Remote Sensing Using Multispectral Camera, April 06-10, 2015, 68. Turkey Geology Congress, Ankara, Turkey.

CONFERENCES AND COURSES ATTENDED

American Geophysical Union (AGU), Fall Meeting in San Francisco, U.S on December 12-16, 2016 as a poster presenter. <http://fallmeeting.agu.org/2016/>

European Geosciences Union (EGU) in Vienna, Austria on April 23-28, 2017 as a poster presenter. <http://www.egu2017.eu/>

8th International Congress on Environmental Modelling and Software (iEMSS) in Toulouse, France, on July 10-14, 2016, as a participant. <http://www.iemss.org/sites/iemss2016/>

8th International Symposium on Eastern Mediterranean Geology (ISEM) in Muğla, Turkey on October 13-17, 2014, as a staff member. <http://isemg.org/>

LANGUAGES AND CERTIFICATES

English (Upper Intermediated- B2), French (Beginner), Turkish (Mother tongue)

2015 : St. Giles English School, Intermediated general English program in Brighton, UK

2015 : British Street Course, English Language Training Program, B2 Levels in Muğla, Turkey

2014 : 8th International Symposium on Eastern Mediterranean Geology (ISEMG), 13-17 October, Mugla Sitki Kocman University, Turkey

2012 : The European Language Portfolio, American Cultural Association Language Schools Elazığ, Turkey

2012 : ArcGIS 10.2 training certificate, Esri, Ankara, Turkey

WORK EXPERIENCE

- 2014-2015 : Research Assistant, Geographic Information System and Remote Sensing Center (CBS-UZAL) Mugla Sitki Kocman University, Mugla, Turkey. www.cbs.mu.edu.tr
- 2013-2014 : GIS Expert, Infomab Geographic Information, Technologies Inc. Ankara, Turkey. <http://www.infomab.com/en/>
- 2008-2012 : Bachelor of Science in Geological Engineering, University of Firat, Elazig, Turkey
- 2010 : Internship – Field Geologist, General Directorate of Mineral Research and Exploration- MTA Ankara/Turkey Feasibility studies in Elbistan Coal mine Project, <http://www.mta.gov.tr/en/>